Fakultät für Medizin

Institut/Klinik/Lehrstuhl für Virologie

Establishment and Characterization of Novel Recombinant Hepatitis B Virus Reporter Systems

Wen-Min Chou

Vollständiger Abdruck der von der Fakultät für Medizin der Technischen Universität München zur Erlangung des akademischen Grades eines

Doctor of Philosophy (Ph.D.)

genehmigten Dissertation.

Vorsitzende/r: Prof. Dr. Stefan Engelhardt

Betreuer/in: Prof. Dr. Ulrike Protzer

Prüfer der Dissertation:

1. Priv.-Doz. Dr. Günter Schneider

2. Prof. Dr. Wolfgang Hammerschmidt

Die Dissertation wurde am 16.08.2018 bei der Fakultät für Medizin der Technischen Universität München eingereicht und durch die Fakultät für Medizin am 17.09.2018 angenommen.

Table of contents

Abbreviations 3
Abstract 5
Zusammenfassung 6
1 Introduction 7
1.1 Hepatitis B virus 7
1.1.1 Structure of the hepatitis B virion 7
1.1.2 HBV replication cycle 9
1.1.3 *In vitro* HBV models and their applications 12
1.2 Recombinant virus live cell reporter systems 14
1.2.1 Fluorescence-based recombinant HBV reporter systems 15
1.2.2 Bioluminescence-based recombinant HBV reporter systems 16
1.2.3 Magnetic-activated cell sorting (MACS)-based isolation systems for virus-infected cells 17
1.2.4 Cre-based recombinant virus reporter systems 18
1.3 Aim of the study 20
2 Results 22
2.1 Establishment of rHBV-LNGFR reporter system 22
2.1.1 Hepatoma cells isolation by magnetic-activated cell sorting (MACS) 23
2.1.2 Production of rHBV-LNGFR 26
2.2 Establishment of rHBV-Cre reporter systems 30
2.2.1 Production of rHBV-Cre revenant 31
2.2.2 Production of rHBV-CreN 33
2.2.3 Generation of a Cre reporter cell line 39
2.2.4 Infection of the Cre reporter cells with rHBV-CreN 42
3 Discussion 47
3.1 Establishment of rHBV-LNGFR reporter system 47
3.1.1 Hepatoma cells isolation by MACS 47
3.1.2 Production of rHBV-LNGFR 49
3.2 Establishment of rHBV-Cre reporter systems 50
3.2.1 Production of rHBV-Cre revenant 51
3.2.2 Production of rHBV-CreN 53
3.2.3 Generation of a Cre reporter cell line 55
3.2.4 Infection of the Cre reporter cells with rHBV-CreN 56
3.3 Conclusion and perspectives 58
4 Materials and Methods 59

4.1 Materials 59
4.1.1 Chemicals and reagents 59
4.1.2 Formula of chemical solutions 60
4.1.3 Enzymes and Kits 61
4.1.4 Oligos 62
4.1.5 Plasmids 63
4.1.6 Antibodies 63
4.1.7 Cell lines and bacteria 64
4.1.8 Cell culture media 64
4.1.9 Laboratory equipment and consumables 64
4.1.10 Software 65
4.2 Methods 66
4.2.1 Molecular cloning 66
4.2.2 Cell culture 68
4.2.3 Transfection 68
4.2.4 Magnetic activated cell sorting (MACS) 68
4.2.5 Cell viability assays 69
4.2.6 Fluorescence activated cell sorting (FACS) 69
4.2.7 Recombinant HBV (rHBV) production 69
4.2.8 PEG precipitation of HBV/rHBV 70
4.2.9 Southern blotting analysis of capsid DNA 70
4.2.10 Southern blotting analysis of viral DNA 71
4.2.11 Heparin affinity chromatography and rDNase on-column digestion 71
4.2.12 Northern blotting analysis of HBV RNA 71
4.2.13 Western blotting analysis 72
4.2.14 HBV/rHBV infection 72
4.2.15 Fluorescence microscopy 73
4.2.16 HBeAg ELISA 73
4.2.17 Real-time quantitative PCR (qPCR) 73
4.2.18 Polymerase chain reaction (PCR) 74
4.2.19 Southern blotting analysis of cccDNA 74
5 Table of figures 75
6 Reference 76
Publications and patent 83
Acknowledgements 84

Abbreviations

(+)	plus strand
(–)	minus strand
APOBEC3A	Apolipoprotein B mRNA editing enzyme catalytic polypeptide-like 3A (cytidine deaminase)
BAC	bacterial artificial chromosome
BFP	blue fluorescent protein
cccDNA	covalently closed circular DNA
CFP	cyan fluorescent protein
CLDN1	claudin 1
Cre	Cre recombinase
CreC/CIR cells	HepG2-NTCP-CreC-CIR cells
ddPCR	droplet digital PCR
dHepaRG	differentiated HepaRG cells
DMSO	dimethyl sulfoxide
dpi	days post-infection
DR1	direct repeats 1
DR2	direct repeats 2
dslDNA, DSL	double-stranded linear DNA
DsRed	red fluorescent protein
EBV	Epstein-Barr virus
ELISA	enzyme-linked immunosorbent assay
EN1	enhancer 1
EN2	enhancer 2
ER	endoplasmic reticulum
FACS	fluorescence activated cell sorting
FLuc	Firefly luciferase
GFP	green fluorescent protein
GLuc	*Gaussia* luciferase
HBc	HBV core protein
HBeAg	HBV e antigen
HBsAg	HBV surface antigen
HBV	hepatitis B virus
HCC	hepatocellular carcinoma
HPCs	hematopoietic progenitor cells
HRSV	human respiratory syncytial virus
IAV	Influenza A virus
IRES	internal ribosome entry sites
KSHV	Kaposi’s sarcoma-associated herpes virus
L	large envelope protein

LNGFR	human low affinity nerve growth factor receptor
M	middle envelope protein
MACS	magnetic-activated cell sorting
MHV-68	murine gammaherpesvirus 68
MOI	multiplicity of infection
MyrB	Myrcludex-B
NLuc	NanoLuc
NTCP	sodium taurocholate cotransporting polypeptide
OCLN	occludin
ORF	open reading frame
PCR	polymerase chain reaction
PEG	polyethylene glycol
PF-rcDNA	protein-free rcDNA
pgRNA	pregenomic RNA
PHHs	primary human hepatocytes
RBEs	recombinase-binding elements
rcDNA, RC	relaxed circular DNA
rHBV	recombinant HBV
RLuc	*Renilla* luciferase
RNAi	RNA interference
RNase H	ribonuclease H
RT	reverse transcriptase
S	small envelope protein
SCARB1	scavenger receptor type B class I
ssDNA	single-stranded DNA
SVPs	subviral particles
TP	terminal protein
TTR	mouse transthyretin enhancer/promoter
UPR	unfolded protein responses
wtHBV	wild-type HBV
YFP	yellow fluorescent protein

Abstract

Screenings for drug candidates, therapeutics, or host factors interfering with hepatitis B virus (HBV) infection are currently performed using wild-type HBV (wtHBV). However, wtHBV infection is rather difficult to detect on a single-cell level, and analyses are both labor-intensive and costly. Recombinant HBV (rHBV) reporter systems represent a potential alternative for performing such screenings. These recombinant viruses express reporters (fluorescent proteins or luciferase) upon infection, providing a convenient means for visualizing and quantifying infection events, as well as allowing for the identification and sorting of infected cells. Despite the ease of tracking reporter expression following infection, available rHBV systems have certain limitations. The primary disadvantage is that reporter expression upon rHBV infection is low-level and transient, which reduces detection sensitivity. As a result, it is challenging to isolate rHBV-infected cells for downstream analyses and monitor infections over longer periods (e.g. weeks).

Three novel reporter HBV systems have been established in the present study, including: 1) rHBV-LNGFR encoding a cell-surface molecule, which allows magnetic sorting of infected cells, 2) rHBV-Cre revenant encoding Cre recombinase upon circularization, which allows the activation of reporter gene expression after infection, and 3) rHBV-CreN encoding the N-terminal portion of Cre recombinase, which induces stable reporter expression via the formation of a functional recombinase with the C-terminal portion of Cre upon infection. rHBV were produced by trans-complementing the lacking virus gene products to synthesis the correct circular form of rHBV genomes. Furthermore, a functionally validated Cre-reporter cell line was generated. The integrity and functionality of the rHBV-CreN reporter system was demonstrated by the formation of covalently closed circular DNA (cccDNA) in rHBV-infected cells expressing the reporter gene. Also, rHBV infection could be blocked through an HBV entry inhibitor, demonstrating that the route of rHBV infection is identical to that of wtHBV.

In conclusion, novel rHBV reporter systems were established, of which rHBV-CreN proved superior to all rHBV reporter systems reported to date. Utilizing the Cre-lox recombination to permanently activate reporters upon rHBV infection allowed for specific, rapid, low-cost, permanent, and sensitive tracking of HBV infection. This system now provides a robust platform to detect HBV infection; therefore, it can be utilized for large-scale screenings regarding HBV infection.

Zusammenfassung

Aktuell werden Screenings für Arzneimittelkandidaten, Therapeutika oder Wirtsfaktoren, welche die HBV-Infektion beeinträchtigen, mit Wildtyp-HBV (wtHBV) durchgeführt. Infektion mit wtHBV ist auf Einzelzelllevel jedoch schwierig zu detektieren und die Analysen dazu sind arbeitsintensiv und teuer. Eine potentielle Alternative sind rekombinante HBV (rHBV)-Reportersysteme, welche Reporterproteine (Fluoreszenzproteine oder Luziferase) nach Infektion exprimieren, was eine komfortable Visualisierung oder Quantifizierung der Infektionsereignisse erlaubt sowie die Identifizierung und Sortierung infizierter Zellen. Trotz der einfachen Verfolgbarkeit der Reporterexpression haben die verfügbaren rHBV-Systeme Limitierungen. Ihr Hauptnachteil ist, dass die Reporterexpression nach rHBV-Infektion nur transient und auf einem niedrigen Level erreicht und daher eine sensitive Detektion erschwert wird. Folglich ist es schwierig, rHBV-infizierte Zellen für folgende Analysen zu isolieren und die Infektion über längere Zeit hinweg zu beobachten.

In dieser Arbeit wurden neue Reporter-HBV-Systeme etabliert: 1) rHBV-LNGFR, welches ein Zelloberflächenmolekül codiert, das das magnetische Sortieren infizierter Zellen ermöglicht, 2) rHBV-Cre Revenant, welches die Cre-Rekombinase nach Zirkularisierung codiert, was die Aktivierung der Reportergenexpression nach etablierter Infektion erlaubt und 3) rHBV-CreN, welches den N-terminalen Teil der Cre-Rekombinase codiert, was die stabile Expression eines Reporters über Bildung einer funktionalen Rekombinase mit dem C-terminalen Teil von Cre induziert. rHBV-Partikel wurden durch Trans-Komplementierung der fehlenden viralen Genprodukte produziert und die korrekte Bildung zirkulärer rHBV-Genome wurde nachgewiesen. Eine Cre-Reporterzelllinie wurde erstellt und funktional validiert. Die Integrität und Funktionalität des rHBV-CreN-Reportersystems wurde anhand der Bildung der kovalent geschlossenen, zirkulären DNA (cccDNA) in rHBV-infizierten Zellen gezeigt. Die rHBV-Infektion konnte durch einen Inhibitor der HBV-Aufnahme blockiert werden, was zeigt, dass rHBV dieselbe Infektionsroute wie wtHBV nutzt.

Insgesamt konnten neue rHBV-Reportersysteme etabliert werden, von welchen rHBV-CreN sich als bestes unter allen bisher beschriebenen rHBV-Reportersystemen präsentierte. Die Verwendung der Cre-lox-Rekombination für die andauernde Reporteraktivierung nach rHBV-Infektion erlaubt das spezifische, schnelle, preiswerte, permanente und sensitive Verfolgen der HBV-Infektion. Dieses System stellt eine robuste Plattform für die Detektion der HBV-Infektion dar und kann deshalb für Screenings nach erfolgreicher HBV-Infektion im großen Maßstab genutzt werden.

1 Introduction

The following sections provide background knowledge on topics related to the present study, including HBV biology, methods and *in vitro* models to study HBV infection, and the introduction of recombinant virus live cell reporter systems.

1.1 Hepatitis B virus

Chronic HBV infection is the leading cause of liver cirrhosis and hepatocellular carcinoma (HCC), which results in approximately 887,000 deaths per year [1]. It is estimated that > 85% of newborns are unable to resolve acute HBV infection that is transmitted vertically from their mothers, leading to chronic hepatitis B [2]. Moreover, the frequency of becoming chronically infected with HBV inversely relates to the age of individuals at the time of infection. Approximately 30% of children (yet only 5-10% of adults) will develop a lifelong chronic infection following acute HBV infection [3]. Currently, 257 million individuals worldwide are chronically infected with HBV (WHO 2018). Approximately 3.6% of the global population is HBV surface antigen (HBsAg) positive, and the highest HBsAg seroprevalence was observed in central and East Asia, sub-Saharan Africa, and the Pacific region [4]. A total of 10 HBV genotypes (A-J) are classified (Figure 1). They may vary in their tendency for chronicity development, HBeAg seroconversion and HBsAg seroclearance, responses to antiviral treatment, and disease progression to liver cirrhosis and HCC development [5].

1.1.1 Structure of the hepatitis B virion

HBV is a small enveloped DNA virus belonging to the Hepadnaviridae family, that has a strict tropism for hepatocytes [6]. The infectious virion has a spherical structure of 42-44 nm consisting of the viral capsid surrounded by a lipid envelope studded with complexes of viral glycoproteins [7, 8]. The capsid contains the viral genome, a partially double-stranded, relaxed-circular DNA (rcDNA, RC) of approximately 3.2 kb that is composed of a negative strand and a partial positive strand [9]. The viral polymerase is covalently attached to the 5’ end of minus-stranded DNA, whereas an oligoribonucleotide—serving as a primer for plus-stranded DNA synthesis—is linked to the 5’ end of the plus-stranded DNA (Figure 2) [10].

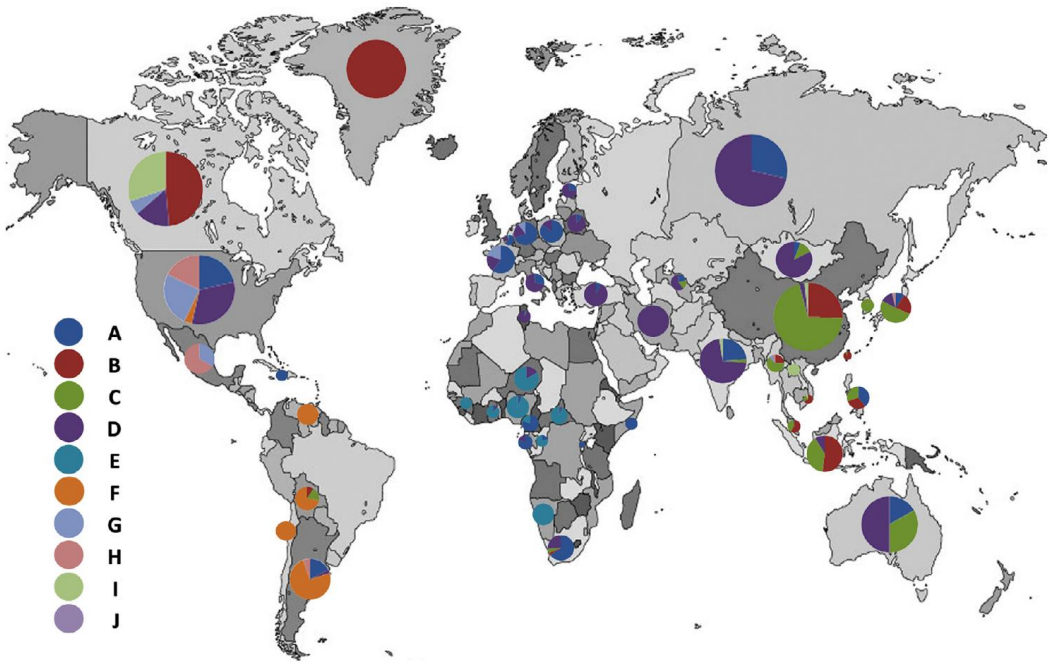

Figure 1: Geographic distribution of HBV genotypes (reprinted from [11])

HBV genotype A is common in sub-Saharan Africa and Northern Europe, genotypes B and C are common in East Asia, genotype D is common in Africa, Europe, Mediterranean countries, and India, genotype E is common in Africa, genotype G is found in France, Germany, and the United States, genotype H is common in Central and South America, genotype I is reported in Vietnam and Laos; and genotype J is found in the Ryukyu Islands of Japan.

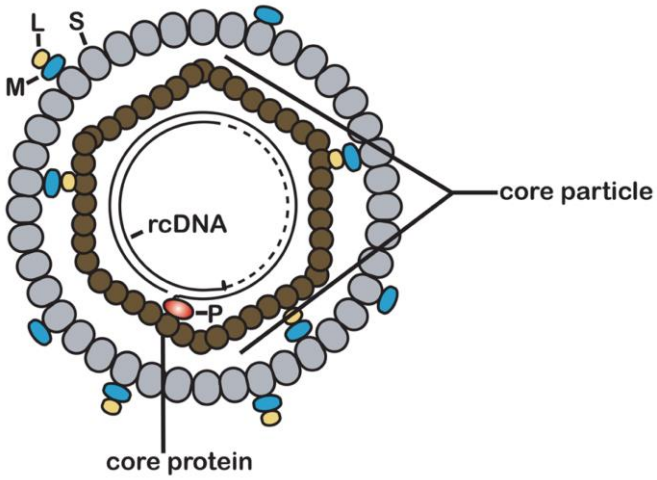

Figure 2: HBV structure (reprinted from [12])

A schematic representation of a mature virion (Dane particle), which consists of two parts: the viralcapsid (or core particle) and a viral envelope. The partially double-stranded DNA genome (rcDNA) bound to the viral polymerase (P) is encapsidated into the icosahedral capsid, which is assembled by the core proteins. The HBV surface proteins (S, M, and L), which contain the same C-terminal S domain (grey) or additional preS1 (yellow) and preS2 (blue) domains, are incorporated into an ER-derived envelope (viral envelope).

1.1.2 HBV replication cycle

The replication cycle of HBV is described in Figure 3. The virus enters the hepatocyte via using a bile acid transporter named sodium taurocholate cotransporting polypeptide (NTCP) [13], which is expressed on the basolateral membrane of hepatocytes and mediates the transport of conjugated bile salts [14]. Upon uncoating viruses release the capsid into the cytoplasm, which then migrates to the nuclear pores and accumulate in nuclear baskets [15]. The interaction between capsids and the cellular transport receptors (importin alpha and beta) allows the HBV genome, an incomplete rcDNA, to be released into the nucleus [15]. In the nucleus, host factors play a role in converting rcDNA to a covalently closed circular DNA (cccDNA) form. However, the identity of the cellular enzymes executing the DNA repair reactions are not fully understood [6].

Notably, cccDNA is the viral persistence form [16], to which the host transcriptional machinery is recruited to produce the viral transcripts necessary for viral protein expression (Figure 4) and virus replication [17]. HBV RNA transcription is regulated by four separated promoters (core, preS1, preS2/S, and X) within the cccDNA, while two enhancers (EN1 and EN2) regulate the activity of these promoters [18]. The 3.5-kb pregenomic RNA (pgRNA) is regulated by the core promoter, serving as the template for encoding HBV core protein (HBc) and polymerase [18]. Core is the subunit of the viral capsid [6], and it spontaneously self-assembles into a capsid-like structure [12]. The polymerase is encoded from the polymerase open reading frame (ORF) using an internal initiation site within the pgRNA [6, 12]. HBV polymerase is functionally divided into three domains: 1) the terminal protein (TP) domain, which is responsible for the packaging of pgRNA and the protein priming of pgRNA reverse transcription [19]; 2) the reverse transcriptase (RT) domain, which reverse transcribes the pgRNA into rcDNA; and 3) the ribonuclease H (RNase H) domain, which degrades the pgRNA during rcDNA synthesis [12]. Additionally, the core promoter regulates the expression of the preCore transcript, which is co-lineared with pgRNA with a short extension at the 5’ end, permitting the translation of preCore protein from the preCore AUG [6, 18]. PreCore protein is the core protein with an N-terminal signal peptide that transports the peptide to the endoplasmic reticulum (ER), where this protein, so-called hepatitis B e antigen (HBeAg), is proteolytically processed at its N and C termini and secreted from infected cells [6, 20]. HBeAg is a serological marker that can be used to diagnose and distinguish between acute and chronic HBV infections [21]. The 2.4-kb sgRNA includes the PreS1, PreS2, and S ORF, is driven by PreS1 promoter, and encodes the large envelope protein (L), whereas the 2.1-kb sgRNA includes the PreS2 and S ORF, is driven by PreS2 promoter, and encodes the middle (M) and small (S) envelope proteins using different AUG sites [12]. All three

envelope proteins share the same C-terminal S domain, while M protein has an additional preS2 domain at the N-terminus and L protein contains the M protein sequence with an N-terminal extension known as preS1 domain [6, 12]. The envelope proteins are directed to the ER, from which they enter the secretory pathway and yield a huge excess of subviral particles (SVPs) over complete virions. These SVPs are referred to as HBsAg in the serum of the patients [22]. HBx is translated from the 0.7-kb transcript, which is driven by the X promoter. HBx has been shown to be associated with HBV cccDNA and crucial for virus replication, especially for the efficient transcription of viral RNAs from cccDNA [23].

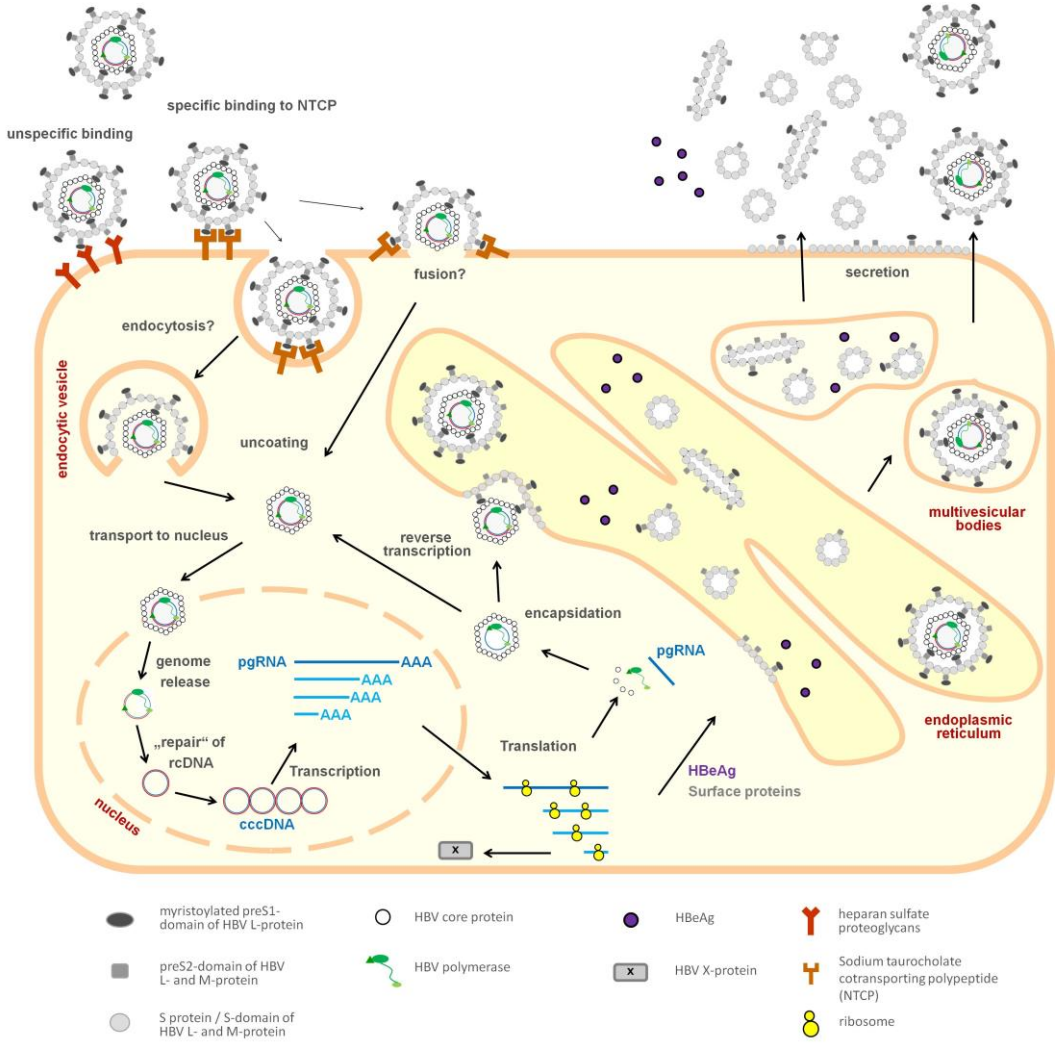

Figure 3: HBV life cycle (reprinted from [16])

After HBV entry into the host cells via NTCP, the uncoated capsid is transported to the cell nucleus to release the HBV genome. Then, rcDNA is repaired to form the cccDNA, which serves as the transcriptional template for pgRNA and subgenomic RNA. In the cytoplasm, the pgRNA and viral polymerase are packaged into capsids, where the pgRNA is reverse transcribed into rcDNA. Capsids can either be recycled back to the nucleus or enveloped in the endoplasmic reticulum and secreted from the cells.

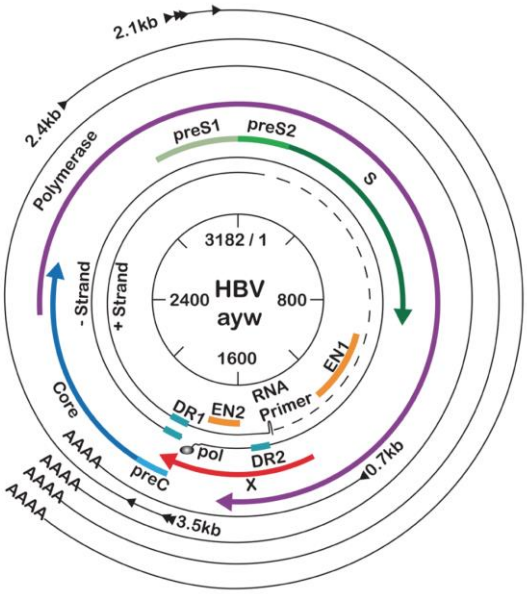

Figure 4: Depiction of the HBV genome organization (reprinted from [12])
The inner circle presents the co-ordinates of the genome, and the genomic position is given relative to the EcoRI site (position 1). The partially double-stranded genome within the capsid consists of a plus (+) and a minus (–) strand that are cohesively complemented at their 5' ends. The (+) strand is attached to the RNA primer, whereas the (–) strand is attached to the polymerase (pol). Upon establishment of HBV infection, cccDNA serves as a template for viral replication. Two enhancers (orange rectangular) regulate the activity of the viral promoters: Enhancer 1 (EN1) stimulates the transcription of pgRNA, preC, and X, whereas Enhancer 2 (EN2) stimulates the transcription of preS1, PreS2/S, and X. Viral open reading frames (ORFs) are indicated by the thicker, colored arrows. The HBV genome has four overlapping ORFs: PreC/C ORF (blue arrow) encodes the core protein and HBeAg, PreS1/PreS2/S ORF (green arrow) encodes the envelope proteins, polymerase ORF (purple arrow) encodes the polymerase, and X ORF (red arrow) encodes the HBx protein. The four outermost black arrows indicate the viral transcripts. Notably, multiple arrowheads at the 5' ends of the PreC/pgRNA (3.5 kb) and PreS2/S (2.1 kb) transcripts indicate heterogeneous transcription start sites. The identical polyA site depicts the common 3' end of all the HBV transcripts. Moreover, the cis-acting regulatory elements, direct repeats 1 and 2 (DR1 and DR2), which play important roles for polymerase translocation during genome replication, are represented by a cyan-colored rectangle.

In addition to being a template for transcribing core proteins and polymerase, pgRNA serves as the template for rcDNA synthesis (the viral genome). Notably, the binding of the polymerase to the stem-loop structure (termed epsilon) at the 5' end of pgRNA triggers the packaging of this protein/RNA complex into the capsid [24]. Inside the capsids, the polymerase primes reverse transcription by its TP domain, and subsequently, reverse transcription of the minus (-) strand DNA is catalyzed by the RT domain of the polymerase [25].

After completing the synthesis of minus (-) strand DNA, the pgRNA is degraded by the RNase H domain of the polymerase, while the non-degraded 5' residues of the pgRNA act as primer for plus (+) strand DNA synthesis. In a majority of capsids, the RNA primer tranlocates and binds to DR2 site of (-) strand DNA, which eventually

becomes the rcDNA (Figure 5). In a minority of capsids, a direct extension of the RNA primer at the DR1 site yields a double-stranded linear DNA (dslDNA, DSL) molecule, which cannot give rise to new pgRNA upon infection [22]. The replication cycle is completed by the DNA-containing capsids being enveloped with viral envelope proteins (S, M, and L) at the ER and virions then being released from cells via multivesicular bodies machinery [26]. Alternatively, an insufficient amount of envelope proteins promotes the recycling of newly synthesized rcDNA back to the nucleus, leading to the amplification of the cccDNA pool [27].

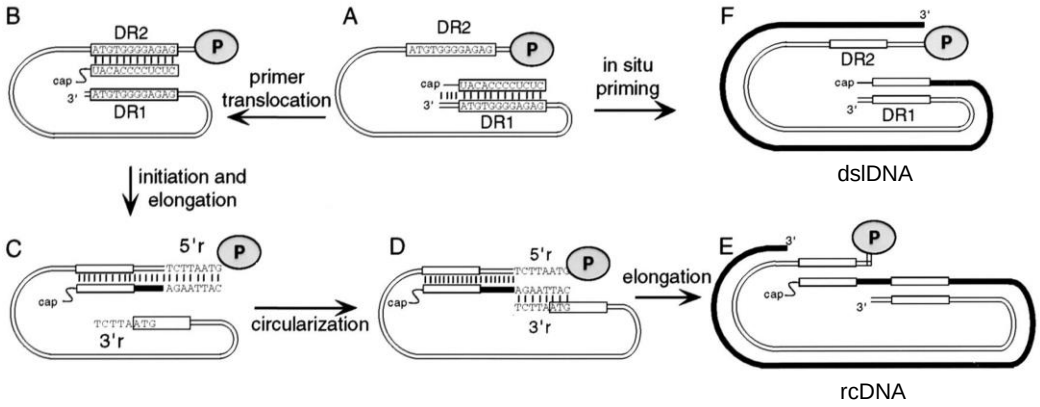

Figure 5: Synthesis of the HBV genome (reprinted from [28])
(A) Following the reverse transcription of (-) strand DNA (thin parallel lines), viral polymerase (gray oval, labeled P) is covalently attached to its 5' end, and the 5' residues of pgRNA then act as primer for (+) strand DNA synthesis. (B) The 5' residues of pgRNA translocate to pair with the DR2 site. (C) Initiation of (+) strand DNA (thick line) synthesis initiates at DR2 site and the elongation to the 5' end of (-) strand DNA takes place. The terminal redundant sequences are labeled as 5'r and 3'r. (D) The nascent (+) strand switches template, becoming complementarity to the 3'r site of (-) strand. (E) Elongation of (+) strand DNA synthesis generates rcDNA. (F) In situ priming of (+) strand DNA synthesis generates dslDNA.

1.1.3 *In vitro* HBV models and their applications

Being faster and more convenient than *in vivo* experiments, *in vitro* cell culture studies are useful to perform cellular analyses and high throughput screenings. HBV *in vitro* models comprise 1) primary human hepatocytes (PHHs), 2) differentiated HepaRG cells (dHepaRG), 3) hepatoma cell lines transfected or transduced with HBV DNA, and 4) hepatoma cell lines expressing the HBV entry receptor NTCP.

PHH is the first available and most physiologically relevant *in vitro* model to represent *in vivo* HBV infection [29]. PHHs are normal cells isolated from patients undergoing liver resection (usually for a hepatic tumor) [30]. Consequently, PHH supply is limited, and high donor-to-donor variability is commonly observed [31,

32]. PHHs do not usually divide after plating and have a limited lifespan (1-2 weeks) during *in vitro* culturing [29, 30, 33]. Moreover, PHHs rapidly dedifferentiate and lose their authentic hepatocyte function in culture, which results in a reduced susceptibility of HBV infection [33, 34]. Despite their limitations, PHHs presumably exhibit typical features of the natural host cells of HBV, such as hepatocyte polarization, the expression of hepatic host factors, and an intact innate immune system [35, 36]. Therefore, PHH is a valuable *in vitro* model, particularly for validating host factors associated with HBV infection [37] and for confirming the activity of antiviral compounds [38].

HepaRG cells are bipotent hepatic progenitor cells that maintain a high degree of morphological and functional features closely resembling that of hepatocytes, and can divide indefinitely [39]. Following several weeks of culturing with dimethyl sulfoxide (DMSO) and hydrocortisone supplementation, the bipotent progenitor cells can differentiate into both biliary-like and hepatocyte-like cells [39]. The differentiated hepatocyte-like cells are capable of supporting HBV infection, and the infection can persist for over 100 days [39]. However, two features of HBV replication cycle—the reimport of rcDNA into the nucleus (cccDNA amplification) [39] and cell-to-cell spreading of the virus [40] —were not observed in HBV-infected dHepaRG cells. Due to their ability to recapitulate the entire HBV replication cycle and exhibit a similar pattern of innate immune components to that of PHH, dHepaRG cells represent a practical *in vitro* model to investigate innate immune responses upon HBV infection. For example, administrating high-dose interferon-α (1000 IU/m) to HBV-infected dHepaRG cells induces the expression of a cytosine deaminase (APOBEC3A), which results in the cytosine deamination of cccDNA, subsequently leading to its degradation [38]. However, the dHepaRG infection model remains restrictive, primarily due to the stringent conditions necessary to maintain the differentiation state of the cells and the relatively low infection efficiency [39-41].

Immortalized hepatoma cell lines—such as HepG2 and Huh7 cells—are very convenient to work with in terms of the handling and genetic manipulation of their genomes; however, they are usually not permissive for HBV infection [41]. Notably, transfecting a plasmid-containing HBV genome into these cells can trigger all the transcriptional and post-transcriptional steps of the HBV replication cycle, including the viral replication as well as the formation of infectious viral particles [42-44]. Therefore, Huh7 cells were thereby employed to address several important issues of the HBV replication cycle, such as HBV encapsidation [24] and the transcriptional regulation of HBV cccDNA [45]. Additionally, due to the higher transfection efficiency compared to HepG2, Huh7 cells are used to produce recombinant HBV via the trans-complementation method [46, 47]. In contrast to

Huh7 cell line, HepG2 cell line can maintain a continuous HBV replication, as shown by HepG2-derived cell lines stably producing HBV (e.g. HepG2.2.15 and HepAD38 cells) [48, 49]. Therefore, HepG2.2.15 and HepAD38 cell lines serve as a source for the production of tissue culture-derived HBV [38]. Moreover, these stable cell lines are used as a platform for drug screening [50] and as a target for examining the cytotoxic activity mediated by engineered T cells against HBV [51].

The discovery of NTCP as an HBV entry receptor, which is not presented on the plasma membrane of hepatoma cells, has opened the door to establishing NTCP-expressing hepatoma cell lines that support authentic infection with HBV [13]. The exogenous expression of NTCP in hepatoma cell lines provides convenient infection models to screen for novel anti-HBV targets such as chemical compounds [52] or RNA interference (RNAi) [53]. Additionally, the HepG2-hNTCP cells infected with HBV can serve as an *in vitro* model to analyze the antiviral efficacy of HBV-specific $CD8^+$ T cells [54]. Despite the ease of using NTCP-expressing hepatoma cell lines to study HBV infection, the cell lines still have their limitations. First, a high multiplicity of infection (MOI) is required for being able to detect HBV infection (in the range of hundreds to thousands). Second, HBV infection in these cells does not result in substantial viral spreading compared to the *in vivo* context. Third, since the hepatoma cells are physiologically impaired in many intracellular pathways and functions. They carry chromosomal abnormalities and mutations, and they differ in gene expression and metabolic properties from PHH. In addition, some unrevealed factors essential for productive HBV infection are likely impaired or even missing in these cells.

1.2 Recombinant virus live cell reporter systems

Traditional diagnostic tools for virus infections, such as enzyme-linked immunosorbent assay (ELISA)-based assays for antigen detection and polymerase chain reaction (PCR)-based assays for viral genome detection, are time consuming and labor intensive. Moreover, these methods cannot distinguish infected cells from uninfected cells. Therefore, generating recombinant virus live cell reporter systems could greatly increase the ease of analyzing viral infections, thereby facilitating large-scale screening studies. The classical approach to creating a recombinant virus is to introduce the coding sequence of the reporters into the viral vector (genome) by direct insertion or replacement of a viral sequence with the reporter sequence. Upon establishing the infection of the recombinant virus carrying reporter sequence in the hosts, the reporter is expressed and can be detected in real-time. Fluorescent proteins and luciferases are the most common reporters utilized to monitor recombinant virus infection [55]. Additionally,

adapting Cre-lox recombination for reporting viral infection [56] or the magnetic sorting of infected cells based on a viral-delivered surface marker have been previously established [57]. These recombinant viruses could provide sensitive and convenient platforms for tracking viral infection and pathogenesis both *in vitro* and *in vivo*. Furthermore, recombinant virus live cell reporter systems serve as powerful tools for conducting screenings of anti-viral agents.

1.2.1 Fluorescence-based recombinant HBV reporter systems

Fluorescent proteins are light-emitting proteins that do not require any co-factor or substrate for their activation [58]. All fluorescent proteins have a similar 3D structure including a barrel-like arrangement consisting of eleven β-sheets surrounding a central α-helix. The α-helix contains the fluorescent center, the chromophore forming-tripeptide [59]. Genetic manipulation of the tripeptide sequence gives rise to variations in spectral characteristics [59, 60]. Green fluorescent protein (GFP) and its variants, including blue fluorescent protein (BFP), cyan fluorescent protein (CFP), and yellow fluorescent protein (YFP), cover the visible spectrum ranges from blue to yellow, whereas the red fluorescent protein (DsRed) and its variants cover the visible spectrum ranges from orange to far-red [59, 61-64]. Fluorescent proteins are widely used for noninvasively visualizing cellular events in cells, especially as markers to track proteins, monitor gene expression, and describe intracellular signal pathways [58, 65]. Additionally, utilizing fluorescent proteins is a common approach for monitoring *in vitro* and *in vivo* viral infection. Instead of detecting infected cells by labeling viral proteins with fluorophore-conjugated antibodies, a recombinant virus encoding fluorescent protein sequence enables the direct visualization of infection using fluorescence microscopy. Furthermore, it allows to direct quantify the frequency of infected cells using fluorescence activated cell sorting (FACS) or fluorescence microplate readers. However, several issues may be encountered when using fluorescent proteins as indicators for viral infection. First, the overexpression of fluorescent proteins in cells—especially the red fluorescent proteins—often induces cell death [66]. Moreover, fluorescence excitation requires a light or laser source, which can also induce phototoxic effects in cells [67]. Second, high levels of cell autofluorescence significantly reduce the signal-to-background ratio, resulting in low fluorescence detection sensitivity [68]. Third, although FACS is one of the most widely used cell isolation platforms, limitations such as high equipment costs, high operation complexity, and limited throughput for direct separation of rare cells hinder the usage of FACS systems to isolate cells [69].

Various recombinant HBV systems carrying the coding sequence of fluorescent proteins have been developed over the past two decades. The first was generated by Protzer et al. using a 1.1-fold wtHBV vector as a template and replacing the HBV small envelope gene with the GFP coding sequence [46]. The production of the recombinant virus (rHBV-GFP) was achieved in a trans-complement manner by expressing the rHBV genome from the rHBV vector and all the viral proteins from a helper construct in Huh7 cells. GFP signal was observed in PHHs infected with the rHBV-GFP. However, a reduced signal-to-background ratio was observed in infected samples due to the high autofluorescence of hepatocytes. The same group reported a modified version of rHBV-GFP by exchanging the PreS/S promoter with mouse transthyretin (TTR) enhancer/promoter since it was proven to exhibit higher transcriptional activity compared to the endogenous HBV promoter in the hepatoma cell lines [55]. Moreover, this study indicated that the use of TTR enhancer/promoter does not affect the replication of the recombinant virus. Moreover, a replication-competent rHBV-GFP vector was also created [70]. In this vector, the GFP sequence—flanked by internal ribosome entry sites (IRES)—together with the N-terminal part of polymerase ORF—an overlapping sequence with the C-terminal part of the core protein—was inserted after the core ORF. This recombinant HBV can be produced *in cis* by transfecting the rHBV vector in hepatoma cell lines without a helper construct to express viral proteins. However, the author observed a significant reduction in replication efficiency due to the genome of the replication-competent rHBV-GFP (3.9 kbp) being much longer than that of wtHBV (3.2 kbp). Although several fluorescence-based HBV recombinants have been available for many years, no follow-up studies using these rHBV have been reported. This is likely due to the restrictions of the rHBV reporter system, such as low virus yield, low infection rate, and low fluorescent signal in infected cells, which impede the use of fluorescence-based recombinant HBV.

1.2.2 Bioluminescence-based recombinant HBV reporter systems

Luciferases are enzymes that catalyze specific substrates and produce light (bioluminescence) [71]. Luciferin-dependent and coelenterazine-dependent luciferases are two common bioluminescence systems. Firefly luciferase (FLuc) is the most widely known luciferase, which uses D-luciferin as its substrate and requires ATP and Mg^{2+} as cofactors [71]. *Renilla* luciferase (RLuc) and *Gaussia* luciferase (GLuc) are luciferases derived from marine organisms. These are ATP-independent luciferases, using coelenterazine as their substrate [71, 72]. Furthermore, NanoLuc (NLuc) is an artificial luciferase (19 kDa) developed from the catalytic subunit of the luciferase derived from *Oplophorus gracilirostris*, and it utilizes furimazine (a coelenterazine derivative) as its substrate [73]. The

extremely low autoluminescent level in tissues results in superior signal-to-background ratio. Therefore, the sensitivity of bioluminescence is much higher than that of fluorescence [68]. Bioluminescence is especially useful for *in vivo* imaging and high-throughput drug screenings based on biological events, such as protein−protein interactions, protein stability, gene regulation, and cell signaling [68, 74]. However, it is not suitable for performing studies at the single-molecular level since detected bioluminescence is an indirect signal derived from the chemical reaction of luciferase and the substrate.

Recombinant viruses encoding luciferase genes have been used to study the early steps of viral infection *in vitro* or to monitor the virus spread *in vivo* [75, 76]. Untergasser and Protzer generated the first recombinant HBV encoding RLuc by replacing the HBV small envelope gene with the RLuc coding sequence in the rHBV vector [55]. In this study, the RLuc activity was elevated 200- to 300-fold in rHBV-infected cells compared to uninfected cells. Moreover, a recent study generated a different type of luciferase-based recombinant HBV that encodes NLuc (named HBV/NL) [77]. Instead of using the HBV small envelope coding region in the rHBV vector, the HBV core region was replaced by the NLuc sequence, and rHBV cccDNA molecules were observed in Huh7-NTCP cells upon HBV/NL infection. Additionally, the kinetic of NLuc activity corresponded to that of HBV RNA expression in HBV/NL-infected cells, whereas HBV rcDNA levels remained unchanged over time due to the replication deficiency of this recombinant HBV. Nevertheless, using their HBV/NL in combination with an RNAi screening, Nishitsuji et al. investigated several host factors that play a role in the early stages of the HBV life cycle [77].

1.2.3 Magnetic-activated cell sorting (MACS)-based isolation systems for virus-infected cells

The MACS system is a biochemical affinity-based cell separation platform, where a magnetic cell separation device is utilized to isolate target cells labeled with magnetic beads [78]. The labeling of target cells with magnetic beads is mediated by an antigen-antibody interaction; the magnetic micro- or nanoparticles are conjugated to antibodies specific to particular cell surface antigens, and the beads can thereby bind to target cells displaying the antigen of interest [69]. The advantages of magnetic cell sorting include: good selectivity, good specificity, high throughput, and convenient integration with other separation methods [69]. The robust antibody–antigen binding between the cells and magnetic particles gives rise to this strong selectivity. Moreover, using magnetic force as the retaining force provides a good contrast between magnetic bead-labeled and non-labeled cells in terms of surface attachment to the magnetic column. In addition, magnetic cell

enrichment devices are capable of processing up to 2×10^{10} cells within 5-30 minutes. Finally, the MACS separation platform can be easily integrated with other separation methods, such as FACS.

MACS has been widely used for isolating the lentiviral or retroviral transduced cells for downstream analyses or applications [79, 80]. The most common procedure is to include the coding sequence of the surface markers, such as human low affinity nerve growth factor receptor (LNGFR) or CD4, to the lentiviral or retroviral vectors. This enables lentiviral or retroviral transduced cells to co-express transgenes and these surface markers. Based on the surface markers displayed on transduced cells, target cells can subsequently be labeled by magnetic beads coupled with the antibodies recognizing these markers for magnetic cell sorting. Besides being a common tool for isolating transduced cells expressing desired transgenes, MACS can also be utilized to isolate virus-replicating cells. The magnetic separation of virus-replicating cells can be achieved by using magnetic beads coupled with antibodies against endogenous viral proteins or against an exogenous surface marker that is encoded by the recombinant virus. Martínez et al. developed a magnetic cell sorting procedure based on the F protein and G protein of human respiratory syncytial virus (HRSV) for isolating the HRSV-positive cells [81]. This approach allowed the researchers to obtain a homogenous population of HRSV-positive cells, which was employed to study the fate of the persistently HRSV-infected cells. In another study, MACS-based isolation of latently HIV-infected hematopoietic progenitor cells (HPCs) was reported. In that study, a recombinant HIV strain (named HXB-ePLAP) carrying a cell surface marker (human placental alkaline phosphatase gene, PLAP) was generated. Upon infection of HPCs with HXB-ePLAP, the actively HIV-infected cells were removed by MACS using a biotin-conjugated PLAP-specific antibody and anti-biotin magnetic beads [57].

1.2.4 Cre-based recombinant virus reporter systems

Cre recombinase (Cre, Causes recombination) is a protein derived from bacteriophage P1 that recognizes a specific 34-bp DNA sequence (the loxp site) [82]. The loxp site contains an 8-bp spacer region flanked by two identical 13-bp palindromic sequences of recombinase-binding elements (RBEs) [83, 84]. When Cre binds to an RBE in the loxP site (named Cre-loxP synapsis), it mediates the site-specific intra- or inter-strand exchange of DNA molecules [85]. Additionally, depending on the orientation of the loxP sites, the DNA segment is either excised or inverted by Cre [85]. The combination of Cre with a Cre-regulated reporter construct (usually fluorescent or bioluminescent reporters) provides the means for heritable labeling of a target cell type, which has enabled *in vitro* and *in vivo*

investigations of cell fate [84]. The major limitation of the Cre-lox recombination system is that the loxp sites must first be introduced into the genome of target cells. The integration of exogenous DNA into a host genome is relatively inefficient in most cell types, and many colonies must be examined to select a clone with a high copy number (activity) of exogenously provided DNA that still maintains the same characteristics as the parental cells. Recently, Cre recombinase was further developed into a "split Cre" approach, where two Cre fragments must be assembled to form an active enzyme in order to achieve temporal regulation of recombinase activity; this approach involves: 1) splitting Cre into two inactive polypeptide chains, 2) expressing these fragments from two individual promoters, and 3) allowing the assembly of active Cre in cells where the transcription of both promoters take place [84, 86].

This system has been adapted for virus-host interaction studies *in vivo* by engineering a virus to carry the Cre coding sequence and the host cells to harbor a Cre-regulated reporter construct. Influenza A virus (IAV) expressing Cre recombinase was applied to transgenic Cre reporter mice to study the long-term fate and transcriptional profile of virus-infected cells within the lungs [87]. Murine gammaherpesvirus 68 (MHV-68), which is closely related to Epstein-Barr virus (EBV) and Kaposi's sarcoma-associated herpes virus (KSHV), was engineered to express Cre recombinase upon infection [88]. Although the virus titer produced from Cre-encoding MHV-68 was ten-fold lower than that of the wild-type virus, the lymphoid sites infected by Cre-encoding MHV-68 could be identified on the basis of EGFP expression in mice containing a Cre-activated EGFP. Additionally, individual MHV-68 infected cells with a high level of EGFP expression following virus-induced Cre-lox recombination could be isolated by FACS [88]. To study HCV infection in mouse cells that do not support robust HCV replication, a bicistronic HCV genome expressing Cre recombinase (named HCV-CRE) was used instead of a firefly luciferase-encoding HCV genome, which did not yield sufficient bioluminescent signal above background in mouse [56]. By transducing human factors, including tetraspanin CD81, scavenger receptor type B class I (SCARB1), claudin 1 (CLDN1), and occludin (OCLN) into fully immunocompetent mice allowed infection of HCV-CRE to occur in the hepatocytes. Moreover, the study demonstrated that HCV-CRE can be blocked by passive immunization and that the system can be used to evaluate vaccines against multiple HCV genotypes *in vivo*.

1.3 Aim of the study

Recombinant virus reporter systems can serve as a robust and convenient platform for monitoring viral infection both *in vitro* and *in vivo*. However, such a platform is not commonly used for detecting HBV infection to date.

Several drawbacks, such as difficulty in isolating HBV-infected hepatocyte, inefficient production of rHBV due to poor replication, or the unstable expression of reporter genes upon rHBV infection hinder the use of a recombinant HBV reporter system to address scientific questions or conduct large-scale screenings. For rare viral infection events, acquiring an enriched population of infected cells could strongly benefit downstream analyses. However, isolating HBV-infected cells by routinely-used FACS is not a feasible approach, as hepatocytes are known to exhibit high autofluorescence and become easily damaged in suspension during prolonged incubation periods. Therefore, a more rapid isolation procedure based on magnetic separation—such as MACS—could represent a potential solution to circumvent these limitations. Several features of HBV result in the low and unstable expression of transgenes in infected cells, thereby causing difficult and impractical reporter detection. Firstly, HBV infection is a relatively inefficient process *in vitro*, and requires extremely high MOI compared to other viruses (e.g., adenovirus). Additionally, replication of recombinant HBV was even poorer in virus-producing cell lines, resulting in lower yields compared to the wild-type HBV. Finally, HBV persistent form cccDNA remains as an episomal molecule in the nuclei of infected cells. Furthermore, cccDNA serves as a template for reporter gene transcription; however, it does not replicate as the cell does. Therefore, reporter signal is gradually lost when rHBV-infected cells divide. Notably, using a genome-editing approach such as Cre-lox recombination could overcome such issues. Since the activation of a reporter gene via genome-editing is a one-time event, even the scarce amount of genome-editing enzyme delivered by a recombinant virus is sufficient for the process to occur. Moreover, Cre-regulated reporter genes are typically integrated in the host genome; therefore, the reporter expression is permanent and inheritable, and thus independent of cccDNA presences in cells.

The aim of the present study was to establish two novel recombinant HBV reporter systems based on: 1) a rHBV encoding LNGFR sequence (rHBV-LNGFR) that could allow convenient magnetic isolation of infected cells via LNGFR, and 2) two rHBV encoding Cre recombinase sequences (rHBV-Cre revenant and rHBV-CreN) that could allow a permanent Cre-dependent expression of reporter genes upon infection. Both of these reporter systems are composed of recombinant HBV and consequent isolation or detection procedures. In order to achieve this goal, several steps must be taken. Firstly, recombinant HBV must be produced and

characterized. Next, the isolation procedure for magnetic sorting of hepatoma cells or the Cre reporter cell line must be established. Finally, the integrity of this system for future applications must be proven in routinely-used hepatoma cell lines expressing NTCP, which is permissive for HBV infection.

2 Results

This section is divided into two subsections, each describing a different type of rHBV reporter system. The rHBV-LNGFR reporter system is described first, which is a system facilitating the transient expression of a surface marker upon infection. Additionally, it allows infected cells to be isolated by magnetic-activated cell sorting. Secondly, two rHBV-Cre reporter systems are described, which are a system that utilizes Cre-lox recombination to edit the host genome, thereby permanently expressing reporter genes upon infection.

2.1 Establishment of rHBV-LNGFR reporter system

Fluorescent protein and luciferase are the most frequently used reporters, which enable hosts to be easily isolated or monitored upon infection with reporter viruses [47]. This work presents a novel strategy for a rHBV reporter system that uses an alternative reporter gene: the truncated LNGFR. The LNGFR coding sequence is delivered via recombinant HBV (rHBV-LNGFR) into the nuclei of host cells. Following the establishment of rHBV-LNGFR cccDNA, the LNGFR will be expressed and displayed on the cell surface. This enables the labeling of infected cells by LNGFR-specific magnetic MicroBeads and the isolation of labeled cells by magnetic separation (Figure 6). The potential for using magnetic separation to isolate infected cells provides a platform that allows cell handling under BSL 2/3 conditions at low cost, requires less time to perform, and easily integrates with other separation methods (such as FACS) [69].

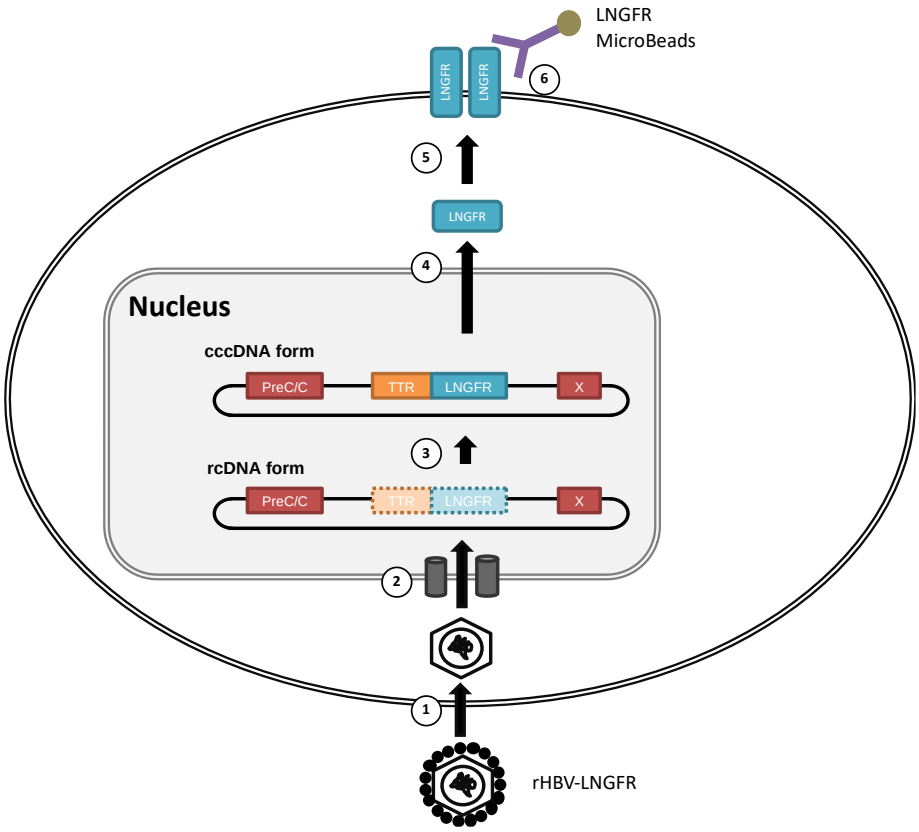

Figure 6: The rHBV-LNGFR reporter system

Step 1, rHBV-LNGFR enters the host cells. Steps 2-3, the rcDNA form of rHBV-LNGFR is delivered into the nucleus and converted into a cccDNA-like structure. Step 4, LNGFR is expressed by using rHBV-LNGFR cccDNA as a transcriptional template. Step 5, LNGFR is transported and displayed on the cell surface. Step 6, LNGFR-expressing cells can be labeled by LNGFR-specific MicroBeads.

2.1.1 Hepatoma cells isolation by magnetic-activated cell sorting (MACS)

First, the magnetic sorting procedure of LNGFR-expressing hepatoma cells was established. HepG2-NTCP cells were transfected with a plasmid expressing LNGFR. Cells were harvested on day 3 post-transfection by trypsin-versene treatment. The cell suspension was divided into two groups: one group was directly stained with anti-LNGFR-PerCP-Cy5.5 antibody, while the other was incubated with LNGFR-specific MicroBeads. The MicroBead-labeled cells were loaded onto a magnetic column, and magnetic separation was then performed by a MidiMACS separator. Flow-through and bound fractions were collected and analyzed by flow cytometry using the MACSelect Control FITC antibody that recognizes the MicroBeads. The frequency of MicroBead-positive cells (Figure 7B) was similar to that of LNGFR-positive cells detected by the anti-LNGFR antibody (Figure 7A). This indicates that the affinity of LNGFR-specific MicroBeads towards LNGFR is comparable to the regular antibody (anti-LNGFR), and that the interaction between antigen and antibody was not hindered by the magnetic beads that are coupled to the antibody. Approximately 7% of MicroBead-positive cells remained in the flow-through

fraction following magnetic separation (Figure 7C). In the bound fraction, 65% of cells were MicroBead-positive (Figure 7D). The affinity of the MicroBeads-labeled cells to the magnetic column was rather stable, since positive cells in the flow-through fraction constituted < 10% of labeled cells. However, approximately 35% of cells remained LNGFR MicroBead-negative among the bound fraction, indicating sub-optimal isolation of positive cells from the sample.

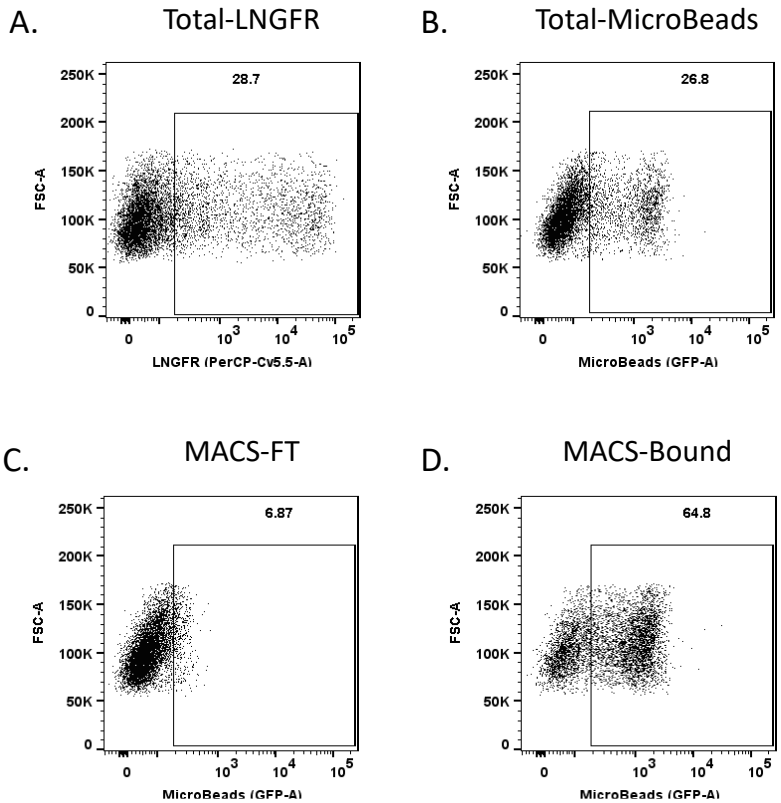

Figure 7: Isolation of LNGFR-expressing cells via MACS

HepG2-NTCP cells were transfected with LNGFR plasmid. The transfected cells were collected after 72 hours. A portion of these cells was stained with anti-LNGFR-PerCP/Cy5.5 antibody (A). The remaining portion of cells was incubated with LNGFR-specific MicroBeads and underwent magnetic separation. The MicroBead-labeled cell (B) flow-through fraction (C) and bound fraction (D) were stained with MACSelect Control FITC antibodies. The frequency of fluorescent-positive cells was determined by flow cytometry. The gates for LNGFR-positive and MicroBead-positive were set on the basis of the fluorescence intensity of cells stained with mouse IgG-PerCP/Cy5.5.

Next, the expansion of MACS-isolated cells was assessed. Four groups of cells were seeded on a collagen-coated tissue culture plate with the same number of cells: the LNGFR-transfected cells, the transfected cells incubated with LNGFR-specific MicroBeads, the flow-through fraction of magnetic-separated cells, and the bound fraction of magnetic-separated cells. Cell viability was analyzed on days 2 and 8 post-seeding. Transfected cells incubated with MicroBeads and cells obtained from the bound fraction presented four times fewer viable cells (Figure 8A), as well as less cell metabolic activity (Figure 8B) compared to MicroBead-free controls on day 2. However, the difference in cell viability between the MicroBead-associated

groups and MicroBead-free groups was reduced to two folds on day 8 post-seeding. This result suggests that the MicroBeads affect cell expansion at an early time point, though their influence decreases when cells are cultured for a longer period.

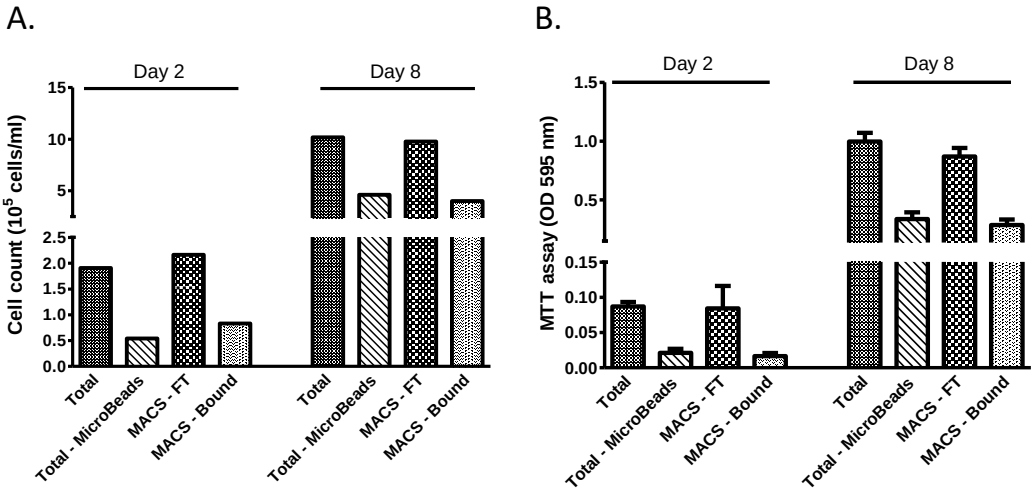

Figure 8: Proliferation of MACS-isolated HepG2-NTCP cells

HepG2-NTCP cells transfected with a LNGFR plasmid were collected on day 3 post-transfection. The transfected cells (Total), MicroBead-labeled cells (Total - MicroBeads), and cells collected from the flow-through fraction (MACS - FT) as well as the bound fraction (MACS – Bound) after magnetic separation were seeded in a collagen-coated 96-well plate. After incubating the cells at 37 °C for 2 and 8 days, cell viability was analyzed by (A) direct cell counting and (B) MTT assay.

Since the purity of LNGFR-expressing cells via the MACS procedure was not ideal, as indicated by approximately 35% MicroBead-negative cells being present in the MACS bound fraction (Figure 7D), an additional FACS step was tested after magnetic separation by using MACSelect Control FITC antibodies. Compared to using magnetic separation alone, the combination of the MACS with the FACS procedure could further enrich the LNGFR MicroBead-positive population in the FACS-purified sample by up to 90 % (Figure 9), suggesting that FACS sorting represents a more effective approach to purifying LNGFR-expressing hepatoma cells.

Combined, the available data indicates that hepatoma cells expressing LNGFR can be purified via a two-step process: by magnetic separation using LNGFR-MicroBeads and subsequent FACS analysis, leading to significant enrichment of LNGFR-positive cells following isolation.

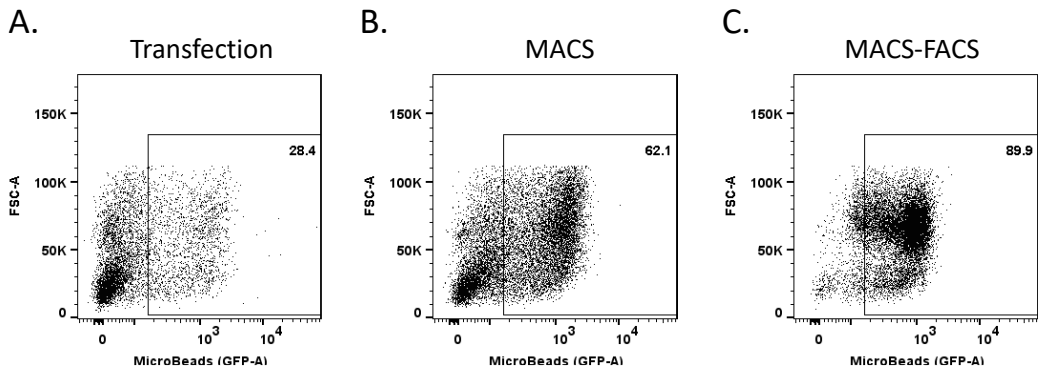

Figure 9: Enrichment procedures for LNGFR-expressing cells
Transfected HepG2-NTCP cells were incubated with LNGFR-specific MicroBeads. An aliquot of labeled cells was used as the control sample (A). Labeled cells were then subjected to magnetic separation, and an aliquot of the bound fraction was taken as the MACS sample (B). The binding fraction was further stained with MACSelect Control FITC antibodies and sorted by flow cytometry (C). The gate for MicroBead-positive was set on the basis of the fluorescence intensity of mock cells.

2.1.2 Production of rHBV-LNGFR

The rHBV-LNGFR transfer plasmid was generated by replacing the PreS/S region of the 1.1-fold wtHBV plasmid (pCH-9/3091) with the TTR promoter/enhancer and LNGFR coding sequence (Figure 10).

rHBV-LNGFR production was performed in a trans-complementation manner [46]. In contrast to the wtHBV production method, in which all viral components required for infectious virus production are derived from a single DNA template, two plasmids are required for recombinant HBV production. The first plasmid, rHBV transfer plasmid, is designed to express rHBV pgRNA and core protein. The second plasmid, an HBV helper plasmid, provides essential proteins for virus assembly. The polymerase plasmid encodes the polymerase and the surface proteins, whereas the helper plasmid encodes all viral proteins (HBc, polymerase, surface proteins, and HBx). The rHBV transfer plasmid and HBV helper plasmid were co-transfected into Huh7 cells. The cells and supernatant were harvested 7 days later.

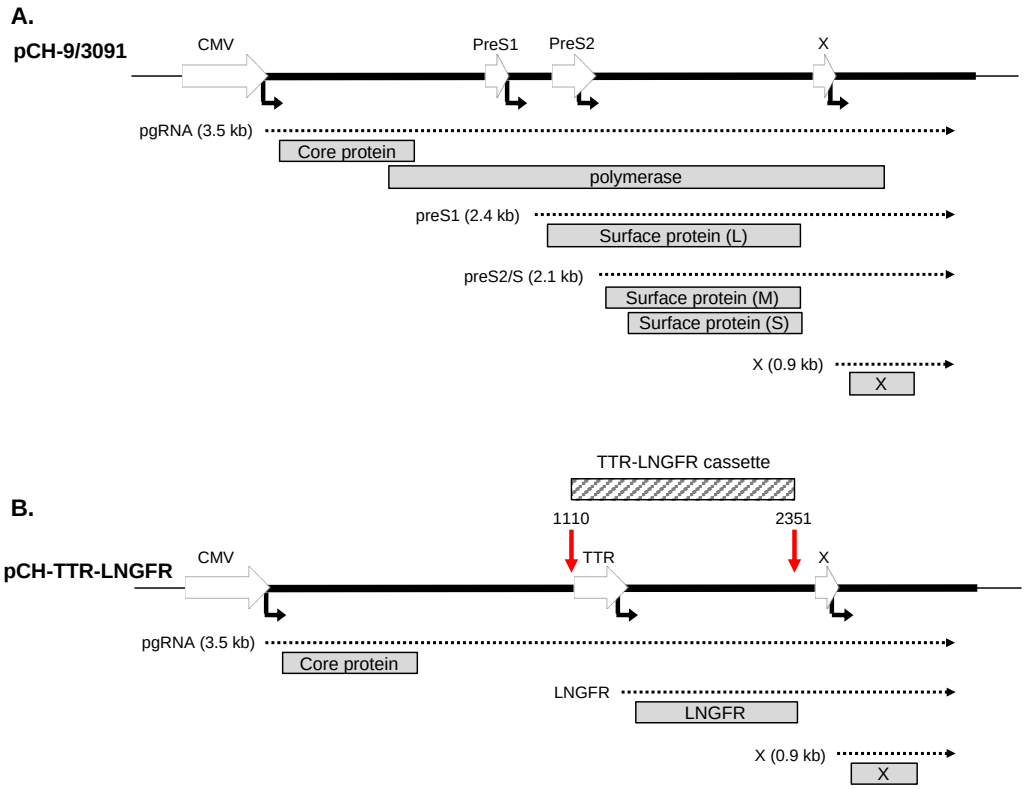

Figure 10: 1.1-fold wtHBV plasmid (pCH-9/3091) and rHBV-LNGFR transfer plasmid (pCH-TTR-LNGFR)

The 1.1-fold wtHBV plasmid (A) contains the terminally redundant HBV genome (thick black lines). This terminally redundant HBV genome is driven by the CMV promoter and mimics the scenario of the pgRNA expression from cccDNA. The plasmid contains four promoters (block arrows), which regulate the transcription of pgRNA, preS1, preS2/S, and X (dashed arrows), respectively. Both the HBV core protein and the polymerase are derived from pgRNA, while the large surface protein is derived from preS1 RNA, medium and small surface proteins are derived from preS2/S RNA, and the HBx protein is derived from X RNA. The rHBV-LNGFR transfer plasmid (B) was obtained by replacing the wtHBV fragment (in pCH-9/3091, position 1110 to 2351) with the TTR-LNGFR cassette (striped rectangles). pgRNA, LNGFR transcript, and X transcript are driven by CMV, TTR, and X promoter, respectively. HBV core protein, LNGFR, and HBx protein are expressed from the plasmid. Since the coding sequences of the polymerase and surface proteins are disrupted by the TTR-LNGFR cassette, these proteins are not expressed from the rHBV-LNGFR transfer plasmid. Transcription start sites are indicated by the attached black arrows. Proteins are indicated by grey boxes.

The viral capsids in cells and viral particles in the supernatant were concentrated by polyethylene glycol (PEG) precipitation. Following DNA extraction from the pellets, the viral genome was analyzed by Southern blot. A positive control was prepared using the cell lysate and supernatant of Huh7 cells transfected with a 1.1-fold wtHBV plasmid (pCH-9/3091). Two bands above 3.2-kb HBV DNA marker were detected on the blot using the cell lysate of wtHBV-producing cells (Figure 11A, Lane 6). Two types of HBV genome, the rcDNA and the dslDNA, could be observed in the capsids and viral particles. The size of both rcDNA and dslDNA was approximately 3.2 kb. Since the electrophoretic mobility of rcDNA is lower than

that of dslDNA, it is usually located slightly above the 3.2-kb HBV DNA marker. Typically, dslDNA migrates to the same position of the 3.2-kb HBV DNA marker, or slightly below it. However, due to the agarose gel preparation and electrophoresis conditions, the position of rcDNA and dslDNA varied between experiments.

To confirm the identity of rcDNA, the digestion of DNA samples with XhoI was used as an alternative method. Since the HBV genome contains one XhoI restriction site at the PreS region, the digestion of rcDNA results in a 3.2-kb linear DNA, whereas digested dslDNA becomes two shorter DNA fragments. Upon visualizing the XhoI-treated DNA sample on the blot, the cut rcDNA migrated to the location of 3.2-kb HBV DNA marker, while the cut dslDNA migrated downwards. As expected, two bands above 3.2 kb shifted in the positive control sample digested with XhoI (Figure 11A, Lane 7), indicating that these bands corresponded to the rcDNA form. No HBV DNA signal was detected in Huh7 cells transfected with rHBV-LNGFR transfer plasmid alone (Figure 11A, Lane 1). Since the coding sequences of the polymerase and surface proteins are disrupted by the TTR-LNGFR cassette, the rHBV-LNGFR transfer plasmid becomes replication-defective and thereby unable to produce rHBV-LNGFR DNA. One predominant band below the 3.2-kb marker and one faint band above the 3.2-bp marker were observed in the DNA sample from cells co-transfected with rHBV-LNGFR transfer plasmid and the polymerase plasmid (Figure 11A, Lane 2). The faint band was not detected in the XhoI-treated sample (Figure 11A, Lane 3). This suggests that a low level of rHBV-LNGFR rcDNA was present. However, in the sample of cells co-transfected with rHBV-LNGFR transfer plasmid and the helper plasmid, only rHBV-LNGFR dslDNA was detected (Figure 11A, Lane 4). The overall signal of HBV DNA in the cells co-transfected with rHBV transfer plasmid and the helper plasmid (Figure 11A, Lane 4) was weaker than that of cells co-transfected with rHBV transfer plasmid and polymerase plasmid (Figure 11A, Lane 2). This implies that the replication efficiency of rHBV-LNGFR might improve with the use of the polymerase plasmid. In the supernatants of co-transfected cells, neither rHBV-LNGFR dslDNA nor the rcDNA was detected (Figure 11B, Lanes 2 and 4). A predominant band above the 3.2-kb marker was observed among the samples from cells transfected with the rHBV-LNGFR transfer plasmid. Since the band was also higher than the location of the wtHBV rcDNA band (Figure 11B, Lane 6), it presumably corresponded to the remaining plasmids in the supernatants.

In summary, although the virion-associated genome of rHBV-LNGFR was not detectable in the supernatant samples, the replication of rHBV-LNGFR took place intracellularly using the trans-complement virus production method.

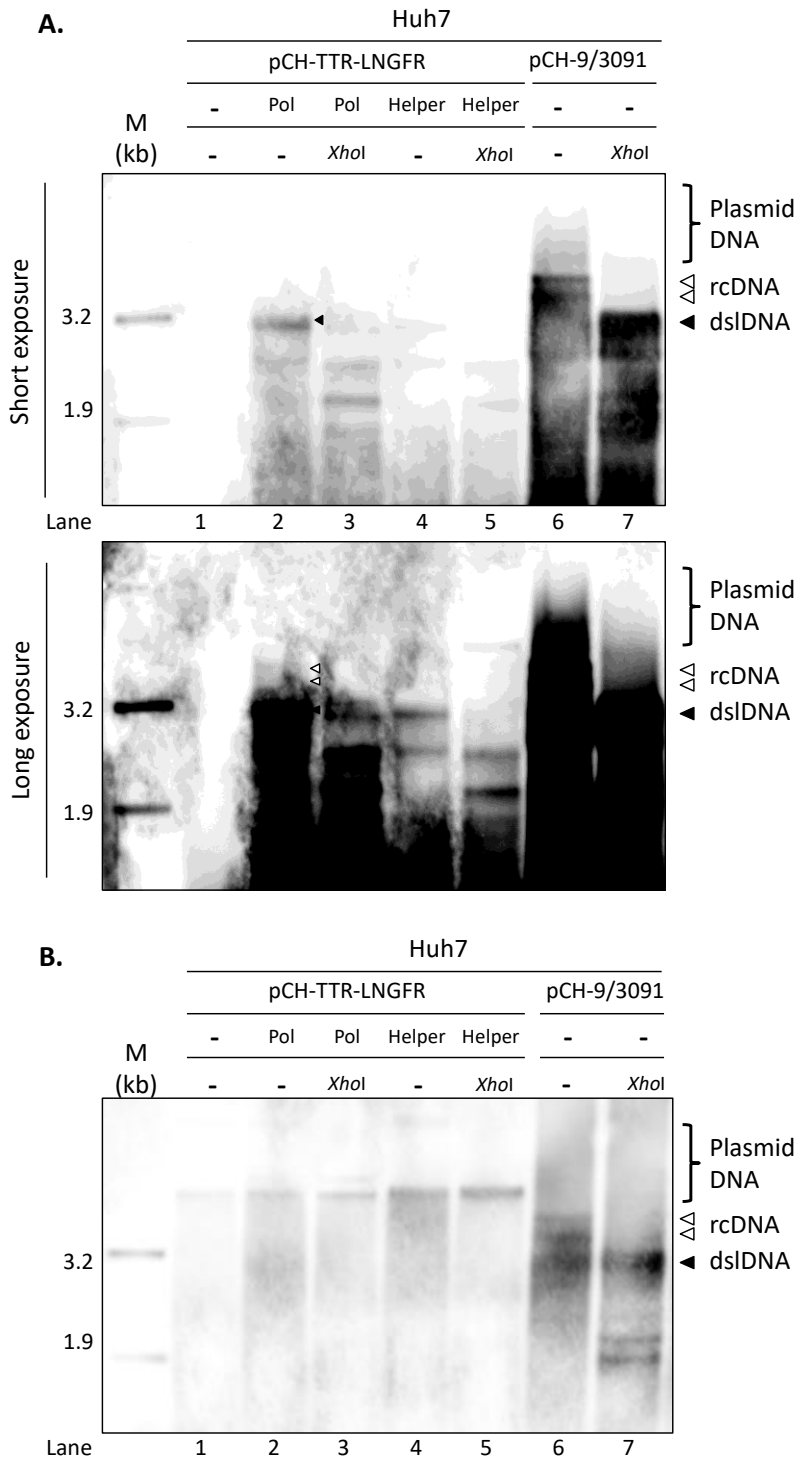

Figure 11: Genome structure of rHBV-LNGFR

Huh7 cells were transfected with rHBV-LNGFR transfer plasmid (pCH-TTR-LNGFR) and an HBV helper plasmid (Pol or Helper). DNA extracted from capsids in the cells (A) and virus in the supernatant (B) were analyzed by Southern blot. DNA species were further confirmed by digesting the DNA sample with XhoI, which linearized the circular DNA. Open triangles indicate the RC form of rHBV DNA. Filled triangles indicate the DSL form of HBV DNA.

2.2 Establishment of rHBV-Cre reporter systems

The reporter gene carried by a recombinant reporter HBV is expressed from the cccDNA template. Thus, its expression relies on the number and stability of the cccDNA. Since cccDNA is an episomal minichromosome that is not integrated into the host genome, the expression of transgenes will be transient. To overcome this issue, an alternative measure of infection reporting involves leaving a permanent mark via genome editing in the host genome upon infection. In this regard, we developed two rHBV-Cre reporter systems: rHBV-Cre revenant and rHBV-CreN. In both systems, the Cre gene is delivered into the Cre reporter hepatoma cells following the route of wtHBV infection. The Cre reporter cells harbor the DsRed coding sequence, which is transcriptionally deactivated by the loxp-stop-loxp cassette prior to the sequence. The cassette can be removed via Cre-lox recombination, and this subsequently leads to the expression of the DsRed gene. Infected cells can therefore be detected by measuring their fluorescence intensity (Figure 12).

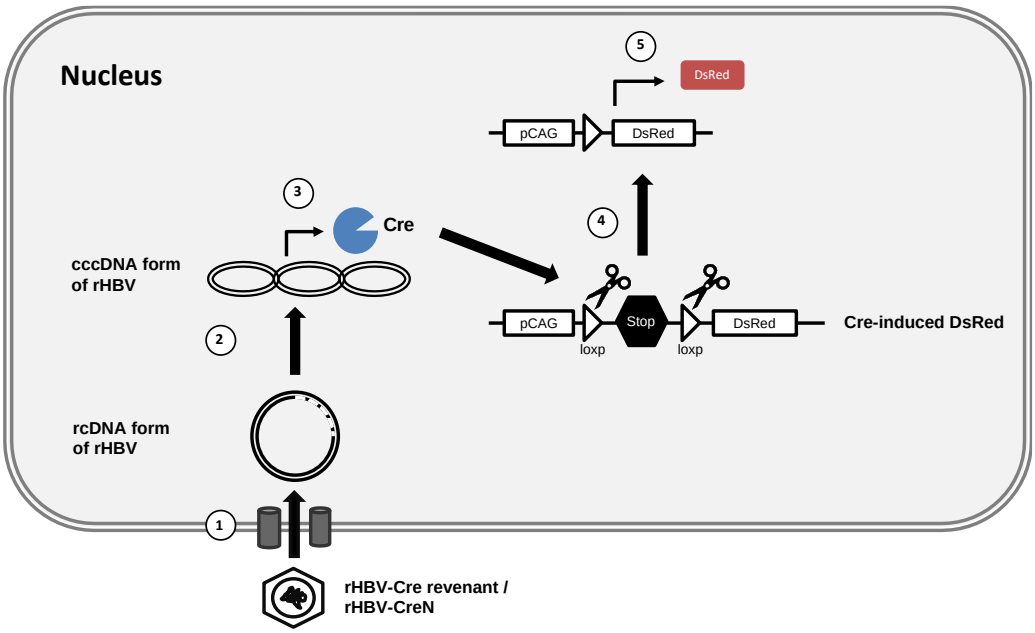

Figure 12: Activation of the DsRed gene via Cre-lox recombination upon rHBV infection
Step 1, rHBV genome carrying the Cre coding sequence is imported into the nucleus of host cells upon rHBV infection. Step 2, the rHBV genome (rcDNA) is converted into a covalently closed circular DNA by host factors. Step 3, the Cre gene is transcribed using cccDNA as its template. Step 4, the loxp-stop-loxp cassette is removed by Cre recombinase. Step 5, DsRed expression is then activated.

2.2.1 Production of rHBV-Cre revenant

The coding sequence of Cre recombinase is greater than 1 kb; therefore, it is not feasible to exchange it with any HBV sequence without resulting in an oversized rHBV genome. Previous studies in our lab have demonstrated that an oversized rHBV genome leads to the inefficient production of recombinant HBV [55]. Moreover, a reporter gene cassette within the rHBV transfer plasmid will be constantly expressed in virus-producing cells. As shown in Section 2.1.2, expression of the reporter gene might have a negative impact on virus-producing cells, thereby inhibiting virus production. Furthermore, expression of the reporter gene can be derived not only from the rHBV cccDNA, but also from the dslDNA genome of the rHBV using an alternative (though sub-optimal) polyA site upstream of the original HBV polyA site.

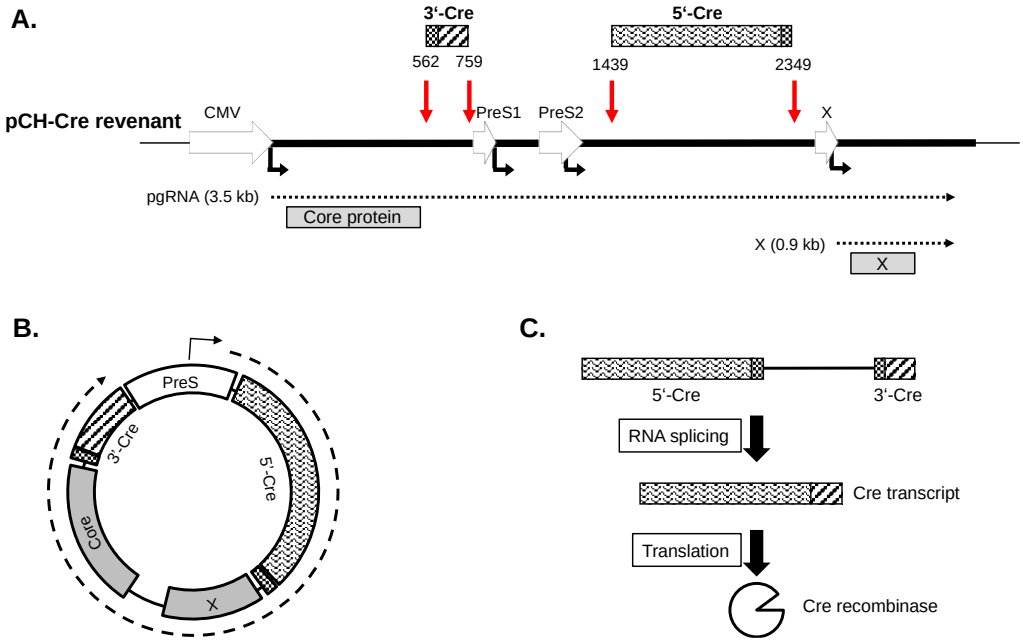

Figure 13: rHBV-Cre revenant transfer plasmid and Cre expression upon circularization
(A) The 3'-Cre (diagonal stripes) was placed after the core protein coding region and before the PreS promoter region. The 5'-Cre (zigzag) was placed between the S region and the X region. Block arrows indicate the promoter or enhancer. Dashed arrows indicate the transcripts. Grey boxes indicate the proteins. (B) Upon circularization, the Cre sequence will be positioned in the correct orientation. The transcription of Cre (dashed line) will be driven by the PreS1 promoter (white box). (C) The long transcript, including the additional HBV sequence between the two Cre fragments, will be spliced out and Cre recombinase will then be translated from the shorter mRNA.

In order to minimize the aforementioned issues, the Cre coding sequence was designed in a way that divided the Cre into two parts (5' Cre and 3' Cre), which were placed in two separate regions of the rHBV genome in a reverse orientation (Figure 13A). The coding region of the small surface protein was replaced by 5' Cre with a splicing donor sequence. The HBV sequence after the core protein coding region and before the PreS1 region was removed. The 3' Cre and a splicing

acceptor sequence were then inserted into this region. This design allows Cre recombinase to be derived solely from the circular form of the rHBV genome (rHBV cccDNA). Upon the establishment of rHBV-Cre revenant cccDNA, Cre expression will be initiated from the PreS1/PreS2 promoters (Figure 13B). RNA polymerase can read through the X and core coding region, and will terminated after 3' Cre region. The segment between 5' Cre and 3' Cre will be removed by RNA splicing and result in the generation of functional Cre recombinase (Figure 13C). In contrast, RNA synthesis using the double-stranded linear form of the rHBV genome (e.g., dslDNA) will be terminated after the X coding region. The transcript cannot be produced as a functional Cre recombinase due to the missing 3' Cre sequence.

The cloning of rHBV-Cre revenant cassette was achieved by assembling three rHBV fragments and two Cre fragments via bacterial artificial chromosome (BAC) recombination. Virus production and genome analysis were performed in a similar manner as described in 2.1.2. Similar to the previous result (Figure 11A, Lane 6), two bands corresponding to wtHBV rcDNA and dslDNA were detected from the DNA sample of capsids derived from wtHBV plasmid-transfected Huh7 cells (Figure 14A, Lane 4). Moreover, an additional predominant band that migrated further than dslDNA was observed. In addition to using the XhoI-digested sample to define the location of rcDNA on the blot (Figure 14A, Lane 5), treating DNA sample with heat (85-95°C) can be used to define the location of HBV single-stranded DNA (ssDNA). This is possible because double-stranded DNA (rcDNA and dslDNA) can be denatured under high temperature, while immediately cooling the sample afterward can prevent the re-annealing of ssDNA. As presented on the blot, the bands referring to rcDNA and dslDNA disappeared in the 95°C-treated sample (Figure 14A, Lane 6). Instead, a band of lower molecular weight was detected. Both the RC and DSL form of rHBV-Cre revenant DNA was presented in the capsids (Figure 14A, Lane 2), indicating that the replication of rHBV-Cre revenant was not impaired due to the Cre sequences. However, the DNA signal of rHBV-Cre revenant was much weaker compared to that of wtHBV. This implies that the replication process of rHBV-Cre revenant is less efficient. The two conformations of rHBV-Cre revenant DNA detected in the capsids were also observed in the virions in supernatant (Figure 14B, Lane 2). This indicates that the capsids containing the Cre sequences were enveloped and secreted from the cells.

In summary, rHBV-Cre revenant transfer plasmid was successfully generated via BAC recombination-mediated fragment assembly, and that the recombinant virus can be produced in Huh7 cells and secreted to the supernatant.

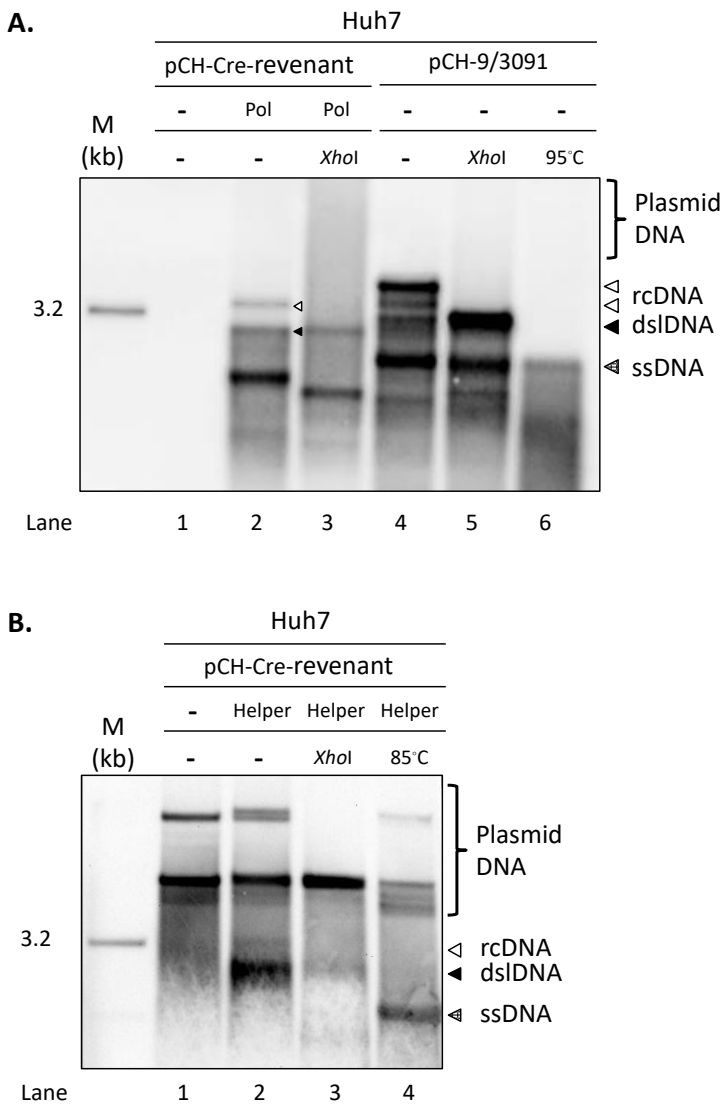

Figure 14: Genome structure of rHBV-Cre revenant

Huh7 cells were transfected with the rHBV-Cre revenant transfer plasmid (pCH-Cre revenant) and an HBV helper plasmid (Pol or Helper). Huh7 cells transfected with a 1.1-fold wtHBV plasmid (pCH-9/3091) served as positive control. DNA extracted from capsids in the cells (A) and virus in the supernatant (B) were analyzed by Southern blot. The identity of DNA species was further confirmed by digesting DNA samples with XhoI (which linearized the circular DNA) or by heating DNA samples to 85-95 °C (which denatured rc-/dsl-DNA to ssDNA). Open triangles indicate rcDNA. Filled triangles indicate dslDNA. Dotted triangles indicate ssDNA.

2.2.2 Production of rHBV-CreN

The Split Cre complementation system is a system in which the activity of Cre recombinase is controlled by a ligand-induced complementation of inactive Cre fragments. It has been used in various contexts, such as monitoring protein-protein interactions [89], providing temporal or optogenetic control of DNA recombination events [90, 91], and pathogen-host interaction [92]. Based on these uses, the Co-InCre system [86] was adapted in this study to monitor virus-host

interaction. The Co-InCre system consists of two components—Co-InCreN and Co-InCreC. Co-InCreN is a fusion of the N-terminal iCre (aa 19-59) and the N-terminal gp41-1, whereas Co-InCreC is a fusion of the C-terminal gp41-1 and the C-terminal iCre (aa 60-343). Cre reconstitution is achieved by the intein-mediated trans-splicing reaction of gp41-1 fragments. Since the size of Co-InCreN (414 bp) is much smaller than that of Co-InCreC (990 bp), the Co-InCreN cassette was cloned into the rHBV transfer plasmid, while the Co-InCreC cassette was integrated into the genome of host cells (Figure 15A). The cloning strategy was similar to that described in Section 2.1.2 (Figure 15B). Since the insert is shorter than the excised HBV fragment, the resulting genome size of rHBV-CreN (2.8 kb) is smaller than that of wtHBV (3.2 kb).

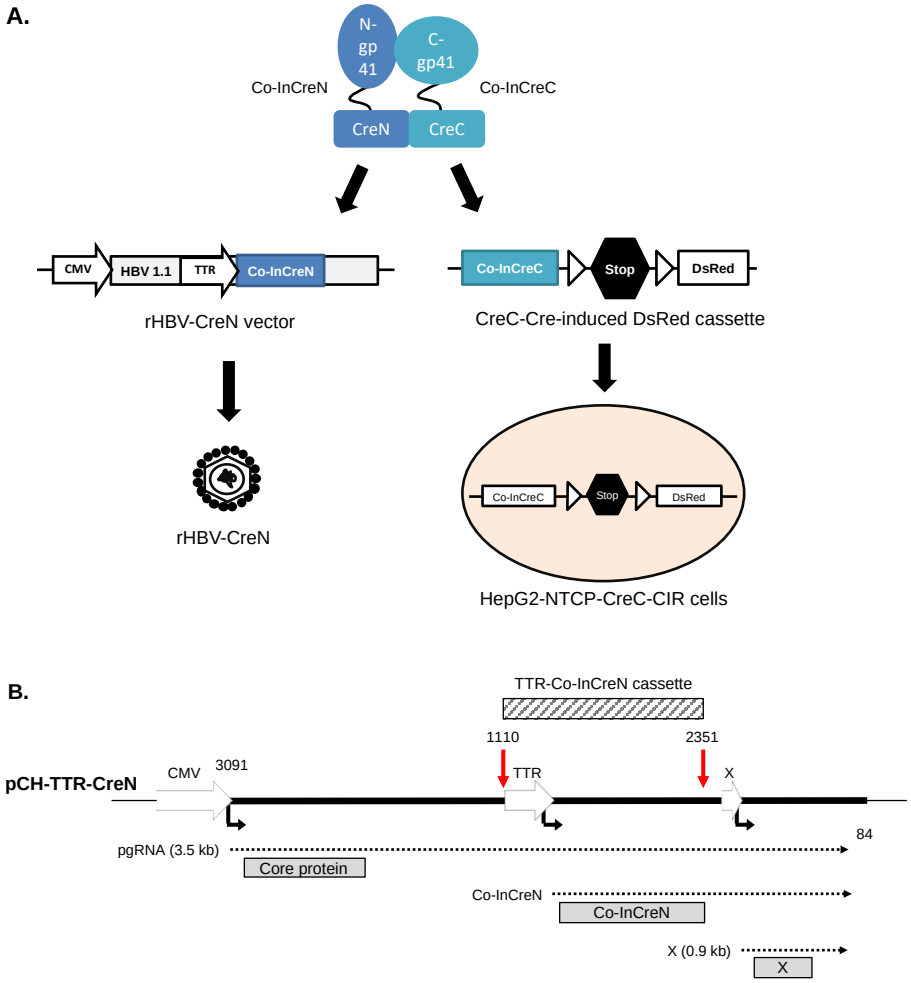

Figure 15: The Co-InCre system and the rHBV-CreN transfer plasmid

(A) The Co-InCreN fragment was placed in the rHBV transfer plasmid, whereas the Co-InCreC fragment and the Cre-induced DsRed cassette were integrated into the genomes of HepG2-NTCP cells. (B) The PreS and S regions of the 1.1-fold HBV plasmid (pCH-9/3091) were replaced by the TTR-Co-InCreN cassette. Block arrows indicate promoters or enhancers. Dashed arrows indicate transcripts. Grey boxes indicate proteins.

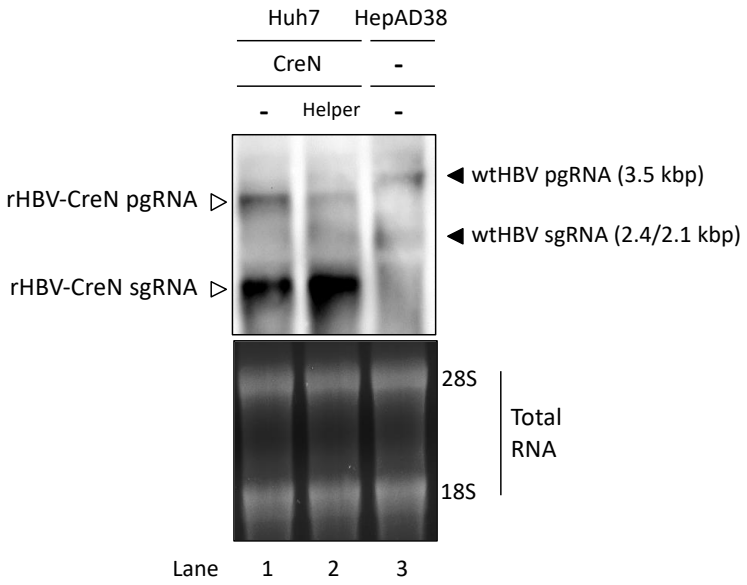

Figure 16: Transcription of viral RNAs derived from the rHBV-CreN transfer plasmid
Huh7 cells were transfected with rHBV-CreN transfer plasmid (CreN) and HBV helper plasmid (Helper), as indicated. A wtHBV replicating cell line, HepAD38 cells, served as the positive control. RNA extracted from the cells was analyzed by agarose gel to determine total RNA level and Northern blot for HBV-specific RNA.

The virus production procedure was similar to that described in Section 2.1.2. However, in this part, in addition to rHBV genome analysis, viral RNAs and proteins were investigated. First step was to analyze the expression of rHBV-CreN pgRNA derived from rHBV-CreN transfer plasmid. RNA was isolated from Huh7 cells transfected with the rHBV-CreN transfer plasmid with or without the helper plasmid and analyzed by Northern blot. Additionally, RNA isolated from HepAD38 cells—a stable cell line constantly producing wtHBV—was included as a positive control. It is known that the 3.5 kb HBV pgRNA and 2.4/2.1 kb HBV sub-genomic RNA (sgRNA) are expressed in HepAD38 cells [49]. As presented on the blot, two bands were detected in the HepAD 38 sample, presumably corresponding to wtHBV pgRNA and wtHBV sgRNA (Figure 16, Lane 3). Furthermore, two bands were observed in the sample transfected with rHBV-CreN transfer plasmid (Figure 16, Lane 1), which migrated faster than that of the HepaAD38 sample. Since the genome size of rHBV-CreN is smaller than that of wtHBV, its pgRNA and sub-genomic RNA are expected to be shorter. Moreover, the expression of rHBV-CreN pgRNA and sgRNA was independent of the helper plasmid. Three bands representing rHBV-CreN pgRNA, wtHBV sgRNA, and rHBV-CreN sgRNA were detected in the sample co-transfected with CreN plasmid and the helper plasmid (Figure 16, Lane 2). Furthermore, rHBV-CreN pgRNA and sgRNA were derived from the rHBV transfer plasmid, whereas the wtHBV sgRNA was derived from the helper plasmid. Compared to the CreN sample, the level of rHBV-CreN pgRNA was lower in the co-transfection sample. Additionally, no wtHBV pgRNA signal was detected

in the co-transfection sample, which indicates that the helper plasmid was unable to generate wtHBV pgRNA.

Thereafter, the expression of viral proteins derived from the rHBV-CreN transfer plasmid and the helper plasmid was analyzed by Western blot. The cell lysate of HepaAD38 cells was included as a positive control. No viral proteins were detected in Huh7 cells, which served as a negative control (Figure 17, Lane 1). HBc protein was the only viral protein detected in cells transfected with rHBV-CreN transfer plasmid alone (Figure 17, Lane 2). As expected, no surface proteins were detected due to the coding sequence of surface proteins being replaced by the Co-InCreN cassette. Although the X promoter and its coding sequence remained intact in the rHBV-Cre transfer plasmid, no HBx protein was detected. In cells co-transfected with the rHBV-CreN transfer plasmid and the helper plasmid, HBc protein, surface proteins, and HBx protein were detected (Figure 17, Lane 3). However, compared to the wtHBV-producing cell line (HepAD38 cells, Figure 17, Lane 4), the level of surface protein expression from the helper plasmid was much lower.

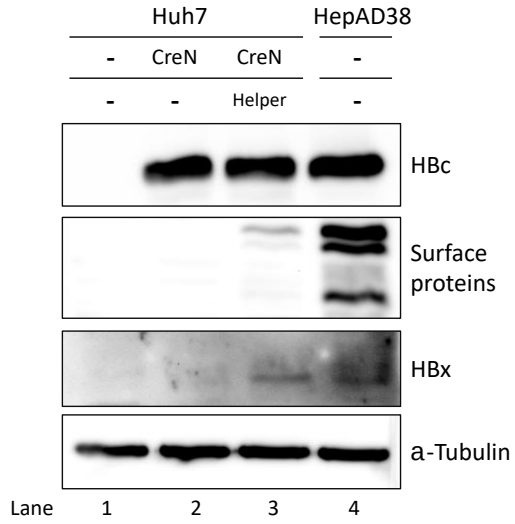

Figure 17: Expression of HBV viral proteins derived from rHBV-CreN transfer plasmid and the helper plasmid

Huh7 cells were transfected with rHBV-CreN transfer plasmid (CreN) alone or with an HBV helper plasmid (Helper). HepAD38 cells, a wtHBV-producing cell line, were used as the positive control. Protein lysates from the cells were analyzed by Western blot using antibodies against HBV core (HBc), surface, and HBx proteins or α-Tubulin, respectively.

Lastly, the rHBV-CreN genomes in the capsid and viral particles were analyzed. Preparation and analysis of the DNA samples was performed in the manner described in Section 2.1.2. However, instead of using Huh7 cells transfected with the wtHBV plasmid, HepAD38 cells were used as a positive control. Similar to previous results showing cells transfected with wtHBV plasmid (Figure 14A, Lane 4), three bands corresponding to rcDNA, dslDNA, and ssDNA were detected in the capsids derived from HepAD38 cells (Figure 18A, Lane 5). Two bands corresponding to rHBV-CreN rcDNA and dslDNA were detected in the capsids derived from Huh7 cells co-transfected with rHBV-CreN transfer plasmid and the helper plasmid (Figure 18A, Lane 2). Since the rHBV-CreN pgRNA was shorter than that of the wtHBV, it was expected that the rHBV-CreN DNA, which is produced from the rHBV-CreN pgRNA (Figure 16, Lanes 1 and 2), is smaller than the wtHBV

genome. The result indicates that the Co-InCreN cassette does not interfere with the rHBV-CreN replication. Differing from the HBV DNA species observed in the capsids derived from HepAD38 cells, two major bands referring to rcDNA and dslDNA were detected in the viral particles in the supernatant of HepAD 38 cells (Figure 18B, Lane 5).

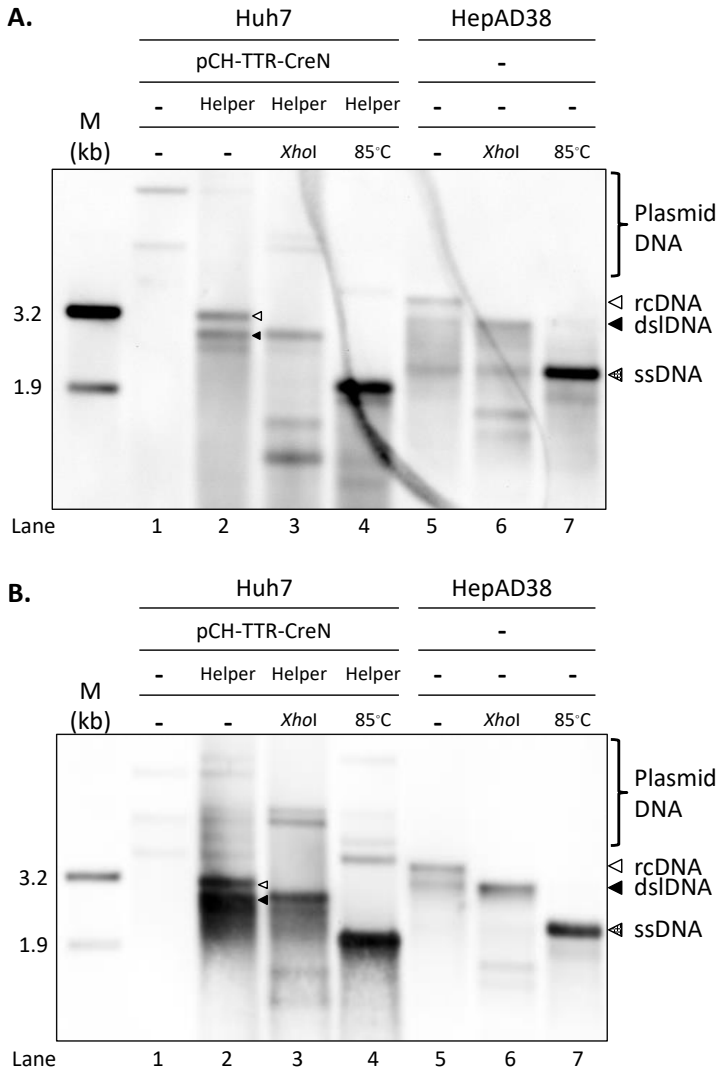

Figure 18: Genome structure of rHBV-CreN

Huh7 cells were transfected with rHBV-CreN transfer plasmid (pCH-TTR-CreN) and HBV helper plasmid (Helper). HepAD38 cells, a wtHBV-producing cell line, were used as the positive control. DNA extracted from capsids in the cells (A) and virus in the supernatant (B) were analyzed by Southern blot. The identity of DNA species was further confirmed by digesting the DNA samples with XhoI, or by heating the DNA samples to 85 °C. Open triangles indicate rcDNA. Filled triangles indicate dslDNA. Dotted triangles indicate ssDNA.

Furthermore, both the RC and DSL forms of rHBV-CreN DNA were detected in viral particles secreted from the co-transfected cells (Figure 18B, Lane 2). This demonstrates the successful production of rHBV-CreN via the trans-complementation manner. However, several bands above the 3.2 kb marker were

detected in the supernatant of rHBV-CreN-producing cells (Figure 18B, Lane 2). This may be due to the plasmid DNA that co-precipitated with the rHBV-CreN.

As shown in Figure 18B, plasmid DNA precipitated alongside virus particles by using PEG solution to increase virus concentration. In order to improve the purity and scale up virus production, heparin affinity chromatography combined with DNase on-column digestion was utilized. HBV viral particles and sub-viral particles bind to the heparin column via the interaction between HBV large surface protein and heparin sulfate proteoglycan [93]. Additional DNase on-column digestion removes the plasmid DNA, which is likely to be associated with viral particles. The extracellular medium was collected from Huh7 cells co-transfected with rHBV-CreN transfer plasmid and the helper plasmid. The collection began on day 5 post-transfection, and media were collected every 4 days for a total of 6 times. DNA samples isolated from PEG-precipitated virus stock and heparin-purified virus stock were analyzed by Southern blot. Notably, both rHBV-CreN rcDNA and dslDNA were also detected in the DNA samples of rHBV-CreN purified using the heparin affinity chromatography (Figure 19). This indicates that the stability of viral particles was unaffected by the use of heparin affinity chromatography combined with DNase on-column digestion for viral purification. Moreover, bands above the 3.2-kb marker were undetectable in the DNA sample from virus purified via the heparin affinity chromatography. This indicates that the purity of virus stock improved greatly due to the elimination of input plasmids.

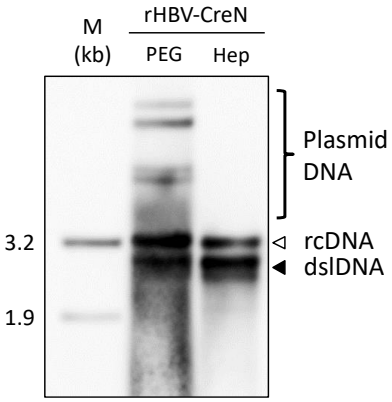

Figure 19: Purification of rHBV-CreN

Huh7 cells were co-transfected with rHBV-CreN transfer plasmid and HBV helper plasmid. The virus-containing supernatants were either subjected to PEG precipitation (PEG) or purified by heparin affinity chromatography coupled with DNase on-column digestion (Hep). DNA extracted from the purified viral stocks was analyzed by Southern blot.

In summary, rHBV-CreN could be efficiently produced in a trans-complementation manner. Heparin affinity chromatography combined with DNase on-column digestion enabled the generation of a pure virus stock.

2.2.3 Generation of a Cre reporter cell line

In order to monitor Cre activity via fluorescence in cells, a Cre-induced DsRed plasmid (pCALNL-DsRed) was utilized (Figure 20) [94]. Since rHBV-CreN only carries the N-terminal component of the Co-InCre system, the C-terminal component of the Co-InCre system, Co-InCreC, is additionally required for executing the recombinase function. To combine the Co-InCreC cassette and the Cre-induced DsRed cassette into one plasmid, the Co-InCreC cassette was inserted into pCALNL-DsRed (Figure 15A). This newly generated plasmid was transfected into HepG2-NTCP-K7 cells, and cells expressing the cassette were selected with neomycin (2 mg/ml). The cell line obtained was named HepG2-NTCP-CreC-CIR (CreC/CIR cells; CIR: Cre-induced red).

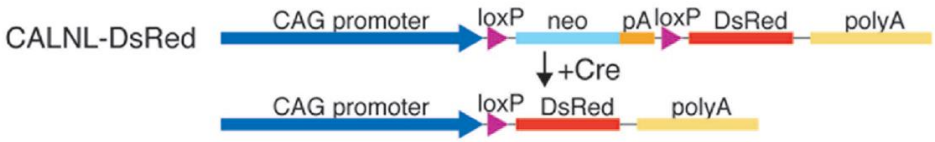

Figure 20: Depiction of the Cre-induced DsRed plasmid (reprint from Matsuda 2007)
This plasmid contains the following elements: the CAG promoter, a loxP-flanked neo-pA cassette, and the DsRed coding sequence. The expression of neomycin phosphotransferase (neo) is driven by the CAG promoter. Due to the polyA site and the neomycin phosphotransferase stop codon, transcription and translation will be terminated at the loxP-flanked neo-pA cassette. DsRed expression will only be initiated upon the removal of the loxP-flanked neo-pA cassette, which is mediated by Cre-lox recombination.

In order to verify the cell line, the functional complementation of the split Cre as well as the activation of the Cre reporter cassette (Cre-induce DsRed) was first evaluated in these cells. The plasmid containing Co-InCreN was transfected into CreC/CIR cells. DsRed expression was examined by fluorescence microscopy and by FACS analysis on day 4 post-transfection. Fluorescence microscopic images indicated that no DsRed signal was observed in CreC/CIR cells transfected with control plasmid (pcDNA3.1) (Figure 21A, left image). This indicates that unspecific Cre-lox recombination did not occur in CreC/CIR cells. In contrast, CreC/CIR cells becoming DsRed-positive was observed upon transfection of a plasmid containing the Co-InCreN cassette (Figure 21A, right image). FACS analysis confirmed that approximately 13% of the CreC/CIR cells transfected with Co-InCreN cassette become DsRed-positive (Figure 21B, right panel). This indicated that DsRed expression was activated in the presence of Co-InCreN and Co-InCreC. This activation was most likely mediated by Cre-lox recombination.

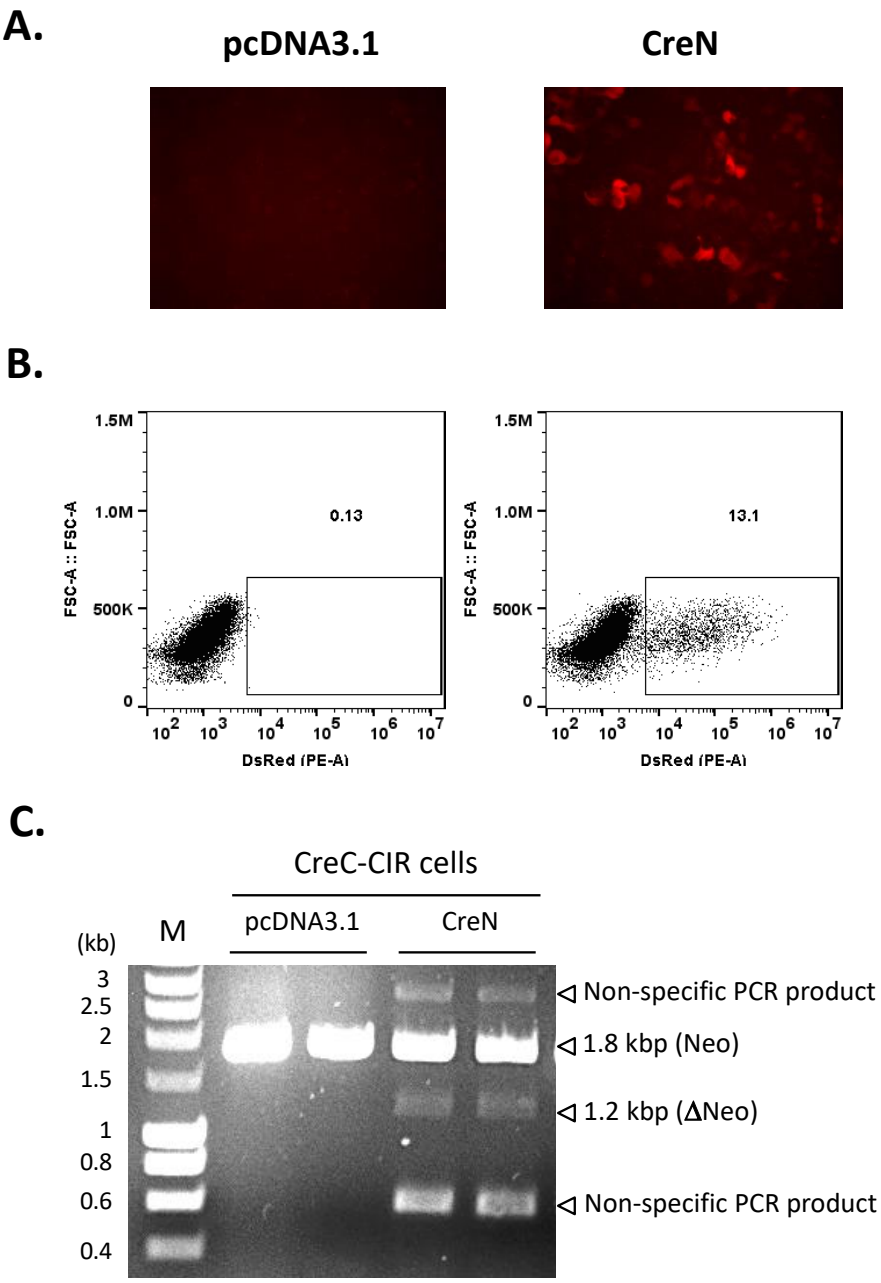

Figure 21: Functional complementation of split Cre in CreC/CIR cells

CreC/CIR cells were transfected with either control plasmid (pcDNA3.1) or plasmid expressing N-terminal Cre (CreN). (A) Red fluorescence was measured by fluorescence microscopy. (B) The numbers of DsRed-positive cells were determined by flow cytometry. The gate for DsRed-positive cells was set on the basis of the fluorescence intensity of the control sample. (C) DNA extracted from the cells was amplified by PCR using primers flanking the loxp-Neo-pA-loxp cassette. PCR products were then subjected to agarose gel electrophoresis. Neo indicates PCR products containing the loxp-Neo-pA-loxp cassette. ΔNeo indicates PCR products without the loxp-Neo-pA-loxp cassette.

Confirming the genome-editing event upon the reassembly of Co-InCreN and Co-InCreC in the CreC/CIR cells represented the next step in the process of validating the cell line. Genomic DNA was isolated from CreC/CIR cells transfected with or without plasmid containing CreN cassette. In the DNA sample of the control group

(pcDNA3.1), a single PCR product (approximately 1800 bp) was detected using primers amplifying the loxp cassette. In the DNA samples isolated from CreN-transfected cells, an additional band of 1.2 kb appeared. This indicated that the DNA flanked by loxP sites was removed. However, two additional non-specific PCR products were detected in the experimental group that could not easily be explained (Figure 21C).

Lastly, the permissiveness of CreC/CIR cells to wtHBV infection was tested to exclude the possibility that clonal selection altered the phenotype of HepG2-NTCP-K7 cells. CreC/CIR cells and their parental cells (HepG2-NTCP-K7 cells) were infected with wtHBV (Figure 22A). On day 4 post-infection, the supernatant was collected to analyze HBeAg expression, and the DNA was isolated from cells to measure the amount of cccDNA. The level of HBeAg in the supernatant of wtHBV-infected CreC/CIR cells was slightly higher than that of HepG2-NTCP-K7 cells (Figure 22B). A similar effect was also observed at the cccDNA level (Figure 22C), which indicated that the permissiveness to HBV infection in CreC/CIR cells was not impaired during the clonal selection procedure.

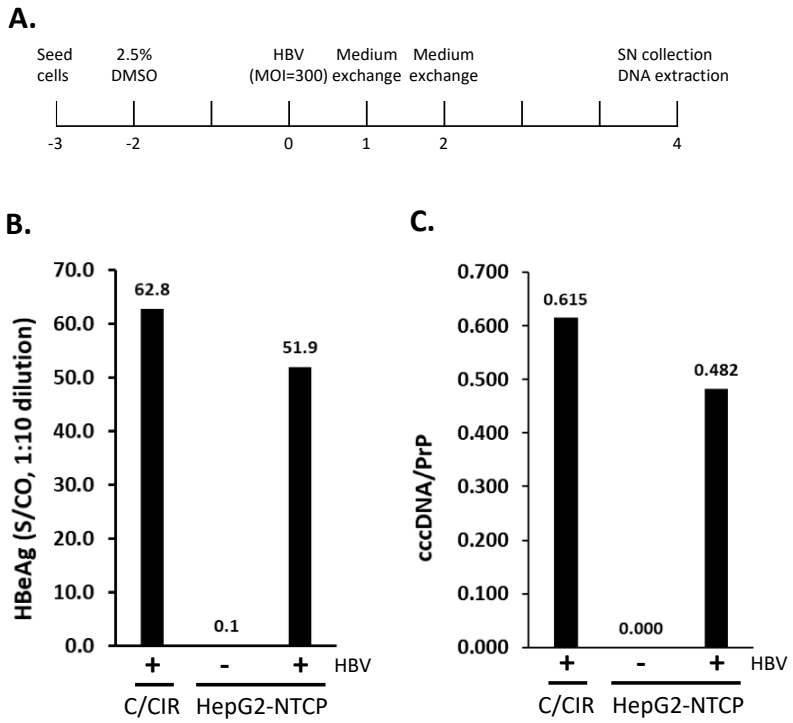

Figure 22: Infectivity of wtHBV in HepG2-NTCP-CreC-CIR cells

CreC/CIR cells were infected with wtHBV, and the experiment was conducted according to the scheme (A). Supernatant was collected for measuring the HBeAg level via HBeAg ELISA (B). The HBeAg level was expressed as sample to cut-off (S/CO) ratio. And the samples with an S/CO value <10 were considered negative. DNA was extracted from cells, and the level of cccDNA was determined by qPCR (C).

Taken together, DsRed expression can be initiated via Cre-lox recombination in CreC/CIR cells. Additionally, cells remained susceptible toward wtHBV infection.

2.2.4 Infection of the Cre reporter cells with rHBV-CreN

Having characterized the reporter cell line and purified the reporter virus, the capability of monitoring rHBV-Cre infection in the Cre/CIR cells was investigated. Characterization of rHBV-CreN infection began by determining the MOI for detecting the DsRed signal. On day 7 post-infection, cells were examined by fluorescence microscopy and then subjected to FACS analysis. Additionally, the supernatant was collected for HBeAg ELISA (Figure 23A). The number of DsRed-positive cells increased proportional to the MOI of rHBV-CreN (Figure 23B, C), which ranged from 1.5% of DsRed-positive cells at MOI = 25 to 7.6% at MOI = 1600, as determined by FACS. Moreover, the increase in DsRed expression was closely correlated with the expression of HBeAg (Figure 23C).

Next, the kinetics of DsRed expression and HBeAg secretion were analyzed. CreC/CIR cells were infected with rHBV-CreN at a MOI of 300 genome equivalents per cell, and harvested at days 1, 4, 7, 10, 13, and 16 post-infection. DsRed expression in infected cells was visible by fluorescence microscopy from 4 days post-infection (dpi) onwards, and the fluorescence signal lasted until 16 dpi (Figure 24A). In contrast, the DsRed signal of uninfected CreC/CIR cells (mock) remained negligible throughout the culture period. A linear increase in the percentage of DsRed-positive cells was observed between 1 to 7 dpi. This increase became modest between 7 and 13 dpi, and then began to decrease (Figure 24B). Additionally, the kinetics of DsRed expression from 4 dpi onwards matched that of HBeAg expression. This suggests that the expression kinetic of DsRed reflects that of the viral protein (HBeAg).

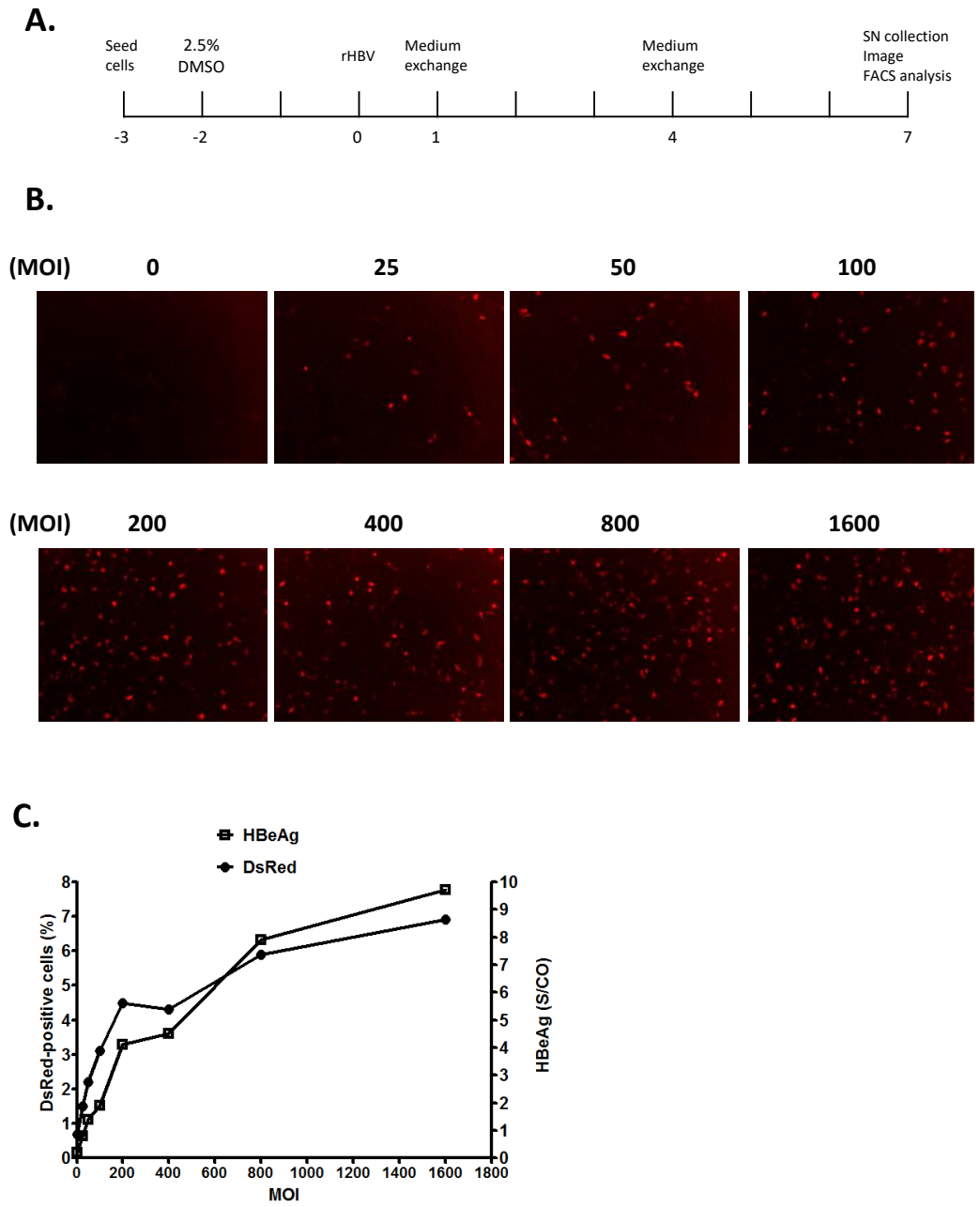

Figure 23: Expression of DsRed upon rHBV-CreN infection in CreC/CIR cells

CreC/CIR cells were infected with rHBV-CreN using different MOI. The experiment was conducted according to the scheme (A). Fluorescence signal was detected by fluorescence microscopy (B). The number of DsRed-positive cells was determined by flow cytometry, and the amount of HBeAg in the supernatant was analyzed by HBeAg ELISA (C). The HBeAg level was reported as sample to cut-off ratio (S/CO), and the samples with a ratio greater than 1 were considered positive.

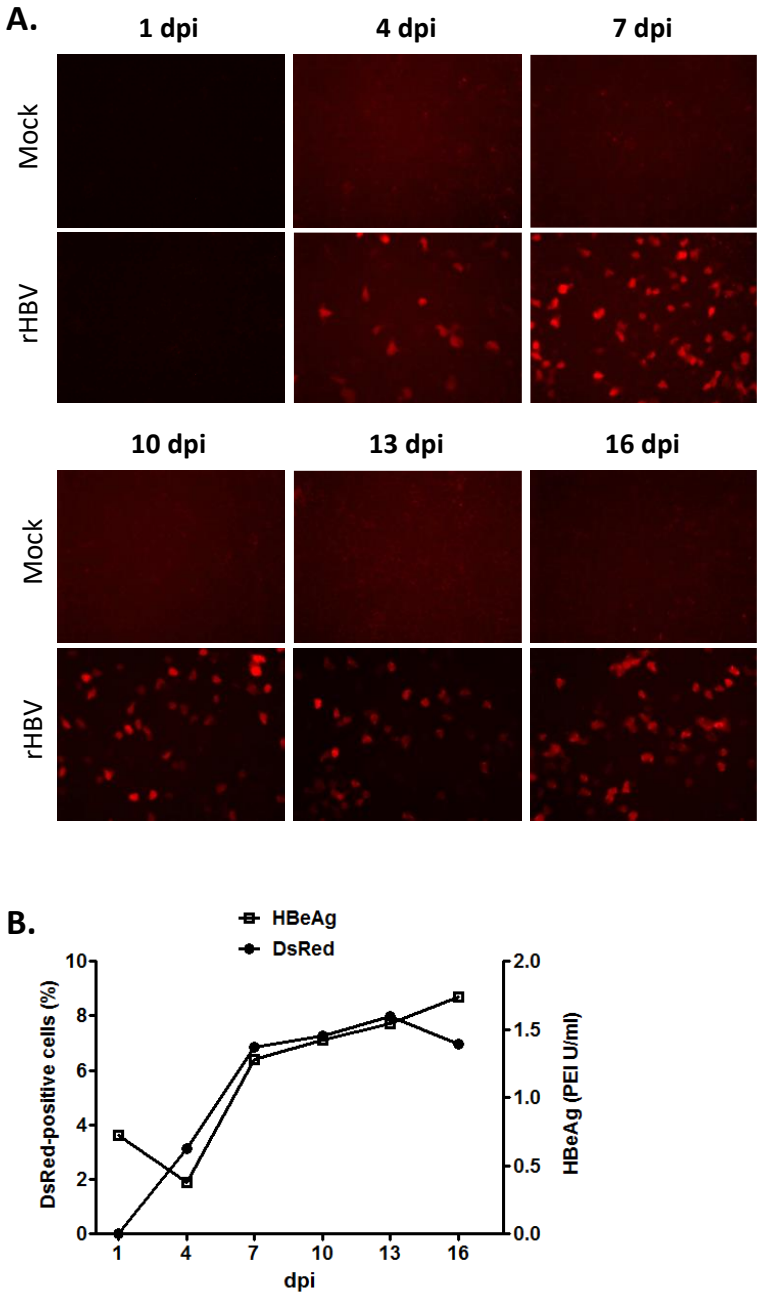

Figure 24: Expression kinetics of DsRed and HBeAg in CreC/CIR cells infected with rHBV-CreN
CreC/CIR cells were incubated with (rHBV) or without (Mock) rHBV-CreN for 24 hours. At the indicated time points, cells were imaged by fluorescence microscopy and analyzed by flow cytometry (A and B). Supernatants were collected simultaneously, and HBeAg levels were determined by HBeAg ELISA (B).

To verify the establishment of rHBV-CreN infection, the kinetic of cccDNA formation was analyzed. CreC/CIR cells were infected with rHBV-CreN (MOI=1000) and harvested at 1, 4, 7, and 10 dpi. DNA was isolated using the Hirt extraction procedure, and the cccDNA and protein-free rcDNA (PF-rcDNA) levels were analyzed by Southern blot. As shown in Figure 25, rHBV-CreN cccDNA was detected on day 4 post-infection, and gradually decreased thereafter. The kinetic of PF-rcDNA was similar to that of cccDNA, peaking at 4 dpi and then declining. This indicates the HBV replication template, cccDNA, was established from the incoming PF-rcDNA in cells infected with rHBV-CreN.

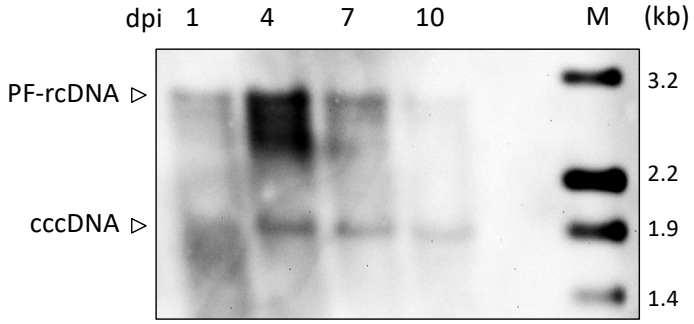

Figure 25: cccDNA formation in CreC/CIR cells infected with rHBV-CreN
CreC/CIR cells were infected with rHBV-CreN. The infected cells were harvested after infection for 1, 4, 7, and 10 days. DNA was isolated by using Hirt extraction and subsequently analyzed by Southern blot.

Finally, the specific uptake of rHBV-CreN via the HBV entry receptor, NTCP, was examined. Myrcludex-B (MyrB) is a lipopeptide consisting of amino acid residues 2–48 of the preS1 region of HBV [37, 95]. MyrB competes with viral particles for NTCP binding, thereby blocking HBV infection. CreC/CIR cells were infected with rHBV-CreN (MOI=250) in the presence of MyrB. DsRed expression in cells, as well as HBeAg expression in the supernatant and cells was analyzed on day 7 post-infection (Figure 26A). Similar to the previous results (Figure 24), DsRed expression was observed in CreC/CIR cells upon rHBV-CreN infection (Figure 26B, middle), as evident in fluorescence imaging and FACS analysis. In the presence of MyrB, the number of DsRed-positive cells was reduced to < 1 %, which is comparable to the mock group (Figure 26B). In addition, the HBeAg level of the MyrB-treated sample was comparable to that of the mock sample (Figure 26C). However, the HBeAg level of the rHBV-infected sample was much lower than that of the wtHBV-infected sample. These results indicate that rHBV-CreN infection was blocked by MyrB and suggests that the rHBV-CreN virus enters cells via the same pathway as wtHBV.

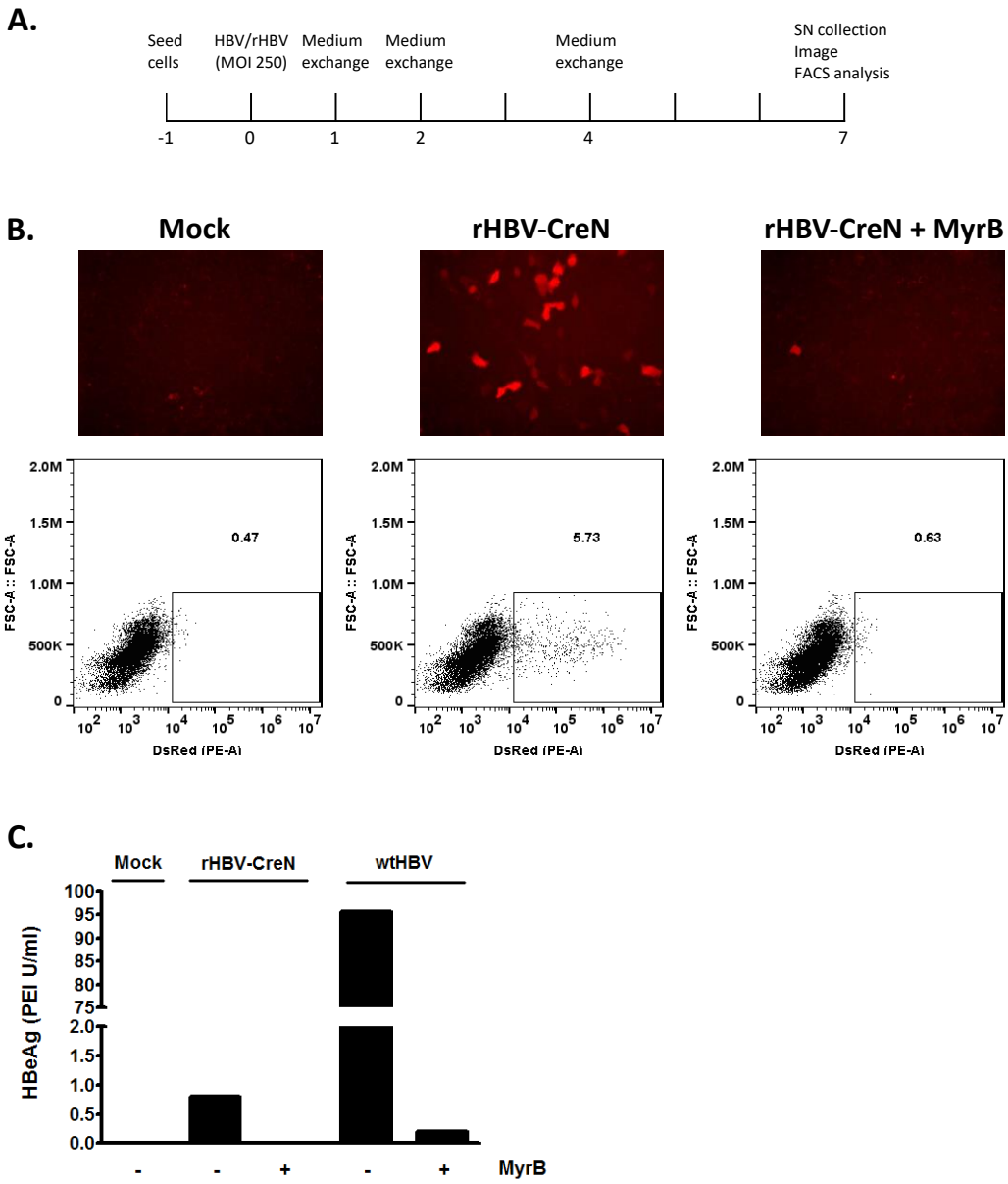

Figure 26: Effect of MyrB on rHBV-CreN infection

CreC/CIR cells were infected with either rHBV-CreN or wtHBV. In addition, MyrB was added to the inoculums. Cells receiving PEG alone served as the control (Mock). The experiment was conducted according to the scheme (A). After 7 days, fluorescence images of the cells were taken and cells were analyzed by flow cytometry (B). In addition, the supernatants of cells were analyzed by HBeAg ELISA (C).

Combined, the results indicate that rHBV-CreN can induce DsRed expression in the Cre reporter cells in a MOI-dependent manner. DsRed and cccDNA signals were detected from 4 days post-infection. Moreover, infection with rHBV-CreN was prevented by MyrB treatment.

3 Discussion

The following section includes an interpretation of the results, a discussion of the utilized methods, the potential optimization of rHBV systems, and details regarding these systems.

3.1 Establishment of rHBV-LNGFR reporter system

The purpose of designing this HBV reporter system is to possess a system that allows for convenient separation of live HBV-permissive cells from naïve cells for further analysis, such as a screening of mouse cells carrying human cDNA library for permissiveness or a study of HBV superinfection (consecutive infection). Moreover, by using a MACS-enriched sample of infected cells for downstream genetic or proteome analyses could “concentrate” the cellular or viral signature derived from infection, thereby reducing certain 'noisy' background from non-infected cells. Therefore, the quantification of viral-associated parameters such as the number of cccDNA copies in infected cells or the transcriptomic/ proteomic profile of the infected cells, could become more precise.

3.1.1 Hepatoma cells isolation by MACS

The isolation of hepatoma cells via MACS or FACS has been previously described [96]. Here, a cell isolation procedure using MACS and FACS was established for the HBV permissive hepatoma cell line, HepG2-NTCP cells expressing LNGFR. In order to evaluate the success of magnetic separation of cells, three main factors are commonly considered: the purity, recovery, and viability of sorted cells. Purity is defined by the percentage of target cells in the bound fraction, whereas recovery is defined by comparing the percentage of target cells before and after separation [69]. The MACS procedure applied in this thesis resulted in a purity rate of approximately 65%, as indicated by the percentage of the MicroBead-positive cells in the bound fraction (Figure 7D), and recovery increased 2.4-fold compared to the percentage of LNGFR MicroBead-labeled cells in the cell suspension before MACS (27%) and after MACS (65%) (Figure 7B, D). As such, the purity and recovery of LNGFR-expressing HepG2-NTCP cells following magnetic sorting is relatively low compared to other types of cells, such as primary PBMCs transduced with a retroviral construct expressing LNGFR [97]. Notably, inefficient separation of hepatoma cells during cell sample preparation could be a major factor in this result. It is known that hepatoma cells—especially HepG2-based cell lines—tend to aggregate; therefore, HepG2 cells are usually cultured in collagen-coated cell

culture vessels for an improved distribution (monolayer) of cells. HepG2-NTCP cells maintained in DMEM containing 2.5% DMSO—which facilitates HBV infection and replication—appear to have an even stronger aggregation tendency. Due to this aggregation characteristic of HepG2-NTCP cells, it is extremely difficult to disperse cells in a single-cell suspension, which is a critical requirement for cell sorting. Applying a stronger cell detachment reagent to harvest cell samples could, on one hand, increase the proportion of single cell in the suspension; however, on the other hand, this could cleave the LNGFR molecule displayed on the cell surface.

Regarding cell viability following magnetic sorting, cells associated with MicroBeads exhibited a survival rate two times lower than that of MicroBead-free cell samples (Figure 8). Cell viability following magnetic sorting is reportedly affected by high concentrations of magnetic beads associated with cells [98]. One potential explanation is that the interaction of cell adhesion molecules to the cell culture vessel is affected by steric hindrance caused by the MicroBeads associated with cells. An enzyme can be applied to cleave the bound MicroBeads on the cell surface, or a saturated protein solution (antibody) can be applied to compete the binding of MicroBeads and to remove magnetic beads from the cells [69]. However, the efficiency of removing beads bound to cells, and the adverse effects of the enzyme or high protein concentration in the cell solution still requires consideration.

Alternatively, two consecutive rounds of isolation could be applied to increase the purity of target cells in the samples in two different ways: 1) by using two different cellular markers with the same isolation procedure, or 2) by using a single marker with two different isolation procedures. Since rHBV vector length is limited, the insertion of two markers into the vector for performing two isolation procedures based on these markers is extremely difficult. Therefore, using two isolation methods chronologically would represent a more reasonable solution for improving purity. Since the LNGFR epitope on the cell surface will be blocked by MicroBeads following incubation with LNGFR-MicroBeads, LNGFR molecules on the MicroBead-labeled cells are no longer accessible for other LNGFR antibodies. However, MicroBeads can be recognized by a fluorochrome-conjugated antibody known as the MACSelect Control FITC Antibody. Therefore, staining of the MACSelect Control FITC Antibody allows MicroBeads-labeled cells to be analyzed and sorted by flow cytometry (Figure 9). Moreover, compared to the FACS procedure alone, MACS-FACS reduced the time requires for isolation, and cell viability should increase due to more rapid preparation [69].

3.1.2 Production of rHBV-LNGFR

After establishing the MACS/FACS isolation procedure for HepG2-NTCP cells expressing LNGFR, the production of rHBV-LNGFR was evaluated. Both RC and DSL form of rHBV-LNGFR DNA were detected in the capsids (Figure 11A, Lane 2). The amount of circular DNA species is much lower than the double-linear DNA species, whereas the RC-to-DSL ratio is 1:1 in the wtHBV setting (Figure 11A, Lane 6). The amount of rcDNA is the most important criterion when evaluating recombinant HBV production, since expression of the reporter gene carried by rHBV requires establishment of rHBV cccDNA, which can only be converted from rcDNA but not from dslDNA. The primary reason for this phenomenon most likely is that alteration of the HBV genome by replacing part of its sequence with TTR-LNGFR cassette affects the circularization process during reverse transcription of pgRNA, which is catalyzed by HBV polymerase strand switch.

The overall rHBV-LNGFR DNA signal in cells co-transfected with rHBV-LNGFR vector and the polymerase plasmid (Figure 11A, Lane 2) was stronger than that of cells co-transfected with the rHBV-LNGFR vector and the helper plasmid (Figure 11A, Lane 4). In the helper plasmid, HBV core protein and HBV polymerase are derived from the same transcript. The translation of HBV polymerase results from leaky scanning of the ribosome during translation initiation. Moreover, small regulatory upstream ORFs (uORFs) have been found upstream of the polymerase ORF, which inhibits the translation of this polymerase [99]. Therefore, the expression level of polymerase from the helper plasmid is expected to be lower than that of the polymerase plasmid, where polymerase expression is directly driven by the CMV promoter. Since this polymerase plays an important role in the synthesis of HBV DNA, the expression level of this protein could determine the efficiency of HBV DNA synthesis.

A very weak double-linear rHBV-LNGFR DNA signal was detected, but no relax-circular rHBV-LNGFR DNA signal was detected in the DNA sample from the supernatant (Figure 11B, Lanes 2 and 4). An artifact derived from the DNA extraction procedure can be excluded, since viral DNA extracted from wtHBV vector-transfected cells was detectable (Figure 11B, Lane 6). Since the circular form of capsid-associated DNA was detected in other types of rHBV, such as rHBV-GFP (data not shown) or rHBV-CreN (Figure 18B), the expression of LNGFR in virus-producing cells represent the primary cause. It is known that secreted and membrane proteins accumulate in the ER for folding and maturation [100]. Previous studies indicate that overexpression of HBV surface proteins results in the accumulation of the small envelope protein (S) on the ER membrane inducing unfolded protein responses (UPR) [101, 102]. The S protein-induced UPR activates

the autophagy pathway in cells, thus enhancing HBV envelopment [102]. However, prolonged ER stress in cells often leads to the activation of apoptosis [100]. Indeed, massive cell death was observed in the present study when producing the rHBV-LNGFR (data not shown). This body of evidence suggests that expression of LNGFR could further enhance ER stress induced by HBs, thereby resulting in ER stress that cannot recover and ultimately induces cell death.

Further investigation of ER stress in virus-producing cells through the analysis of UPR markers could be useful for evaluating the production efficiency of a recombinant virus. Moreover, in such a case where the reporter gene has a negative influence on virus-producing cells, a design of the rHBV vector that harbors a transcriptionally inactive reporter gene in the virus-producing cells is required. Several strategies can be utilized to achieve this purpose; for example, using a Tet-responsive promoter to replace the TTR enhancer for temporal control of transgene expression; or splitting the transgene into two inactive fragments, and either placing the fragments in reverse orientation or only including one of the fragments in the rHBV vector [90, 103]. Alternatively, the transgene could be integrated into the host genome and regulated by a genome-editing event, such as the Cre-lox recombination or the Crispr/Cas9 system.

3.2 Establishment of rHBV-Cre reporter systems

Based on the difficulty encountered while establishing rHBV-LNGFR (3.1.2), and to overcome the reported limitations of rHBV in the previous studies, rHBV reporter systems using the Cre-mediated genome engineering to track HBV infection were designed. The idea was to introduce the coding sequence of Cre recombinase into cells via recombinant HBV, subsequently activating the transcription of reporter genes at the genomic level via Cre-lox recombination. Using Cre-lox recombination to reporter viral infection has three major advantages: 1) it requires less virus input, 2) it permanently expresses the reporter genes after infection, and 3) it allows for the expression of multiple reporter genes upon infection.
Since the activation of reporter genes via Cre-lox recombination is a one-time event, a small amount of Cre recombinase expressed from the rHBV cccDNA is sufficient for executing the recombination. Therefore, establishing a high copy number of rHBV cccDNA in individual infected cells is not necessary. Furthermore, HBV cccDNA is an episomal DNA, which does not integrate into the host genome, and will therefore not duplicate as the host genome during cell division, which subsequently leads to a loss of cccDNA [16]. Hence, when compared to reporter gene expression from the rHBV cccDNA, the expression of host genome reporter genes will be more stable. Moreover, multiple reporter gene sequences can be

joined into one DNA cassette via 2A self-cleaving peptides or internal ribosome entry sites; therefore, several reporter genes can be simultaneously expressed by a Cre-regulated promoter. This enables infected cells to display different characters based on the reporter function and can be utilized for various purposes. For example, analysis at the single-cell level can be achieved based on the fluorescence intensity of infected cells, and the overall level of infection can be quantified based on the luciferase activity of infected cells. Isolation of infected cells can also be accomplished by magnetic sorting or antibiotic selection.

Since the activation of reporter genes via Cre-lox combination is irreversible, infected cells are permanently marked upon infection—regardless of cccDNA stability. As a result, it is not possible to track virus clearance in infected cells by observing reporter signal or activity, though conventional HBV marker, such as HBeAg secretion, can be used to track the virus in this case. Another limitation of this system is that it requires a cellular counterpart in order to detect infection, such as a stable cell line harboring a Cre reporter cassette. This makes the system less convenient in changing between different *in vitro* HBV infection models and even more so in the *in vivo* models. A potential solution for improving the portability and flexibility of this system could be the use of an adenoviral vector carrying the Cre reporter cassette.

3.2.1 Production of rHBV-Cre revenant

HBV cccDNA formation is the ultimate step in the establishment of HBV infection [16]. To design an HBV reporter system in which the reporter gene is exclusively expressed upon cccDNA formation, a Cre coding sequence divided in two fragments (5'-Cre and 3' Cre) is placed in reverse orientation in the rHBV vector. This design prevents the expression of Cre in virus-producing cells, which is known to affect cell viability [104]. HBV pgRNA is terminally redundant due to read-through of the viral polyA site, indicating that the endogenous polyA site of HBV is not effective at terminating transcription [105]. Taking advantage of this effect, one could initiate transcription of the Cre recombinase from the PreS1/PreS2 promoters of the circular DNA template (cccDNA). The elongation of Cre mRNA could then pass once through the polyA site between X and the core coding region, and then termination will only occur when RNA polymerase reaches the polyA site again. The frequency of these transcripts will be low, since the majority of transcription events will be terminated while RNA polymerase reaches the HBV polyA signal for the first time. However, since Cre-lox recombination is very efficient, achieving a high amount of Cre transcripts from the rHBV cccDNA in the rHBV infected cells is not necessary.

Southern blot is a robust method used for the analysis of various species of the HBV genome. However, the sensitivity of Southern blot is low, and requires at least three picograms of HBV DNA (10^6 HBV DNA copies) to detect a signal (data not shown). As shown in Figures. 11 and 14, rHBV production efficiency is much lower than that of wtHBV. Therefore, a high amount of virus or virus-producing cells is necessary to detect the rHBV DNA signal by Southern blot. Alternatively, the membrane must be overexposed to possess a sufficient rHBV DNA signal. In the previous result (Figure 11A, Lane 2 and 3), the background partially masked the rHBV-LNGFR DNA signal during prolonged membrane exposure and interfered with proper interpretation of the results.

Several factors, including the DNA probes, handling of the membrane, and membrane washing procedure, could influence the background of the Southern blot method (DIG application manual, Roche Diagnostics, 2008). Hybridization tubes or hybridization bags are commonly used for the hybridization of DNA probes and the membrane in Southern blot procedures. The hybridization tube is a re-usable material, and it requires less hybridization buffer, whereas the hybridization bag is a disposable material that requires a higher volume of hybridization buffer. However, in the present study, Southern blot background using a hybridization bag was largely reduced (Figure 14) compared to the use of a hybridization tube (Figure 11). Potential reasons for the hybridization bottle resulting in higher background include: 1) insufficient cleaning of the hybridization tube, which leads to leftovers of DIG-labeled DNA probe in the tubes, or 2) incomplete closing of the hybridization tube, which can lead to partial dry-out of the membrane during the hybridization procedure.

Both circular and double-linear forms of rHBV-Cre revenant DNA were present in the capsids as well as in the secreted virions (Figure 11). However, two differences were noted between the rHBV-Cre revenant DNA and wtHBV DNA. First, two distinct bands of rcDNA were observed in the wtHBV sample (Figure 11A, Lane 4). In contrast, only one circular form of rHBV DNA was observed in the rHBV-Cre revenant DNA sample (Figure 11A, Lane 2). Notably, neither the difference nor the identity of these two circular forms of wtHBV DNA is known. Moreover, an artifact introduced at the DNA isolation step was excluded since the DNA extraction of all samples was performed in parallel. Therefore, this data may imply that the replication of rHBV-Cre revenant in the virus-producing cells could differ slightly from that of wtHBV. Second, the dslDNA of rHBV-Cre revenant (Figure 11A, Lane 2) migrated further than wtHBV dslDNA during electrophoresis (Figure 11A, Lane 4). Since the size difference between rHBV-Cre revenant and wtHBV is 40 bp, it is unlikely to observe a size difference by agarose gel electrophoresis. This suggests

that either the transcription of rHBV-Cre revenant pgRNA or the reverse transcription of rHBV-Cre revenant dslDNA was affected by the Cre sequence.

Although the first step of this system was successfully supported with the 5'Cre and 3'Cre positioned in the correct order in the circular form of rHBV-Cre revenant DNA in the virion, the transcription of Cre using rHBV-Cre revenant cccDNA as a template in rHBV-infected cells and the functionality of Cre recombinase derived from the transcript must be investigated further.

3.2.2 Production of rHBV-CreN

In parallel to the development of the rHBV-Cre revenant, the other type of rHBV vector carrying the N-terminal of the Cre-coding sequence (Co-InCreN, 413 bp) was designed. The primary advantage of inserting a partial Cre sequence is that alteration of the HBV sequence in the rHBV vector is minimized. Since cloning was conducted by exchanging the transgene cassette in the rHBV vector, rHBV-CreN genome size was smaller than that of wtHBV or other rHBVs. However, the rHBV-CreN production rate was higher than that of rHBV-CreN3.2 (data not shown). Additionally, rHBV-CreN and rHBV-CreN3.2 both carry the CreN sequence, and the only difference between them is that the rHBV-CreN3.2 vector contains an additional HBV sequence at the 3' of the Co-InCreN cassette, including the EN1 sequence, which results in an identical genome size to wtHBV (3.2 kb). This suggests that the smaller genome leads to more efficient production of the recombinant virus. Detailed analysis using the trans-complementation method to produce rHBV-CreN demonstrated the transcription of all viral RNAs, translation of the viral proteins, and the replication of rHBV DNA.
In rHBV-producing cells, two features are included in the helper plasmid to prevent the packaging of wtHBV pgRNA: removal of the 5' epsilon (ε) sequence of HBV, and substitution of the HBV polyadenylation signal with that of rabbit β-globin [55]. The 5' ε sequence is known to be crucial for the encapsidation of pgRNA, and for its subsequent reverse-transcription [106]. Furthermore, replacing the HBV polyA signal with rabbit β-globin polyA signal results in a much longer transcript, thereby significantly reducing the likelihood of packaging this RNA and making reverse transcription within the sized-limited capsid impossible [55]. Using Northern blot analysis, the present study determined that wtHBV pgRNA was barely detectable in cells transfected with the helper plasmid (Figure 16, Lane 2). Moreover, the expression level of rHBV-CreN pgRNA in cells transfected with rHBV-CreN vector (Figure 16, Lane 1) was higher compared to cells co-transfected with the rHBV vector and the helper plasmid (Figure 16, Lane 2). In contrast, the level of rHBV-CreN sgRNA increased slightly in co-transfected cells compared to that of rHBV-

CreN transfected cells. Change in rHBV-CreN pgRNA and sgRNA levels in different cell samples is likely due to the competition of transcription factors among the different promoters, which drive the expression of pgRNAs and sgRNAs. Since pgRNA is the template for producing the HBV genome, the lower expression level of rHBV-CreN pgRNA observed in the cells co-transfected with the rHBV vector and the helper plasmid (e.g. the virus-producing cells) could be a cause for the low efficiency of rHBV production observed using the trans-complementation method.

Two unexpected results were observed during viral protein analysis by Western Blot (Figure 17). First, the expression level of surface proteins from the helper plasmid was much lower compared to that of HepAD38 cells. Since the analysis was only performed once, repetitions of this analysis are required to draw final conclusions regarding this observation. Second, no HBx protein signal was detected in cells transfected with the rHBV-CreN vector. Since Western blot analysis of HBx is generally difficult to perform, it is challenging to address whether no HBx expression occurred in the rHBV-CreN vector transfected cells or if HBx expression derived from the rHBV-CreN vector was too low. It is known that EN1 promotes the expression of HBx; therefore, partial deletion of the EN1 sequence in the rHBV-CreN vector could affect the expression level of HBx derived from the vector [18]. This could be verified by an examination of the cells transfected with the rHBV-CreN3.2 vector where the EN1 sequence remains intact in the vector.

Plasmid DNA in the virus-containing supernatant was efficiently removed by using heparin affinity chromatography together with DNase on-column digestion (Figure 19). Although Southern blot is particularly useful for examining different DNA species sharing the same sequence, this method is insensitive to detection of smaller amounts of DNA. Therefore, a small amount of plasmid DNA—below the detection limit of Southern blot—could remain in the virus stock. Alternatively, a PCR-based assay, such as droplet digital PCR (ddPCR), could provide a more sensitive and quantitative measurement of the amount of rHBV-CreN DNA (genome equivalent, GE) and plasmid DNA.

To broaden the application of this CreN-based HBV reporter system, different rHBV-CreN vector designs to fulfill various research purposes would be useful to explore. Since Cre-lox recombination does not require a large amount of Cre recombinase, it is not necessary to use a strong promoter or enhancer, such as TTR, to regulate the expression of Co-InCreN. Instead, using the endogenous HBV preS/S promoter to drive Co-InCreN expression would be closer to the nature of viral protein expression upon HBV infection. Furthermore, HBV surface proteins are not expressed from the current rHBV-CreN vector (Figure 17, Lane 2); therefore, it cannot be used for studies where HBsAg is involved (for example, the

anti-viral activity of S-CAR–expressing $CD8^+$ T cells) [51, 107]. In the present study, generating another rHBV-CreN vector by replacing the HBc coding region with a Co-InCreN cassette allows surface proteins to be expressed from the cccDNA derived from this vector, which could subsequently serve as a tool for such applications. Moreover, a replication-competent rHBV-CreN vector can be utilized for studies or screenings that demand virus generated from infected cells, such as analyzing the cell-to-cell spread of HBV. This type of vector can be achieved by inserting the Co-InCreN cassette into the site between the HBc coding region and the polymerase coding region of the HBV replication-competent vector [70]. Since the Co-InCreN sequence does not affect rHBV replication and the production of rHBV-CreN provides a high yield, it is technically feasible to adapt this cassette to other types of rHBV vectors, from which a range of possible applications can arise.

3.2.3 Generation of a Cre reporter cell line

A HepG2-NTCP cell line engineered to express C-terminal Cre and to detect Cre-lox recombination was generated by delivering the Co-InCreC and loxP-flanked neo-pA cassette into the host cell genome (named HepG2-NTCP-CreC-CIR cells, CreC/CIR). CreC/CIR cells were permissive for wtHBV infection and the level of cccDNA and HBeAg observed in infected CreC/CIR cells was comparable to that of its parental cells, HepG2-NTCP (Figure 22). In addition, Cre recombinase activity was tightly controlled by the complementation of Co-InCreN and Co-InCreC in CreC/CIR cells, since the constant expression of Co-InCreC did not lead to the expression of DsRed in CreC/CIR cells, as indicated by a lack of red fluorescence signal detected in the cells (Figure 21A, left image). Moreover, in the presence of Co-InCreN in the CreC/CIR cells, DsRed-positive cells were observed by microscopy, and the number of DsRed-positive cells could be determined by FACS analysis (Figure 21A, right image, and Figure 21B), confirming the functionality of the Cre complementation.

Notably, the percentage of DsRed-positive cells was quite low (13%), and the fluorescence intensity was below the detection limit of the fluorescence microplate reader (data not shown). This can be explained by low transfection efficiency, the homogeneity of CIR/CreC cells, and the cytotoxic effect of DsRed. A possible complementation efficiency problem in the Co-InCre system could be excluded, as Cre activity following the complementation of Cre fragments was comparable to that of the wild-type Cre, which was previously confirmed in HepG2-NTCP cells (data not shown). To tackle the issue of low DsRed-positive cell numbers in the presence of CreN in the CreC/CIR cells, a second round of cell clone selection was conducted using the limiting dilution method. Preliminary results

showed a higher percentage of DsRed-positive cells in the presence of Co-InCreN (data not shown), indicating that the homogeneity of CIR/CreC cells could be the main reason for low DsRed-positive cell numbers being observed in the present study. Further analysis of copy numbers of the Co-InCreC cassette, as well as of the Cre-induced DsRed cassette via ddPCR, will provide us with more detailed information regarding the homogeneity of the cell line.

It is known that red fluorescent proteins are cytotoxic, and replacing the Cre-induced DsRed with a non-cytotoxic DsRed variant (DsRed-Express2) can circumvent this issue [66]. In addition, other types of reporter genes can be utilized for reporting the Cre-lox recombination upon rHBV-CreN infection, such as LNGFR, could be used for rapid isolation of infected cells [69]; alternatively, luciferase could promote a more convenient and sensitive readout of the infection [77]. The flexibility of using multiple reporters simultaneously regulated by Cre recombinase makes the Cre reporter cell line convenient for meeting a variety of experimental requirements.

3.2.4 Infection of the Cre reporter cells with rHBV-CreN

The infection of CreC/CIR cells with an increasing MOI of rHBV-CreN resulted in a concomitant increase in the percentage of DsRed-positive cells (Figure 23). However, the highest percentage of DsRed-positive cells was approximately 8% while using an extremely high MOI (MOI = 1600). Two aspects could influence the low frequency of DsRed-positive cells: Cre reporter cells and infection with rHBV-CreN. As described in the previous section (3.2.3), a sub-optimal homogeneity of reporter cells could lead to the underestimation of Cre-lox recombination events since infected cells might not express Co-InCreC and not contain the Cre-induced DsRed cassette. Furthermore, it is known that HBV envelope proteins are also secreted as empty subviral particles (SVPs) that do not contain any HBV genome [108]. Part of these SVPs (e.g. the filamentous form containing L protein) are co-purified from the heparin column and can compete with infectious particles for binding of the HBV entry receptor on the cells (NTCP). Thus, SVPs in the virus stock can affect the uptake efficiency of rHBV-CreN and lead to a reduced infection rate of rHBV-CreN.

The kinetics of DsRed expression levels in the rHBV-infected cells closely correlated with HBeAg level in infected cells between 4 and 13 dpi (Figure 24), suggesting that a change in the DsRed signal level of rHBV-CreN infected cells could be used to monitor rHBV infection. Moreover, detection of HBeAg in the supernatant at 1 dpi was most likely due to remaining HBeAg (or empty capsid)

derived from the inoculum. The modest decrease of DsRed-positive cells observed at 16 dpi is likely due to the cytotoxic effect of DsRed in the cells, as described in 3.2.3.

The establishment of cccDNA pool is prerequisite for HBV infection [16]. Additionally, the cccDNA level in rHBV-CreN-infected cells decreased after 4 dpi (Figure 25), whereas the cccDNA level in wtHBV-infected HepG2-NTCP cells remained stable for up to a 6-week culture period [109]. This difference could be attributed to the influence of the foreign sequence (Co-InCreN) on the host factor-mediated repair of cccDNA or the maintenance of cccDNA in CIR/CreC cells. Nevertheless, the lack of both: 1) rcDNA re-import into the nucleus of the rHBV-CreN infected cells, and 2) secondary infection events mediated by newly-produced virions should also be taken into account, which could also attribute to lower cccDNA content in rHBV-infected cells [109]. Since the coding sequences of the polymerase and surface proteins are disrupted in rHBV-CreN cccDNA, the replication of rHBV-CreN in infected cells cannot occur. Therefore, no capsid containing rHBV-CreN DNA will be produced and subsequent re-import and superinfection events will not occur. Notably, the kinetics of PF-rcDNA in the rHBV-CreN-infected cells was similar to that of wtHBV-infected cells (data not shown) indicating equal efficiency of initial infection establishment (rcDNA to cccDNA conversion).
The receptor dependency of rHBV-CreN was examined using an entry inhibitor (MyrB) that competes with HBV surface protein binding to the HBV entry receptor, NTCP [37, 95]. As shown in Figure 26, rHBV-CreN infection was blocked in the presence of MyrB, since neither the DsRed signal nor the HBeAg expression was detectable in the MyrB-treated cells.

Surprisingly, the HBeAg level of rHBV-CreN infected CreC/CIR cells was much lower than that of wtHBV-infected CreC/CIR cells (Figure 26C). Since HBeAg expression is closely related to the size of the cccDNA pool, the lower amount of cccDNA detected in CreC/CIR cells infected with rHBV-CreN compared to that of cells infected with wtHBV (data not shown) most likely causes the lower HBeAg level. Moreover, in contrast to the rHBV-CreN stock preparation, SVPs in the wtHBV virus stock were further removed using sucrose density gradient centrifugation following heparin affinity chromatography. Therefore, the reduced amount of cccDNA presented in the cells infected with rHBV-CreN could be the result of inefficient rHBV-CreN uptake due to the competition of SVPs binding for entry receptors. Therefore, including an additional purification step with sucrose density gradient centrifugation to remove the SVPs in the rHBV-CreN stock would address this issue. Another potential factor influencing this phenomenon is the efficiency of rHBV-CreN cccDNA formation, since the HBV PreS/S regions were replaced by

the TTR-Co-InCreN cassette sequence and part of the HBV EN1 sequence was deleted. Therefore, the host DNA repair machinery—which is utilized by wtHBV—might be less efficient at converting rHBV-CreN rcDNA to rHBV-CreN cccDNA.

Nevertheless, the blockade of rHBV-CreN entry by MyrB treatment, rHBV-CreN cccDNA formation, and HBeAg expression in rHBV-infected CreC/CIR cells demonstrated that the infection of in the CreC/CIR cells is analogous to that of wtHBV. Moreover, DsRed expression, which is closely correlated to that of HBeAg expression, highlights the functionality of the rHBV-CreN reporter system and the suitability of this reporter system for monitoring HBV infection.

3.3 Conclusion and perspectives

This thesis demonstrates different strategies for constructing a recombinant reporter HBV vector, including the adaptation of novel types of reporter genes and the utilization of innovative measures to insert the reporter gene sequence into the rHBV vector. Detailed analyses of the rHBV production using the trans-complementation method are described. In addition, methods including the magnetic sorting of hepatoma cells and materials such as the Cre reporter cell line were established and characterized. Finally, rHBV-CreN infection in the CreC/CIR cells was investigated. The rHBV-CreN reporter system proved superior and represented all features of a natural HBV infection. It could be employed in various applications, including screening of inhibitors or host factors involved in the early stages of HBV infection (cccDNA formation), monitoring the fate of infected cells after immunotherapies (e.g. antibody-based T cells therapies, IFNs), and the transcriptomic or proteomic profiling of infected cells. Altogether, the establishment of a novel reporter system using the infection of CreC/CIR cells with rHBV-CreN reporter virus provides a new platform for conducting HBV infection studies in a more convenient fashion.

4 Materials and Methods

Following section provides the list of the materials and the description of the methods utilized in the present study.

4.1 Materials

All the materials, including chemicals, reagents, enzymes, kits, oligos, antibodies, laboratory equipment and consumables are listed in this section. The information of plasmids and cell lines are provided. The formulas of chemical solutions and cell culture media are described.

4.1.1 Chemicals and reagents

Name	**Supplier**
25X Protease inhibitor cocktail	Roche, #11836153001
Agar	Roth, 5210.3
Agarose	Peqlab, # 35-1020
Ampicillin	Roth, #K029.1
Bovine Serum Albumin V (BSA)	Roth, #8076.3
Bromphenolblue (BPB)	Roth, #A512.1
Chloroform (Trichlormethan)	Roth, #3313.1
Collagen R solution, 0.2%	Serva, #47256
Di-Sodium hydrogen phosphate (Na_2HPO_4)	Roth, #P030.1
Dimethyl sulfoxide- hybri max (DMSO)	Sigma, #D2650
Dulbecco's Modified Eagle Medium (DMEM, high glucose), 1X	Gibco, #11960-044
Dulbecco's Modified Eagle Medium: Nutrient Mixture F-12 (DMEM/F-12), 1X	Gibco, #11320-074
Ethylendiamin-tetraaceticacid (EDTA)	Roth, #8043.2
Ethidium bromide (solution), 0.027%	Roth, #HP47.1
FBS, Qualified, HI	Gibco, #10500-064
Formaldehyde, 37%	Roth, #CP10.1
Formamide	Roth, #6749.1
FuGeneHD	Promega
Geneticin	Gibco, #10131-027
Gentamicin	Ratiopharm
Glycerol	Roth, #3783.1
Glycine	Roth, #3908.2
Glycogen (5 mg/ ml)	Ambion, #AM9510
Glucose solution, 200 g/L	Gibco, #A24940-01
Hepes buffer solution, 1M	Gibco, #15630-056
Hydrochlorid acid (1N)	Roth, #K025.1
Hydrocortisone	Pfizer

Insulin	Sanofi Aventis
L-Glutamine, 200 mM	Gibco, #25030-024
Methanol	Roth, #4627.5
Milk powder	Roth, #T145.2
MOPS	Roth, #6979.4
Non-essential amino acids, 100X	Gibco, #11140-035
3-(4,5-Dimethylthiazol-2-yl)-2,5-Diphenyltetrazolium Bromide (MTT)	Provided by I. Jeremias
NP-40	Fluka, #74385
PBS, 10X, pH 7.4	Gibco, #70011-036
Penicillin-Streptomycin	Gibco, #15140-122
Phenol/chloroform/isoamyl alcohol (25:24:1)	Roth, A156.2
Polyethylene glycol (PEG) 6000	Merck, #8.07491.1000
RIPA buffer	Pierce, #89900
RNase A (50 mg/ml)	Applichem, #2760.0100
Salmon sperm DNA	SIGMA, #D1626
Sodium acetate	Roth, #X891.2
Sodium chloride (NaCl), 99.5%	Roth, #3957.2
Sodium dihydrogen phosphate (NaH_2PO_4)	Roth, #T879.2
Sodium dodecansulfate (SDS), ultra-pure, 99.5%	Roth, #2326.2
Sodium hydroxide (NaOH)	Roth, #P031.2
Sodium pyruvate, 100 mM	Gibco
Tris-HCl	Roth, #4855.3
Tris base	Roth, #4855.3
Tri-Sodium citrate ($C_6H_5Na_3O_7$)	Roth, #3580.1
TRIzol	Ambion, #15596-018
Trypsin-EDTA, 0.5%	Gibco, #15400-054
Tryptone	Roth, #8952.2
Tween 20	Roth, #9127.1
Versene, 1:5000	Gibco, #15040-033
William's E medium, 1X	Gibco, #22551-022
Xylene cyanol FF	In-house
Yeast extract	Roth, #2363.3

4.1.2 Formula of chemical solutions

Name	**Formula**
6X cccDNA loading dye	10 mM EDTA (pH 8.0), 50 % glycerol, 0.25 % (w/v) BPB
10X NB loading dye	10 mM EDTA (pH8.0), 50 % glycerol, 0.25 % BPB, 0.25 % Xylene cyanol FF
20X SSC	3 M NaCl, 0.3 M Tri-Sodium citrate dihydrate, pH 7
6X DNA loading buffer	10 mM Tris-HCl (pH 7.5), 60 mM EDTA, 60% glycerol, 0.1% BPB, 0.1% Xylene cyanol FF
Heparin column Binding buffer	0.8 mM KH_2PO_4, 116.4 mM NaCl, and 2.2 mM Na_2HPO_4 (75 % of 1X PBS)

Heparin column rDNase solution	20 mM Tris, pH7.5, 10 mM MgCl2, 5 mM CaCl2, and 200 U rDNase
Heparin column Elution buffer	3.2 mM KH_2PO_4, 466 mM NaCl, and 8.9 mM Na_2HPO_4 (3X PBS)
Hirt lysis buffer	50 mM Tris–HCl, pH 7.4, 10 mM EDTA, 150 mM NaCl, and 1% SDS
LB medium	10 g/L Tryptone, 5 g/L Yeast extract, 10 g/L NaCl
LB agar plate	10 g/L Tryptone, 5 g/L Yeast extract, 10 g/L NaCl, 15 g/L agar
MOPS buffer	20 mM MOPS, pH 7.0, 2 mM sodium acetate, and 1 mM EDTA
NaPi, 1M, pH 7.2	31.6 ml of 1M NaH_2PO_4 and 68.4 ml of 1M Na_2HPO_4
PEG precipitation solution	26% PEG 6000, 350 mM NaCl, 10 mM EDTA
Pre-Hybridization buffer	1 % BSA, 1 mM EDTA, 500 mM NaPi, 0.7 % SDS
SB core Lysis buffer	50 mM Tris-HCl (pH 8.0), 100 mM NaCl, 1 mM EDTA, 1% NP-40
SDS-PAGE running buffer	3 g/L Tris base, 14.4g/L glycine, 1 g/L SDS
SSC washing solutions	2X or 0.5X SSC with 0.1 % SDS
TBST	200 mM Tris base, 1.5 M NaCl, 0.1% Tween 20
TNE buffer	10 mM Tris-HCl (pH 7.5), 150 mM NaCl, and 1 mM EDTA
Western blot transfer buffer	3 g/L Tris base, 14.4g/L glycine, 20 % methanol

4.1.3 Enzymes and Kits

Name	**Suppliers**
Amersham ECL Prime Western Blotting Detection Reagent	GE Healthcare
CloneJET PCR Cloning Kit	Thermo Scientific, #K1231
DIG Luminescent Detection Kit	Roche, #1 363 514
DNase I (10 U/ml)	Roche, #04716728001
Enzygnost HBe monoclonal	Siemens, #OQDM11
FastDigest *Kpn*I	Thermo Scientific, #FD0524
FastDigest *Kpn2*I	Thermo Scientific, #FD0534
FastDigest *Hind*III	Thermo Scientific, #FD0504
FastDigest *Pvu*I	Thermo Scientific, #FD0624
FastDigest *Spe*I	Thermo Scientific, #FD1253
FastDigest *Sph*I	Thermo Scientific, #FD0604
GeneJET Gel Extraction Kit	Thermo Scientific, #K0691
GeneJET Plasmid Miniprep Kit	Thermo Scientific, #K0503
KOD Hot Start DNA Polymerase	Novagen, # 71086
NucleoSpin® Tissue	Macherey-Nagel, #740952.250
LightCycler 480 SYBR Green I Master mix	Roche
LIVE/DEAD™ Fixable Near-IR Dead Cell Stain Kit	Invitrogen, #L10119
MACSelect LNGFR MicroBeads	Miltenyi Biotec, #130-091-330
Phusion® Hot Start Flex DNA Polymerase	NEB, #M0535S

QIAamp® DNA Mini kit	Qiagen, #51304
QIAamp® MinElute® Virus Spin Kit	Qiagen, #57704
QIAGEN Plasmid Plus Midi Kit	Qiagen, #12943
QIAquick Gel Extraction Kit	Qiagen, #28704
T4 DNA Ligase	Thermo Scientific, #EL0011
T5 exonuclease	New England BioLab, #M0363L

4.1.4 Oligos

Cloning primers	**Sequence**
F-*Kpn*I-LNGFR-WC	GGTACCATGGGGGCAGGTGCCACC
R-*Hind*III-LNGFR-WC	AAGCTTTCAGTTCCACCTCTTGAAGG
F-*Kpn*I-SV40 NLS_WC	GGTACCATGCCCAAGAAGAAGAGGAAG
R-*Hind*III-gp41_WC	AAGCTTTCACTCCTTCACGTACAGGC
B-Cm-5	GATTTTCAGGAGCTAAGGAAGC
17-1-3(v)	TAGGCAGAGGTGAAAAAGTTGCATGGTGGCCTATAGTGAGTCGTATTAAG
resD-for	CGCCTCCCCAATCCAGGTCC
17-2-3a	GGGAGAGAGGAGGGAAGAGGAGTCAAGGAATACTAACATTGAGATTCCCG
17-2-3b	TCCAGACCAGGCCAGGTATCTCTGACCTGTGGGAGAGAGGAGGGAAGAGG
17-4-3a	GGTCAGTAAATTGGACATGGTGGCTTATTAATGTTCAGCGCAGGGTCCCC
17-4-3b	GACCGGTAATGCAGGCAAATTTTGGTGTACGGTCAGTAAATTGGACATGG
17-5-3a	GATTGAATACATGACTTACCTGAGTCATCCTTAGCGCCGTAAATCAATCG
17-5-3b	TTGGCGAGAAAGTGAAAGCCTGCTTAGATTGAATACATGACTTACCTGAG
parC-rev	AACCGGGCTGCATCCGATGC
17-3D-5	GGTGCGCCTGCTGGAAGATGGCGATTAGGTTACCAAATATTTACCATTGG
17-4(K)-3	GAGGATTGCTGGTGGAAAGATTCTGCCCTCAGAAGAACTCGTCAAGAAGG
12-1-3new	AACCGGGCTGCATCCGATGCAAGTGTGTCGGTCTGACAGTTACCAATGC
17-6-5	TTCTGACTTCTTTCCTTCAGTACGAGATCGCACAATTCGAGCTCGGTACC
17-7-5	ACCATATTCTTGGGAACAAGATCTACAGCTGAGGGCAGAATCTTTCCACC

Southern/Northern blotting probes	**Sequence**
Forward primer for Full-length HBV probe	TTCTAGATACCGCCTCAGCTCT
Reverse primer for Full-length HBV probe	TGGTGCGCAGACCAATTTAT
Forward primer for HBc probe	TTCAGGCAACTCTTGTGG
Reverse primer for HBc probe	TGAGGCGCTATGTGTTGT
Forward primer for HBx probe	ATGGCTGCTAGGCTGTGCTG
Reverse primer for HBx probe	TGGTGCGCAGACCAATTTAT

PCR/qPCR primers	Sequence
F-CALNL-4658_WC	CAACGTGCTGGTTATTGTGC
R-CALNL-6442_WC	TGGTCTTCTTCTGCATCACG
cccDNA 92 fw	AGCTGAGGCGGTATCTA
cccDNA 2251 rev	GCCTATTGATTGGAAAGTATGT
PRNP fw	TGCTGGGAAGTGCCATGAG
PRNP rev	CGGTGCATGTTTTCACGATAGTA

4.1.5 Plasmids

Name	Suppliers
pCAG-Co-InCreC	A gift from Pawel Pelczar (Addgene plasmid # 51268)
pCAG-Co-InCreN	A gift from Pawel Pelczar (Addgene plasmid # 51267)
pCALNL-DsRed	A gift from Connie Cepko (Addgene plasmid # 13769)
pCDH-EF1a-Cas9-T2A-NGFR	A gift from Irmela Jeremias, Ludwig Maximilians University (IJ258)
pCMV-Pol	A gift from Wang-Shick Ryu, Yonsei University
pCH-TTR-Puro	Generated in-house
pCH-9/3091	Generated in-house (No. 25)
pJET1.2	Thermo Scientific, #K1231
pMH 3142 An ß glob	Generated in-house (No. 28)

4.1.6 Antibodies

Name	Application/Dilution	Suppliers
Anti-LNGFR-PerCP-Cy5.5	FACS/1:100	BioLegend (provided by I. Jeremias) [110]
Anti-mouse IgG-PerCP-Cy5.5	FACS/1:100	BioLegend (provided by I. Jeremias)
Mouse Anti-α-Tubulin	WB/1:5000	Sigma-Aldrich, #T5168
Mouse Anti-HBc (8C9)	WB/1:1	Provided by E. Kremmer
Rabbit Anti-HBs (H863)	WB/1:5000	Provided by H.Schaller
Mouse Anti-HBx (2F9)	WB/1:500	Virostat
Anti-mouse	WB/1:10,000	Sigma-Aldrich, #A0168
Anti-rabbit	WB/1:10,000	Sigma-Aldrich, #A0545
MACSelect Control FITC Antibody	FACS/1:30	Miltenyi Biotec, #130-090-326

4.1.7 Cell lines and bacteria

Name	Description
HepAD38	HepG2-based wtHBV-producing cell line [49]
HepG2-NTCP-K7	HepG2-based NTCP-overexpressing cell line [109]
Huh7	Huh7 cells was derived from a well-differentiated HCC [111]
Stbl3	Chemically Competent E. coli (Invitrogen)
SW102	E. coli contains a bacterial artificial chromosome (BAC) and a defective temperature-sensitive λ prophage [112]

4.1.8 Cell culture media

Media	Ingredients (including supplements)
DMEM/F12-full medium	DMEM/F-12, 10% FBS, 50,000 U Penicillin-Streptomycin
DMEM-full medium	DMEM (high glucose), 10% FBS, 50,000 U Penicillin-Streptomycin, 2 mM glutamine, 1 mM sodium pyruvate, 0.1 mM non-essential amino acids
DMEM transfection medium	DMEM (high glucose), 2 mM Glutamine, 1 mM sodium pyruvate, 0.1 mM non-essential amino acids
OPTI-MEM Reduced Serum medium	-
rHBV production medium I	0.5X DMEM (high glucose), 0.5X William's E medium, 5% FBS, 0.025% Glucose, 10 mM Hepes (pH 7.4), 2 mM Glutamine, 50,000 U Penicillin-Streptomycin, 3% DMSO, 20 mg of Gentamicin, 1.3 mg of hydrocortisone, and 6.4 IE of Insulin, 0.5 mM sodium pyruvate, 0.05 mM non-essential amino acids
rHBV production medium II	William's E medium, 5% FBS, 0.05 % Glucose, 20 mM Hepes (pH 7.4), 2 mM Glutamine, 50,000 U Penicillin-Streptomycin, 2% DMSO, 40 mg of Gentamicin, 2.6 mg of hydrocortisone, and 12.8 IE of Insulin

4.1.9 Laboratory equipment and consumables

Items	Supplier
Amersham Hybond-XL (charged nylon membrane)	GE Healthcare, #RPN303 S
ARCHITECT HBeAg assay	Abbott Laboratories
BEP III system	Siemens Healthcare
BD Falcon 35um Cell Strainer	BD, #352235
CELLSTAR® Polypropylene Tube, 15/50 ml	Greiner Bio-One
Centrifuges	Beckman Coulter, Avanti J-26 XP

Centrifuges	Eppendorf, #5417C, #5417R, #5810R, #5920R
Corex glass tube, 15 ml	-
Countess™ Automated Cell Counter	Invitrogen
CRYO.S, 2 ml	Greiner Bio-One, #122263
CytoFLEX S	Beckman Coulter
FACSAria	BD Biosciences
FACSCanto	BD Biosciences
Fluorescence microscopy CKX41	Olympus
Fusion FX7 imaging system	Peqlab
HiTrap Heparin HP (5 ml)	GE Healthcare, #17-0407-03
Hybridization bags	Roche, #11 666 649 001
Hybridization oven	Thermo Scientific, #HBSNSR220
Immun-Blot PVDF membrane	Bio-Rad, # 162-0177
Intas ECL ChemoCam	INTAS Science Imaging
LightCycler 480 Instrument	Roche Molecular Systems
LS column (MACS column)	Miltenyi Biotec
Micro-plate reader	TECAN
MidiMACS™ Separator	Miltenyi Biotec
Mini Trans-Blot® Cell	Bio-Rad
Multimode Plate reader Infinite F200	Tecan Group Ltd
NanoDrop microvolume spectrophotometers	Thermo Scientific
PerfectBlue™ Gel System Mini L	Peqlab
Peristaltic pump, Masterflex L/S	Core-Parmer
Peristaltic tubes	Core-Parmer
Serological Pipettes	Greiner Bio-One
Stericup® filter unit	Merckmillpore, #SCHVU05RE
qPCR 96-well plates	4titude
Thermocycler T3000	Biometra
ThermoMixer F1.5	Eppendorf
Tissue culture test plates	TPP Techno Plastic Products AG
Tissue culture test flasks	TPP Techno Plastic Products AG
Ultrafiltration tube, Vivaspin Turbo 15 (50,000 MWCO)	Sartorius
UV-Crosslinker	Vilber Lourmat, #BLX-E254

4.1.10 Software

Name	**Supplier**
cellSens Standard (1.7.1)	Olympus
CytExpert (2.1)	Beckman Coulter
FlowJo (v10)	FlowJo, LLC
ImageJ (1.46r)	National Institutes of Health, USA
i-Control for infinite reader (1.10)	Tecan Group Ltd
LightCycler 480 SW (1.5.1)	Roche

Prism 5 (5.01.336)	GraphPad Software
Serial cloner (2.6.1)	Serial Basics

4.2 Methods

All the experimental procedures applied in the present study are described in the following section.

4.2.1 Molecular cloning

Sequences of *Kp*nI and *Hind*III restriction sites were introduced to the 5' and 3' of the coding sequence of LNGFR and Co-InCreN, respectively, by polymerase chain reaction (PCR) using Phusion® Hot Start Flex DNA Polymerase. The PCR mixture was composed of 10 ng of plasmid DNA, 1X Phusion HF Buffer, 0.2 mM dNTPs, 0.5 μM primers, 3% DMSO, 1 unit of Phusion Hot Start Flex DNA Polymerase in nuclease-free water. The reaction was performed by using the following thermocycle: 1 cycle of denaturation at 98 ˚C for 30 seconds, 35 cycles of amplification (98 ˚C for 10 seconds, 60 ˚C for 30 seconds, 72 ˚C for 1 minute), and 1 cycle of extension at 72 ˚C for 1 minute. The PCR products were analyzed by agarose gel electrophoresis and the bands with the correct size were cut out. DNA was extracted from the gel piece by using GeneJET Gel Extraction Kit following the manufacturer's instructions with an elution volume of 30 μl. The isolated DNA fragment was ligated into a blunt-end vector, pJET1.2, using CloneJET PCR Cloning Kit. The ligation mixture (5 μl) was incubated with 50 μl of Stbl3 chemically competent E. coli cells (prepared in-house) at 4 °C for 30 minutes. Following 50 seconds of heat-shock and two minutes of 4 °C incubation, 850 μl of LB medium was added to the transformed bacteria and the bacteria were grown in a 37 °C shaking incubator for at least one hour. The bacteria culture (300 μl) was then spread on a LB agar plate containing 100 μg/ml ampicillin and the plate was incubated at 37 °C overnight. On the next day, colonies were picked and incubated in 2 ml of LB medium containing 100 μg/ml ampicillin at 37 °C overnight. The plasmid DNA was isolated from the bacteria culture using GeneJET Plasmid Miniprep Kit. To confirm the insertion of the transgenes, the purified plasmid was subjected to restriction enzyme digestion using FastDigest enzymes following the manufacturer's instructions, then the digested DNA was analyzed by agarose gel electrophoresis.

The correct pJET plasmids containing the LNGFR or the Co-InCreN cassette were then used for sub-cloning the cassette into the rHBV vector. The sub-cloning procedure began with obtaining the insert DNA (LNGFR or Co-InCreN) and the vector DNA (an rHBV vector, named pCH-TTR-Puro) by digesting the plasmids with restriction enzymes *Kp*nI and *Hind*III. The digested samples were subjected to

agarose gel electrophoresis and the DNA fragments with the expected sizes were extracted using GeneJET Gel Extraction Kit. Ligation of the insert and vector (in a 3:1 ratio) was achieved by using a T4 DNA Ligase following the manufacturer's instructions. Transformation and plasmid DNA isolation were performed as described above. The positive clones were identified by restriction enzyme digestion, and subsequently subjected to Sanger sequencing (Eurofins genomics co.) for analyzing the sequence of the insert. The large-scale preparation of plasmids for transfection was conducted by using a 100 ml bacterial culture and the QIAGEN Plasmid Plus Midi Kit following the manufacturer's instructions.

Cre revenant cassette was assembled by joining the 5'Cre and 3'Cre with the HBV fragments (core, preS and X) using bacterial artificial chromosome (BAC) recombineering (Fig. 27) [112, 113]. Homologous recombination sites were introduced to 5' and 3' end of the insert DNA by PCR using KOD Hot Start DNA Polymerase. The PCR mixture was prepared according to the manufacturer's instruction with 50 ng of a restriction enzyme-digested templated DNA. The thermocycle was set up as followed: 1 cycle of denaturation at 95 ˚C for 2 minutes, 35 cycles of amplification (95 ˚C for 20 seconds, 55 ˚C for 20 seconds, 70 ˚C for 25 seconds/kb), and 1 cycle of extension at 70 ˚C for 3 minutes. The PCR product was first analyzed by agarose gel electrophoresis and subsequently extracted from the gel using QIAquick Gel Extraction Kit. SW102 bacteria containing the target BAC was heat-shocked at 42 ˚C to allow the recombinase activation, and subsequently the purified PCR product was electroporated into the bacteria [112]. BAC derived from the colonies was isolated using BAC minipreps method [112]. The verification of the recombination was conducted by using PCR to amplify the recombination region and subsequently analyzed by agarose gel electrophoresis. The assembled Cre revenant cassette was then sub-cloned into the rHBV vector using *Kpn*2I and *Sph*I restriction sites.

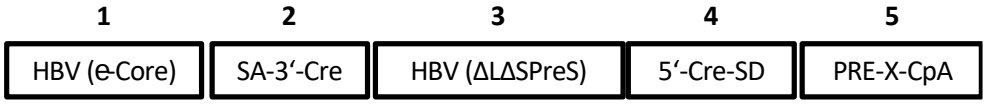

Fig. 27 Assembling of Cre revenant cassette by BAC recombineering

Fragment 1 contains the sequence of epsilon and HBV core coding sequence, fragment 2 contains sequences of splicing acceptor and 3' Cre, fragment 3 contains the sequence of PreS region with mutations at the ATG sites of the large and small envelope proteins coding sequences, fragment 4 contains sequences of 5' Cre and splicing donor, and fragment 5 contains the sequence of EhnI, X, and polyA site.

The plasmid (named pCAG-CreC-CANLNL-dsRed) containing the Co-InCreC cassette and the loxp-Neo-loxp-DsRed cassette was generated by sub-cloning procedure described above. The Co-InCreC cassette was obtained from pCAG-Co-InCreC digested with *Pvu*I and *Spe*I, and subsequently inserted into the Cre-induce dsRed plasmid (pCALNL-dsRed).

4.2.2 Cell culture

HepG2-NTCP-K7 cells, CreC/CIR cells and Huh7 cells were maintained in DMEM-full medium. HepG2-NTCP-K7 cells is a HepG2-based cell clone stably expressing NTCP. It was generated in-house using the lentiviral transduction procedure to integrate the CMV-NTCP cassette into the genome of HepG2 cells. CreC/CIR cells is a HepG2-NTCP-based cell clone containing the cassette loxp-Neo-loxp-DsRed and stably expressing the Co-InCreC. The cell line was generated by transfecting the plasmid pCAG-CreC-CALNL-dsRed (see 4.2.1) into HepG2-NTCP-K7 cells. Subsequent selection of neomycin-resistant clones was achieved by culturing the cells in the presence of geneticin (2 mg/ml). HepAD38 cells were maintained in DMEM/F12-full medium. It is a cell line containing two integrated HBV genomes (serotype type ayw) and constantly producing wtHBV [Lander 1997].

4.2.3 Transfection

Approximately 0.4 million of HepG2-NTCP cells were seeded on a 12-well plate one day prior to transfection. OPTI medium (45 μl) was added to the microcentrifuge tube containing 1 μg of DNA, then 4.5 μl of FuGeneHD transfection reagent was added to the OPTI-DNA solution. The mixture was incubated at room temperature for 15 minutes. Cells at 80% confluency was changed to DMEM transfection medium (0.5 ml) and the transfection mixture was slowly applied to the cells. After incubation for 16 hours at the a 37 °C cell culture incubator, the medium was replaced by DMEM-full containing 2.5% DMSO.

4.2.4 Magnetic activated cell sorting (MACS)

HepG2-NTCP-K7 cells were detached from the culture vessels using a trypsin-versene mixture (1:1). The cell suspension was passed through a cell strainer. Cells were pelleted by centrifugation and resuspended in PBE (PBS supplemented with 0.5% BSA and 5 mM EDTA) to a concentration of 2×10^6 cells/ml. An aliquot of cells was taken as the transfection sample. MACSelect LNGFR MicroBeads (1 ml per 25000 cells) were added to the cells and the reaction was conducted at 4 °C for 20 minutes. The volume of the mixture was adjusted to 2 ml and passed through a cell strainer again. An aliquot of cells was taken as the MicroBeads-labeled sample. Then, the cells were loaded onto the LS column in aliquots of 500 μl. The column was washed with 3 ml of PBE for four times. The flow-through was collected as the negative fraction sample. The column was removed from the separator and the cells (positive/bound fraction) were eluted with 5 ml of PBE.

4.2.5 Cell viability assays

Cell counting was performed by using Countess™ Automated Cell Counter according to the manufacturer's instructions. MTT assay was perform by incubating cells with MTT for two hours in a 37 °C cell culture incubator. The MTT formazan precipitate was dissolved in DMSO, then the absorbance (595 nm) was measured using a micro-plate reader. The value of MTT solution (blank) was subtracted from raw values detected for all samples and the average of three biological replicates is shown. The data was plotted using Prism 5.

4.2.6 Fluorescence activated cell sorting (FACS)

The procedure of cell collection was identical as described in 4.2.4, except that the cells were resuspended in 300 μl of FACS buffer (PBS containing 0.1% BSA) instead of PBE. For the staining of LNGFR molecules or MicroBeads, anti-LNGFR-PerCP-Cy5.5, or anti-Mouse IgG-PerCP-Cy5.5, or MACSelect Control FITC Antibody was added to the cells, respectively. The samples were incubated at 4 °C for 15 minutes and subsequently washed with FACS buffer for three times (350 xg, 5 minutes) to remove the unbound antibodies. Finally, the samples were analyzed by FACSCanto or sorted by FACSAria (with a 100 Micron nozzle). For analyzing the DsRed intensity and the DsRed-positive population of the cell samples, the cell samples were first incubated with LIVE/DEAD™ Fixable Near-Infrared dead cell stain kit at 4 °C for 30 minutes and washed with FACS buffer twice (350 xg, 5 minutes). The samples were then analyzed by CytoFLEX S. All the obtained data was analyzed by FlowJo software.

4.2.7 Recombinant HBV (rHBV) production

Huh7 cells were seeded on 9 cm dishes (6010 mm^2) and incubated until approx. 80% confluency was reached. Transfection was conducted by mixing 16 μg of DNA together with 0.8 ml of OPTI medium, and 48 μl of FuGene HD transfection reagent. The transfection mixture was incubation for 15 minutes at room temperature and then gently applied to the cells supplemented with 9 ml of DMEM transfection medium. On the next day, the transfected cells were first changed to the rHBV production medium I. After additional 24 hours of incubation, medium was changed to the rHBV production medium II. Thereafter, supernatant was collected every 4 days for 6 times. Cell debris was removed from the supernatant by centrifugation at 1,500 xg for 15 min. The virus-containing supernatant was stored at 4 °C until six collections were completed.

4.2.8 PEG precipitation of HBV/rHBV

The collections of supernatants derived from the virus-producing cells (4.2.7) were mixed with PEG precipitation solution in a 3:1 ratio. The reaction took place in a 15 ml Corex glass tube at 0 °C overnight. The precipitate was pelleted by centrifugation at 5,000 xg for 25 minutes at 4 °C. After removal of the supernatant, the pellet was dissolved in 200 μl TNE buffer.

4.2.9 Southern blotting analysis of capsid DNA

One million transfected Huh7 cells were lysed in 500 μl of SB lysis buffer and incubated on ice for 15 minutes. The cell debris was pelleted by centrifugation (12,000 rpm, 15 minutes, 4 °C) and the supernatant (cell lysate) was collected. DNaseI (0.01 Units) and RNaseA (100 μg) were then added to the cell lysate solution supplemented with 10 mM $MgCl_2$. The solution was incubated at 37 °C for three hours to digest the DNA and RNA from cell lysates. Centrifugation was used to remove the debris additionally, and the supernatant containing the capsids was collected. The precipitation of the capsids was achieved by incubating the capsid-containing solution with PEG (final concentration: 7% PEG 8000, 10 mM EDTA) overnight at 4 °C. The precipitate was collected by centrifugation (12,000 rpm for 15 minutes at 4 °C) and then dissolved in 200 μl of TNE buffer. DNA was isolated by using QIAamp® DNA Mini kit following the manufacturer's instructions and eluted in a volume of 25 μl. DNA samples (20 μl) were mixed with 6X DNA loading dye prior to agarose gel electrophoresis. The procedure of Southern blot capillary transfer was performed as described [114]. The cross-linked membrane was incubated with the pre-hybridization buffer at 65 °C for 2 hours. HBV-specific DNA probe was mixed with 100 μl of ssDNA and heated at 98 °C for three minutes, immediately followed by a cooling step. The probe solution was then added to the fresh pre-hybridization buffer, and the membrane was incubated with the solution overnight at 65 °C. After washing the membrane with SSC washing solutions, the membrane was developed using the DIG Luminescent Detection Kit following the manufacturer's instructions. Chemiluminescent signals were detected by an ECL Imager.

4.2.10 Southern blotting analysis of viral DNA

Viral DNA was isolated from virus stocks (see 4.2.8 or 4.2.11) by using QIAamp® MinElute® Virus Spin Kit (Qiagen). The isolation procedure was performed according to the manufacturer's instructions and the DNA was eluted in a volume of 25 μl. DNA was then subjected to Southern blotting analysis following the procedure described in 4.2.9.

4.2.11 Heparin affinity chromatography and rDNase on-column digestion

All collections of virus-containing supernatant (4.2.7) were pooled together and filtrated with a Stericup® filter unit (0.45 μm) to remove the cell debris and aggregates. Heparin affinity chromatography was set up by placing the peristaltic tube on the peristaltic pump, and then the heparin column was connected to the tube. The column was first washed with the elution buffer and then equilibrated with the binding buffer. The virus-containing supernatant was loaded onto a heparin column with a speed of 5 ml per minute, then the column was washed with 5 column volumes of the binding buffer. The column was removed from the peristaltic system and 6 ml of rDNase solution were applied to the column with a syringe. The column was incubated at room temperature for 1 hour, and then washed with 5 column volumes of the binding buffer. Virus was eluted with 4 column volumes of the elution buffer with a speed of 2 ml/minute. The eluate was first dilute in 1X PBS containing FBS. Subsequently, ultrafiltration tubes were used to reduce the total salt content and to concentrate the virus solution to a final volume of 0.1-0.2 ml. FBS (final concentration: 50%) and OPTI-MEM (final concentration: 25%) were then added to the virus stock and it was stored at -80 °C.

4.2.12 Northern blotting analysis of HBV RNA

RNA was isolated using TRIzol® reagent following the manufacturer's instructions and dissolved in 15 μl of ddH_2O. The amount of RNA was measured by NanoDrop microvolume spectrophotometers. 10 μg RNA was prepared in a solution containing 1X MOPS buffer, 2.2 M formaldehyde, 50% formamide and 0.5 μg of EtBr, and the RNA solution was heated at 65 °C for 10 minutes to remove RNA secondary structures. The RNA samples were then mixed with 10X NB loading dye and subjected to the electrophoresis with a 1% formaldehyde agarose gel, which was prepared by dissolving 1 gram of agarose in 1X MOPS buffer containing 7% formaldehyde. The gel was first exposed to UV light to examine the level of the reference RNA (28S/18S rRNA), then the gel was submerged in 50 mM NaOH solution for 5 minutes and in 20X SSC buffer for 20 minutes before the capillary

transfer. The procedure of membrane hybridization and development was identical to that of the Southern blot analysis (4.2.9).

4.2.13 Western blotting analysis

Medium was removed from the cells and then 250 µl of RIPA buffer containing 1X protease inhibitor cocktail was applied to the cells per well of a 6-well plate. After 5 minutes of incubation on ice, cell debris was pelleted by centrifugation (12,000 xg, 15 minutes, 4 °C) and the supernatant (protein lysate) was collected. Protein lysate was mixed with Laemmli buffer and denatured at 98 °C for 3 min. The protein samples were subjected to 12 or 15% Sodium dodecyl sulphate-polyacrylamide gel electrophoresis (SDS-PAGE). The electrophoresis was conducted in Western blot gel running buffer at 100 V (stacking gel) and subsequently at 140 V (separating gel) for two hours. The protein samples on the gel were blotted onto a PVDF membrane using a Mini Trans-Blot® Cell device (Bio-Rad). The transfer was conducted in Western blot transfer buffer at 300 mA for two hours. The blotted membrane was blocked with 5% milk-TBST at room temperature for one hour. The primary antibodies were diluted in 1.5% milk-TBST and the membranes were incubated in the antibody solutions at 4 °C overnight. On the next day, membranes were washed three times for 10 minutes each with TBST. The secondary antibodies were diluted in 1.5% milk-TBST and the membranes were incubated in the antibody solutions at room temperature for two hours. Finally, membranes were washed three times for 10 minutes each with TBST and developed using Amersham ECL Prime Western Blotting Detection Reagent. The chemiluminescent signal was detected by an ECL Imager.

4.2.14 HBV/rHBV infection

HepG2-NTCP cells or CreC/CIR cells were seeded in collagen-coated plates in DMEM-full medium with a density of 1.34×10^3 cells/mm^2. On the next day, medium was changed to the DMEM-full medium containing 2.5% DMSO. Infection was conducted either on the same day or two days later. The inoculum was prepared by first mixing PEG solution (final concentration: 4%) with DMEM-full medium containing 2.5% DMSO, and then the indicated amount of virus (4.2.11) according to the required MOI (25 to 1600) was added to the solution. Cells were incubated with the inoculum for 24 hours, and then were washed three times with PBS. Thereafter, the cells were cultured in DMEM-full medium containing 2.5% DMSO for indicated duration according to the experimental set-ups.

4.2.15 Fluorescence microscopy

Cells cultured on the cell culture vessel were analyzed under the fluorescence microscope (100x or 200x magnification). Red fluorescence signal (green excitation/ red emission) of the cells was recorded with an exposure time of 2 seconds. The bright field at the same position was taken with an exposure time of 250 micro-seconds.

4.2.16 HBeAg ELISA

Supernatant was collected from the HBV/rHBV-infected cells, cell debris was removed by centrifugation at 12, 000 rpm for three minutes at 4 ◦C. The samples were diluted 1:3 in PBS in a total volume of 300 µl. Absolute HBeAg concentration was quantified using ARCHITECT HBeAg assay. Alternative, relative HBeAg values were measured using a commercial qualitative immunoassay—Enzygnost HBe monoclonal and automated BEP III system.

4.2.17 Real-time quantitative PCR (qPCR)

Genomic DNA of the infected cells was isolated by using NucleoSpin® Tissue Kit according to the manufacturer's instructions. DNA samples were then treated with T5 exonuclease to reduce the amount of other HBV DNA species, including rcDNA, dslDNA, and PF-rcDNA. The T5 digestion was conducted by mixing 8.5 µl of total DNA sample with 5 units of T5 exonuclease in 1X T5 buffer, and then the mixture was incubated at 37 °C for 30 minutes. Subsequent heating at 99 °C for 5 minutes was required to inactivate the exonuclease. The T5-treated DNA samples were diluted four times in nuclease-free water to avoid that salts in the samples interfere with the downstream qPCR reaction. The diluted DNA (4 µl) was mixed with 2 µM of primers and 1X LightCycler 480 SYBR Green I Master mix in a total volume of 10 µl. The qPCR mixtures were loaded on a qPCR-grade 96-well plate, and HBV cccDNA and Prion protein (PRNP) gene were quantified using LightCycler 480 system instrument according to the literature [115]. The acquired data was analyzed using the advanced relative quantification method considering primer efficiency and normalization to the reference gene, PRNP.

4.2.18 Polymerase chain reaction (PCR)

Genomic DNA of the transfected cells was isolated using NucleoSpin® Tissue Kit according to the manufacturer's instructions. The PCR was set up as described in 4.2. 1, with an input of 250 ng of genomic DNA. PCR sample (5 μl) was mixed with 1 μl of 6X DNA loading buffer, and then the DNA was examined using agarose gel electrophoresis.

4.2.19 Southern blotting analysis of cccDNA

Cells derived from one well of the 6-well plate were incubated with 1 ml of Hirt lysis buffer for one hour at 37 °C. To precipitate proteins and protein-associated DNAs from the samples, KCl solution (0.5 M final concentration) was applied to the cell lysate and incubated for 16 hours at 4 °C. The precipitates were then removed by centrifugation (14,000 xg, 30 minutes, 4 °C) and the DNA in the supernatant was isolated using phenol/chloroform extraction procedure. Briefly, equal volume of phenol/chloroform/isoamyl alcohol (mixture in 25:24:1 ration) was added to the DNA-containing supernatant, and the separation of aqueous phase (DNA) and organic phase (proteins) was achieved by centrifugation (3,500 xg, 10 minutes, 4 °C). The phenol/chloroform extraction step was repeated twice to increase the purity of the DNA in the solution before precipitating the DNA by adding equal volume of isopropanol and 20 μg of glycogen. The precipitation was conducted at -20 °C for 16 hours. The DNA precipitates were collected by centrifugation (14,000 xg, 30 minutes, 4 °C), and the pellets were washed once with 70% ethanol. DNA was air-dried first to remove the residual ethanol before dissolving in 20 μl of ddH_2O. DNA samples (20 μl) were mixed with 10X cccDNA loading dye and the agarose gel electrophoresis was conducted at 20 V for 16-20 hours. The subsequent procedures, including Southern blot capillary transfer, membrane hybridization and membrane development, were identical to the procedure in 4.2.9.

5 Table of figures

Figure 1: Geographic distribution of HBV genotypes (reprinted from [11])....8
Figure 2: HBV structure (reprinted from [12])....8
Figure 3: HBV life cycle (reprinted from [16])....10
Figure 4: Depiction of the HBV genome organization (reprinted from [12])....11
Figure 5: Synthesis of the HBV genome (reprinted from [28])....12
Figure 6: The rHBV-LNGFR reporter system....23
Figure 7: Isolation of LNGFR-expressing cells via MACS....24
Figure 8: Proliferation of MACS-isolated HepG2-NTCP cells....25
Figure 9: Enrichment procedures for LNGFR-expressing cells....26
Figure 10: 1.1-fold wtHBV plasmid (pCH-9/3091) and rHBV-LNGFR transfer plasmid (pCH-TTR-LNGFR)....27
Figure 11: Genome structure of rHBV-LNGFR....29
Figure 12: Activation of the DsRed gene via Cre-lox recombination upon rHBV infection....30
Figure 13: rHBV-Cre revenant transfer plasmid and Cre expression upon circularization....31
Figure 14: Genome structure of rHBV-Cre revenant....33
Figure 15: The Co-InCre system and the rHBV-CreN transfer plasmid....34
Figure 16: Transcription of viral RNAs derived from the rHBV-CreN transfer plasmid....35
Figure 17: Expression of HBV viral proteins derived from rHBV-CreN transfer plasmid and the helper plasmid....36
Figure 18: Genome structure of rHBV-CreN....37
Figure 19: Purification of rHBV-CreN....38
Figure 20: Depiction of the Cre-induced DsRed plasmid (reprint from Matsuda 2007)....39
Figure 21: Functional complementation of split Cre in CreC/CIR cells....40
Figure 22: Infectivity of wtHBV in HepG2-NTCP-CreC-CIR cells....41
Figure 23: Expression of DsRed upon rHBV-CreN infection in CreC/CIR cells....43
Figure 24: Expression kinetics of DsRed and HBeAg in CreC/CIR cells infected with rHBV-CreN....44
Figure 25: cccDNA formation in CreC/CIR cells infected with rHBV-CreN....45
Figure 26: Effect of MyrB on rHBV-CreN infection....46

6 Reference

1. Mohsen, W. and M.T. Levy, *Hepatitis A to E: what's new?* Intern Med J, 2017. **47**(4): p. 380-389.
2. Beasley, R.P., et al., *The e antigen and vertical transmission of hepatitis B surface antigen.* Am J Epidemiol, 1977. **105**(2): p. 94-8.
3. McMahon, B.J., et al., *Acute hepatitis B virus infection: relation of age to the clinical expression of disease and subsequent development of the carrier state.* J Infect Dis, 1985. **151**(4): p. 599-603.
4. Schweitzer, A., et al., *Estimations of worldwide prevalence of chronic hepatitis B virus infection: a systematic review of data published between 1965 and 2013.* Lancet, 2015. **386**(10003): p. 1546-55.
5. Sunbul, M., *Hepatitis B virus genotypes: global distribution and clinical importance.* World J Gastroenterol, 2014. **20**(18): p. 5427-34.
6. Seeger, C. and W.S. Mason, *Molecular biology of hepatitis B virus infection.* Virology, 2015. **479-480**: p. 672-86.
7. Robinson, W.S. and R.L. Greenman, *DNA polymerase in the core of the human hepatitis B virus candidate.* J Virol, 1974. **13**(6): p. 1231-6.
8. Dane, D.S., C.H. Cameron, and M. Briggs, *Virus-like particles in serum of patients with Australia-antigen-associated hepatitis.* Lancet, 1970. **1**(7649): p. 695-8.
9. Summers, J., A. O'Connell, and I. Millman, *Genome of hepatitis B virus: restriction enzyme cleavage and structure of DNA extracted from Dane particles.* Proc Natl Acad Sci U S A, 1975. **72**(11): p. 4597-601.
10. Kaplan, P.M., et al., *DNA polymerase associated with human hepatitis B antigen.* J Virol, 1973. **12**(5): p. 995-1005.
11. Shi, W., et al., *Hepatitis B virus subgenotyping: history, effects of recombination, misclassifications, and corrections.* Infect Genet Evol, 2013. **16**: p. 355-61.
12. Lamontagne, R.J., S. Bagga, and M.J. Bouchard, *Hepatitis B virus molecular biology and pathogenesis.* Hepatoma Res, 2016. **2**: p. 163-186.
13. Yan, H., et al., *Sodium taurocholate cotransporting polypeptide is a functional receptor for human hepatitis B and D virus.* Elife, 2012. **1**: p. e00049.
14. Stieger, B., *The role of the sodium-taurocholate cotransporting polypeptide (NTCP) and of the bile salt export pump (BSEP) in physiology and pathophysiology of bile formation.* Handb Exp Pharmacol, 2011(201): p. 205-59.
15. Rabe, B., et al., *Nuclear import of hepatitis B virus capsids and release of the viral genome.* Proc Natl Acad Sci U S A, 2003. **100**(17): p. 9849-54.
16. Ko, C., T. Michler, and U. Protzer, *Novel viral and host targets to cure hepatitis B.* Curr Opin Virol, 2017. **24**: p. 38-45.
17. Quasdorff, M. and U. Protzer, *Control of hepatitis B virus at the level of transcription.* J Viral Hepat, 2010. **17**(8): p. 527-36.
18. Moolla, N., M. Kew, and P. Arbuthnot, *Regulatory elements of hepatitis B virus transcription.* J Viral Hepat, 2002. **9**(5): p. 323-31.

19. Bartenschlager, R. and H. Schaller, *The amino-terminal domain of the hepadnaviral P-gene encodes the terminal protein (genome-linked protein) believed to prime reverse transcription.* Embo j, 1988. **7**(13): p. 4185-92.
20. Wang, J., A.S. Lee, and J.H. Ou, *Proteolytic conversion of hepatitis B virus e antigen precursor to end product occurs in a postendoplasmic reticulum compartment.* J Virol, 1991. **65**(9): p. 5080-3.
21. Tang, L.S.Y., et al., *Chronic Hepatitis B Infection: A Review.* Jama, 2018. **319**(17): p. 1802-1813.
22. Nassal, M., *HBV cccDNA: viral persistence reservoir and key obstacle for a cure of chronic hepatitis B.* Gut, 2015.
23. Lucifora, J., et al., *Hepatitis B virus X protein is essential to initiate and maintain virus replication after infection.* J Hepatol, 2011. **55**(5): p. 996-1003.
24. Bartenschlager, R. and H. Schaller, *Hepadnaviral assembly is initiated by polymerase binding to the encapsidation signal in the viral RNA genome.* Embo j, 1992. **11**(9): p. 3413-20.
25. Zoulim, F. and C. Seeger, *Reverse transcription in hepatitis B viruses is primed by a tyrosine residue of the polymerase.* J Virol, 1994. **68**(1): p. 6-13.
26. Watanabe, T., et al., *Involvement of host cellular multivesicular body functions in hepatitis B virus budding.* Proc Natl Acad Sci U S A, 2007. **104**(24): p. 10205-10.
27. Summers, J., P.M. Smith, and A.L. Horwich, *Hepadnavirus envelope proteins regulate covalently closed circular DNA amplification.* J Virol, 1990. **64**(6): p. 2819-24.
28. Havert, M.B., L. Ji, and D.D. Loeb, *Analysis of duck hepatitis B virus reverse transcription indicates a common mechanism for the two template switches during plus-strand DNA synthesis.* J Virol, 2002. **76**(6): p. 2763-9.
29. Rijntjes, P.J., H.J. Moshage, and S.H. Yap, *In vitro infection of primary cultures of cryopreserved adult human hepatocytes with hepatitis B virus.* Virus Res, 1988. **10**(1): p. 95-109.
30. Thomas, E. and T.J. Liang, *Experimental models of hepatitis B and C - new insights and progress.* Nat Rev Gastroenterol Hepatol, 2016. **13**(6): p. 362-74.
31. Galle, P.R., et al., *In vitro experimental infection of primary human hepatocytes with hepatitis B virus.* Gastroenterology, 1994. **106**(3): p. 664-73.
32. Andrus, L., et al., *Expression of paramyxovirus V proteins promotes replication and spread of hepatitis C virus in cultures of primary human fetal liver cells.* Hepatology, 2011. **54**(6): p. 1901-12.
33. Gripon, P., et al., *Hepatitis B virus infection of adult human hepatocytes cultured in the presence of dimethyl sulfoxide.* J Virol, 1988. **62**(11): p. 4136-43.
34. Elaut, G., et al., *Molecular mechanisms underlying the dedifferentiation process of isolated hepatocytes and their cultures.* Curr Drug Metab, 2006. **7**(6): p. 629-60.

35. Thomas, E., et al., *HCV infection induces a unique hepatic innate immune response associated with robust production of type III interferons.* Gastroenterology, 2012. **142**(4): p. 978-88.
36. Verrier, E.R., et al., *Cell Culture Models for the Investigation of Hepatitis B and D Virus Infection.* Viruses, 2016. **8**(9).
37. Ni, Y., et al., *Hepatitis B and D viruses exploit sodium taurocholate co-transporting polypeptide for species-specific entry into hepatocytes.* Gastroenterology, 2014. **146**(4): p. 1070-83.
38. Lucifora, J., et al., *Specific and nonhepatotoxic degradation of nuclear hepatitis B virus cccDNA.* Science, 2014. **343**(6176): p. 1221-8.
39. Gripon, P., et al., *Infection of a human hepatoma cell line by hepatitis B virus.* Proc Natl Acad Sci U S A, 2002. **99**(24): p. 15655-60.
40. Hantz, O., et al., *Persistence of the hepatitis B virus covalently closed circular DNA in HepaRG human hepatocyte-like cells.* J Gen Virol, 2009. **90**(Pt 1): p. 127-35.
41. Witt-Kehati, D., M. Bitton Alaluf, and A. Shlomai, *Advances and Challenges in Studying Hepatitis B Virus In Vitro.* Viruses, 2016. **8**(1).
42. Sureau, C., et al., *Production of hepatitis B virus by a differentiated human hepatoma cell line after transfection with cloned circular HBV DNA.* Cell, 1986. **47**(1): p. 37-47.
43. Chang, C.M., et al., *Production of hepatitis B virus in vitro by transient expression of cloned HBV DNA in a hepatoma cell line.* Embo j, 1987. **6**(3): p. 675-80.
44. Yaginuma, K., et al., *Hepatitis B virus (HBV) particles are produced in a cell culture system by transient expression of transfected HBV DNA.* Proc Natl Acad Sci U S A, 1987. **84**(9): p. 2678-82.
45. Pollicino, T., et al., *Hepatitis B virus replication is regulated by the acetylation status of hepatitis B virus cccDNA-bound H3 and H4 histones.* Gastroenterology, 2006. **130**(3): p. 823-37.
46. Protzer, U., et al., *Interferon gene transfer by a hepatitis B virus vector efficiently suppresses wild-type virus infection.* Proc Natl Acad Sci U S A, 1999. **96**(19): p. 10818-23.
47. Bai, W., et al., *Engineering Hepadnaviruses as Reporter-Expressing Vectors: Recent Progress and Future Perspectives.* Viruses, 2016. **8**(5).
48. Sells, M.A., M.L. Chen, and G. Acs, *Production of hepatitis B virus particles in Hep G2 cells transfected with cloned hepatitis B virus DNA.* Proc Natl Acad Sci U S A, 1987. **84**(4): p. 1005-9.
49. Ladner, S.K., et al., *Inducible expression of human hepatitis B virus (HBV) in stably transfected hepatoblastoma cells: a novel system for screening potential inhibitors of HBV replication.* Antimicrob Agents Chemother, 1997. **41**(8): p. 1715-20.
50. van de Klundert, M.A., H.L. Zaaijer, and N.A. Kootstra, *Identification of FDA-approved drugs that target hepatitis B virus transcription.* J Viral Hepat, 2016. **23**(3): p. 191-201.
51. Bohne, F., et al., *T cells redirected against hepatitis B virus surface proteins eliminate infected hepatocytes.* Gastroenterology, 2008. **134**(1): p. 239-47.

52. Iwamoto, M., et al., *Evaluation and identification of hepatitis B virus entry inhibitors using HepG2 cells overexpressing a membrane transporter NTCP.* Biochem Biophys Res Commun, 2014. **443**(3): p. 808-13.
53. Verrier, E.R., et al., *A targeted functional RNA interference screen uncovers glypican 5 as an entry factor for hepatitis B and D viruses.* Hepatology, 2016. **63**(1): p. 35-48.
54. Hoh, A., et al., *Hepatitis B Virus-Infected HepG2hNTCP Cells Serve as a Novel Immunological Tool To Analyze the Antiviral Efficacy of CD8+ T Cells In Vitro.* J Virol, 2015. **89**(14): p. 7433-8.
55. Untergasser, A. and U. Protzer, *Hepatitis B virus-based vectors allow the elimination of viral gene expression and the insertion of foreign promoters.* Hum Gene Ther, 2004. **15**(2): p. 203-10.
56. Dorner, M., et al., *A genetically humanized mouse model for hepatitis C virus infection.* Nature, 2011. **474**(7350): p. 208-11.
57. McNamara, L.A., J.A. Ganesh, and K.L. Collins, *Latent HIV-1 infection occurs in multiple subsets of hematopoietic progenitor cells and is reversed by NF-kappaB activation.* J Virol, 2012. **86**(17): p. 9337-50.
58. Misteli, T. and D.L. Spector, *Applications of the green fluorescent protein in cell biology and biotechnology.* Nat Biotechnol, 1997. **15**(10): p. 961-4.
59. Ormo, M., et al., *Crystal structure of the Aequorea victoria green fluorescent protein.* Science, 1996. **273**(5280): p. 1392-5.
60. Shaner, N.C., G.H. Patterson, and M.W. Davidson, *Advances in fluorescent protein technology.* J Cell Sci, 2007. **120**(Pt 24): p. 4247-60.
61. Heim, R., D.C. Prasher, and R.Y. Tsien, *Wavelength mutations and posttranslational autoxidation of green fluorescent protein.* Proc Natl Acad Sci U S A, 1994. **91**(26): p. 12501-4.
62. Matz, M.V., et al., *Fluorescent proteins from nonbioluminescent Anthozoa species.* Nat Biotechnol, 1999. **17**(10): p. 969-73.
63. Shaner, N.C., et al., *Improved monomeric red, orange and yellow fluorescent proteins derived from Discosoma sp. red fluorescent protein.* Nat Biotechnol, 2004. **22**(12): p. 1567-72.
64. Wang, L., et al., *Evolution of new nonantibody proteins via iterative somatic hypermutation.* Proc Natl Acad Sci U S A, 2004. **101**(48): p. 16745-9.
65. Lippincott-Schwartz, J. and G.H. Patterson, *Development and use of fluorescent protein markers in living cells.* Science, 2003. **300**(5616): p. 87-91.
66. Strack, R.L., et al., *A noncytotoxic DsRed variant for whole-cell labeling.* Nat Methods, 2008. **5**(11): p. 955-7.
67. Wiedenmann, J., F. Oswald, and G.U. Nienhaus, *Fluorescent proteins for live cell imaging: opportunities, limitations, and challenges.* IUBMB Life, 2009. **61**(11): p. 1029-42.
68. Troy, T., et al., *Quantitative comparison of the sensitivity of detection of fluorescent and bioluminescent reporters in animal models.* Mol Imaging, 2004. **3**(1): p. 9-23.
69. Plouffe, B.D., S.K. Murthy, and L.H. Lewis, *Fundamentals and application of magnetic particles in cell isolation and enrichment: a review.* Rep Prog Phys, 2015. **78**(1): p. 016601.

70. Wang, Z., et al., *Replication-competent infectious hepatitis B virus vectors carrying substantially sized transgenes by redesigned viral polymerase translation.* PLoS One, 2013. **8**(4): p. e60306.
71. England, C.G., E.B. Ehlerding, and W. Cai, *NanoLuc: A Small Luciferase Is Brightening Up the Field of Bioluminescence.* Bioconjug Chem, 2016. **27**(5): p. 1175-1187.
72. Matthews, J.C., K. Hori, and M.J. Cormier, *Purification and properties of Renilla reniformis luciferase.* Biochemistry, 1977. **16**(1): p. 85-91.
73. Hall, M.P., et al., *Engineered luciferase reporter from a deep sea shrimp utilizing a novel imidazopyrazinone substrate.* ACS Chem Biol, 2012. **7**(11): p. 1848-57.
74. Kaskova, Z.M., A.S. Tsarkova, and I.V. Yampolsky, *1001 lights: luciferins, luciferases, their mechanisms of action and applications in chemical analysis, biology and medicine.* Chem Soc Rev, 2016. **45**(21): p. 6048-6077.
75. Koutsoudakis, G., et al., *Characterization of the early steps of hepatitis C virus infection by using luciferase reporter viruses.* J Virol, 2006. **80**(11): p. 5308-20.
76. Luker, G.D., et al., *Noninvasive bioluminescence imaging of herpes simplex virus type 1 infection and therapy in living mice.* J Virol, 2002. **76**(23): p. 12149-61.
77. Nishitsuji, H., et al., *Novel reporter system to monitor early stages of the hepatitis B virus life cycle.* Cancer Sci, 2015. **106**(11): p. 1616-24.
78. Dainiak, M.B., et al., *Methods in cell separations.* Adv Biochem Eng Biotechnol, 2007. **106**: p. 1-18.
79. Lepelley, A., et al., *Innate sensing of HIV-infected cells.* PLoS Pathog, 2011. **7**(2): p. e1001284.
80. Ottaviani, S., et al., *A MAGE-1 antigenic peptide recognized by human cytolytic T lymphocytes on HLA-A2 tumor cells.* Cancer Immunol Immunother, 2005. **54**(12): p. 1214-20.
81. Martinez, I., et al., *Cultures of HEp-2 cells persistently infected by human respiratory syncytial virus differ in chemokine expression and resistance to apoptosis as compared to lytic infections of the same cell type.* Virology, 2009. **388**(1): p. 31-41.
82. Hoess, R.H., M. Ziese, and N. Sternberg, *P1 site-specific recombination: nucleotide sequence of the recombining sites.* Proc Natl Acad Sci U S A, 1982. **79**(11): p. 3398-402.
83. Van Duyne, G.D., *Cre Recombinase.* Microbiol Spectr, 2015. **3**(1): p. Mdna3-0014-2014.
84. Meinke, G., et al., *Cre Recombinase and Other Tyrosine Recombinases.* Chem Rev, 2016. **116**(20): p. 12785-12820.
85. Missirlis, P.I., D.E. Smailus, and R.A. Holt, *A high-throughput screen identifying sequence and promiscuity characteristics of the loxP spacer region in Cre-mediated recombination.* BMC Genomics, 2006. **7**: p. 73.
86. Hermann, M., et al., *Binary recombinase systems for high-resolution conditional mutagenesis.* Nucleic Acids Res, 2014. **42**(6): p. 3894-907.
87. Heaton, N.S., et al., *Long-term survival of influenza virus infected club cells drives immunopathology.* J Exp Med, 2014. **211**(9): p. 1707-14.

88. Dutia, B.M., et al., *A novel Cre recombinase imaging system for tracking lymphotropic virus infection in vivo.* PLoS One, 2009. **4**(8): p. e6492.
89. O'Brien, S.P. and M.P. DeLisa, *Split-Cre recombinase effectively monitors protein-protein interactions in living bacteria.* Biotechnol J, 2014. **9**(3): p. 355-61.
90. Hirrlinger, J., et al., *Split-cre complementation indicates coincident activity of different genes in vivo.* PLoS One, 2009. **4**(1): p. e4286.
91. Kennedy, M.J., et al., *Rapid blue-light-mediated induction of protein interactions in living cells.* Nat Methods, 2010. **7**(12): p. 973-5.
92. Koshy, A.A., et al., *Toxoplasma secreting Cre recombinase for analysis of host-parasite interactions.* Nat Methods, 2010. **7**(4): p. 307-9.
93. Sureau, C. and J. Salisse, *A conformational heparan sulfate binding site essential to infectivity overlaps with the conserved hepatitis B virus a-determinant.* Hepatology, 2013. **57**(3): p. 985-94.
94. Matsuda, T. and C.L. Cepko, *Controlled expression of transgenes introduced by in vivo electroporation.* Proc Natl Acad Sci U S A, 2007. **104**(3): p. 1027-32.
95. Meier, A., et al., *Myristoylated PreS1-domain of the hepatitis B virus L-protein mediates specific binding to differentiated hepatocytes.* Hepatology, 2013. **58**(1): p. 31-42.
96. Zhu, Z., et al., *Cancer stem/progenitor cells are highly enriched in CD133+CD44+ population in hepatocellular carcinoma.* Int J Cancer, 2010. **126**(9): p. 2067-78.
97. Qasim, W., et al., *T cell transduction and suicide with an enhanced mutant thymidine kinase.* Gene Ther, 2002. **9**(12): p. 824-7.
98. McGuckin, C., et al., *Culture of embryonic-like stem cells from human umbilical cord blood and onward differentiation to neural cells in vitro.* Nat Protoc, 2008. **3**(6): p. 1046-55.
99. Chen, A., Y.F. Kao, and C.M. Brown, *Translation of the first upstream ORF in the hepatitis B virus pregenomic RNA modulates translation at the core and polymerase initiation codons.* Nucleic Acids Res, 2005. **33**(4): p. 1169-81.
100. Walter, P. and D. Ron, *The unfolded protein response: from stress pathway to homeostatic regulation.* Science, 2011. **334**(6059): p. 1081-6.
101. Ji, C. and N. Kaplowitz, *ER stress: can the liver cope?* J Hepatol, 2006. **45**(2): p. 321-33.
102. Li, J., et al., *Subversion of cellular autophagy machinery by hepatitis B virus for viral envelopment.* J Virol, 2011. **85**(13): p. 6319-33.
103. Das, A.T., L. Tenenbaum, and B. Berkhout, *Tet-On Systems For Doxycycline-inducible Gene Expression.* Curr Gene Ther, 2016. **16**(3): p. 156-67.
104. Pugach, E.K., et al., *Prolonged Cre expression driven by the alpha-myosin heavy chain promoter can be cardiotoxic.* J Mol Cell Cardiol, 2015. **86**: p. 54-61.
105. Tavis, J.E. and M.P. Badtke, *Hepadnaviral Genomic Replication*, in *Viral Genome Replication*, K.D. Raney, M. Gotte, and C.E. Cameron, Editors. 2009, Springer US: Boston, MA. p. 129-143.

106. Beck, J. and M. Nassal, *Hepatitis B virus replication.* World J Gastroenterol, 2007. **13**(1): p. 48-64.
107. Krebs, K., et al., *T cells expressing a chimeric antigen receptor that binds hepatitis B virus envelope proteins control virus replication in mice.* Gastroenterology, 2013. **145**(2): p. 456-65.
108. Chai, N., et al., *Properties of subviral particles of hepatitis B virus.* J Virol, 2008. **82**(16): p. 7812-7.
109. Ko, C., et al., *Hepatitis B virus genome recycling and de novo secondary infection events maintain stable cccDNA levels.* J Hepatol, 2018.
110. Ebinger, S., et al., *Characterization of Rare, Dormant, and Therapy-Resistant Cells in Acute Lymphoblastic Leukemia.* Cancer Cell, 2016. **30**(6): p. 849-862.
111. Nakabayashi, H., et al., *Growth of human hepatoma cells lines with differentiated functions in chemically defined medium.* Cancer Res, 1982. **42**(9): p. 3858-63.
112. Warming, S., et al., *Simple and highly efficient BAC recombineering using galK selection.* Nucleic Acids Res, 2005. **33**(4): p. e36.
113. Muck-Hausl, M., et al., *Ad 2.0: a novel recombineering platform for high-throughput generation of tailored adenoviruses.* Nucleic Acids Res, 2015. **43**(8): p. e50.
114. Cai, D., et al., *A southern blot assay for detection of hepatitis B virus covalently closed circular DNA from cell cultures.* Methods Mol Biol, 2013. **1030**: p. 151-61.
115. Xia, Y., et al., *Analyses of HBV cccDNA Quantification and Modification.* Methods Mol Biol, 2017. **1540**: p. 59-72.

Publications and patent

a) Publications

1. Ko C, Chakraborty A, **Chou W-M**, Hasreiter J, Wettengel JM, Stadler D, Bester R, Asen T, Zhang K, McKeating J.A., Ryu W-S, and Protzer U.
   Hepatitis B virus (HBV) capsid recycling and de novo secondary infection events maintain stable cccDNA levels. ***Journal of Hepatology*** 2018 accepted for publication.
2. Xia Y*, Stadler D*, Lucifora J, Reisinger F, Webb D, Hösel M, Michler T, Wisskirchen K, Cheng X, Zhang K, **Chou W-M**, Wettengel J, Malo A, Bohne F, Hoffmann D, Eyer F, Thimme R, Thasler WE, Heikenwalder M and Protzer U.
   Interferon-γ and Tumor Necrosis Factor-α Produced by T cells Reduce the HBV Persistence Form, cccdna, Without Cytolysis. ***Gastroenterology*** 2016, 150:194-202.
3. Lucifora J*, Xia Y*, Reisinger F, Zhang K, Stadler D, Cheng X, Sprinzl M, Koppensteiner H, Li Y, Makowska Z, Volz T, Remouchamps C, **Chou W-M**, Thasler W, Hüser N, Durantel D, Münk C, Heim MH, Browning JL, Dejardin E, Dandri M, Schindler M, Heikenwalder M* and Protzer U*
   Specific and non-hepatotoxic degradation of nuclear hepatitis B virus cccDNA. ***Science*** 2014, 343: 1121-1128.

   * Equal contribution

b) Patent

Wen-Min Chou, Ulrike Protzer, Martin Mück-Häusl, Chunkyu Ko, Jochen Wettengel
Novel recombinant HBV reporter system based on cre-lox recombination.
Filing for US patent.

Acknowledgements

First, I would like to thank my supervisor, Prof. Ulrike Protzer, for providing me the opportunity to conduct my study at the Institute of Virology and for guiding me throughout. I have learned much from you, not only in the ability to conduct a research project but also in the attitude as a scientist.

I would like to thank the members of my thesis committee, Prof. Wolfgang Hammerschmidt and Dr. Günter Schneider, for intensively discussing my project and giving me very useful scientific advice. Meeting with you was always very helpful.

I would like to thank Anna Kosinska, Chunkyu Ko, and Daniela Stadler for thoroughly reviewing my thesis. It significantly improved with your suggestions, and I have learned much from you regarding scientific writing.

I would like to thank Martin Mück-Häusl for designing the rHBV-Cre revenant system and inspiring me to develop the rHBV-CreN system. I would like to thank Wen-Hsin Liu (AHS, Helmholtz Zentrum München) for giving me an idea to generate the rHBV-LNGFR system and kindly providing the technical support to establish the MACS procedure. I would like to thank Chunkyu Ko, Daniela Stadler, and Anindita Chakraborty for your scientific discussions and suggestions regarding the projects. These projects would not have been possible without your inputs.

I would like to thank Chunkyu Ko for teaching me the methods of analyzing HBV replication. I would like to thank Sebastian Altstetter, Jochen Wettengel, and Samuel Jeske for teaching me heparin affinity chromatography and providing me equipment. I would like to thank Julia Hasreiter, Lisa Wolff, and Marvin Festag for helping me to establish the FACS analysis procedure for hepatoma cells. I would like to thank Hilary Ganz, who did an internship with me, for performing the cloning of rHBV-LNGFR and rHBV-CreN. I could not have achieved the progress thus far without your help.

I would like to thank Romina Bester for her excellent technical support with the experiments. Moreover, I would like to thank Theresa Asen, Hortenzia Jacobi, Philipp Hagen, and Susanne Kolano for organizing the lab laboratory supplies and their technical support with HBeAg and HBsAg measurements. I would also like to thank Martin Kächele for sharing the responsibility of managing the liquid nitrogen tanks. Your efforts greatly reduced my workload, and I truly appreciated your assistant.

As my colleagues and as my good friends, I would like to thank Julia Hasreiter, Sophia Schreiber, Lisa Wolff, and Marvin Festag. Your friendship is one of the best things I have ever had, not only has helped me through the tough times but also has motivated me to become a better person.

I would like to thank my colleagues, Andreas Oswald, Anindita Chakraborty, Christoph Blossey, Martin Kächele, Jinpeng Su, Julia Sacherl, Lili Zhao, Oliver Quitt, and Sebastian Altstetter, for creating such a pleasant work environment and for warmly supporting me there. In addition, I would like to thank Yuchen Xia, Xiaoming Cheng, and Julie Lucifora for your supervision when I started in the lab and for helping me settle in when I first came to Munich.

I would like to thank the Medical Life Science PhD program for providing me a one-year scholarship and Deutscher Akademischer Austauschdienst (DAAD) for providing me a three-year scholarship.

I would like to thank Prof. Irmela Jeremias (AHS, Helmholtz Zentrum München) and Prof. Lloyd M. Smith (University of Wisconsin–Madison) for hosting me in your labs to learn the experiment techniques.

I would like to thank my mentors, Li-Rung Huang and Ming-Kang Chang. I am grateful for your time, advice, and support, which help me to further develop and inspire me in various ways.

I would like to thank my parents for providing me additional financial support at the beginning for pursuing my study in Germany.

To my friends in Taiwan, in Munich, and in Zurich. Thank you for being there for me when I needed you. It is your warm support and all the joyful moments we have shared that helped me get through those difficult times.

Lastly, to my girlfriend, Ching-Hua, thank you for accompanying me through all these good and bad days. Your unconditional love gives me the strength to stand up again every time I fall.

Thank you all for standing by me throughout my study. I never would have achieved this without you. For this, I am forever grateful.